

POLITECNICO DI TORINO

Department of Mechanical and Aerospace Engineering

Master's Thesis
in
Mechanical Engineering

Human Body Model and Passive Safety in Vehicles: Side Impact Crash with Offset Studied with FE Simulation



**Politecnico
di Torino**

Tutors

Prof. Eng. Alessandro Scattina

Prof. Eng. Giovanni Belingardi

Candidate

Andrea Silvestro

July 2021

Abstract

The objective of this thesis is to reproduce in a FE environment a side impact crash test with offset between a Moving Deformable Barrier (AE-MDB) and a mid-size sedan. A further goal is to investigate the possible injuries that a driver may suffer in this type of impact using a Human Body Model (HBM). This typology of crash test is not regulated by Euro NCAP, but reference is made to their protocol for recreating the impact. The FE environment simulates a 2012 Toyota Camry in which a (HBM) driver is inserted. The HBM chosen for this thesis work is the THUMS model. In order to include the HBM in the car model it is necessary to make some steps to recreate the real situation in the FE environment. The driver's seat has to be statically deformed due to the weight of the occupant and then a standard driving position has to be recreated by changing the initial position of the HBM through a simulation, to this aim the PIPER tool was used. After this process, seat belts are created to secure the driver to his seat. Once the impact simulation has been completed, the results are analysed to measure possible injuries and to investigate the body parts most at risk in this type of crash. The biomechanical data obtained are compared with those obtained from a side impact and far side impact. The impact without offset results to be more critical for the upper body especially for the head, while the back is more stressed in the far side due to the wide excursion. The legs are more loaded in the case taken into consideration but result however out of danger of injury. The advantage of using a HBM model, that is much more detailed and realistic than a rigid dummy, allows for more accurate results on injury analysis.

Index

Summary

| | |
|--|-----------|
| INDEX | 1 |
| PREFACE | 8 |
| INTRODUCTION..... | 8 |
| PURPOSE | 9 |
| ROADMAP | 10 |
| CHAPTER 1: LITERATURE REVIEW | 11 |
| 1.1 EURO NCAP | 11 |
| 1.1.1 Introduction..... | 11 |
| 1.1.2 Side impact testing protocol..... | 12 |
| 1.1.3 Sensors Euro NCAP legislation on the side impact | 13 |
| 1.2 INJURY CRITERIA | 15 |
| 1.2.1 Introduction..... | 15 |
| 1.2.2 Head Injury Criteria (HIC)..... | 15 |
| 1.2.3 Neck Injury Criteria (Nij) | 15 |
| 1.2.4 Tibia Index (TI) | 16 |
| 1.2.5 Viscous Criterion (VC)..... | 16 |
| CHAPTER 2: FINITE ELEMENT MODELS | 19 |
| 2.1 INTRODUCTION..... | 19 |
| 2.2 ADVANCED EUROPEAN MOVABLE DEFORMABLE BARRIER MODEL | 20 |
| 2.3 2012 TOYOTA CAMRY MODEL..... | 23 |
| 2.4 HUMAN BODY MODEL | 26 |
| 2.4.1 Introduction..... | 26 |
| CHAPTER 3: PRE-SIMULATION PROCESS | 29 |
| 3.1 SETTING CRASH SIMULATION | 29 |
| 3.1.1 Introduction..... | 29 |
| 3.1.2 Description of the simulation settings..... | 29 |
| 3.2 SITTING SIMULATION..... | 32 |
| 3.2.1 Introduction..... | 32 |
| 3.2.2 Description of the process..... | 32 |
| 3.3 THUMS POSITIONING | 36 |
| 3.3.1 Introduction..... | 36 |
| 3.3.2 Positioning through PIPER software | 36 |
| 3.4 SEATBELT MODELLING | 41 |
| 3.4.1 Introduction..... | 41 |

| | | |
|------------------------------------|---|------------|
| 3.4.2 | Seatbelt routine | 41 |
| 3.4.3 | Retractor | 44 |
| 3.4.4 | D-rings | 45 |
| 3.4.5 | Pretensioner | 46 |
| 3.4.6 | Sensors | 47 |
| 3.5 | SET-UP OF THE SENSOR | 48 |
| 3.5.1 | Head sensor | 49 |
| 3.5.2 | Neck sensors | 50 |
| 3.5.3 | Thorax and pelvis sensors | 51 |
| 3.5.4 | Rib cage sensor | 52 |
| 3.5.5 | Internal organs volume sensor | 53 |
| 3.5.6 | Lower limbs | 55 |
| CHAPTER 4: RESULTS..... | | 56 |
| 4.1 | OVERVIEW | 56 |
| 4.2 | ENERGY BALANCE..... | 60 |
| 4.3 | CAR AND TROLLEY SENSOR ANALYSIS..... | 62 |
| 4.4 | THUMS SENSOR ANALYSIS..... | 63 |
| 4.4.1 | THUMS – Head | 63 |
| 4.4.2 | Head Injury Criteria (HIC)..... | 64 |
| 4.4.3 | THUMS - Neck..... | 66 |
| 4.4.4 | Neck Injury Criteria | 68 |
| 4.4.5 | THUMS – Thorax T1 | 69 |
| 4.4.6 | THUMS – Thorax T4 | 70 |
| 4.4.7 | THUMS – Thorax T12 | 71 |
| 4.4.8 | THUMS – Ribs | 73 |
| 4.4.9 | THUMS – Backplate | 75 |
| 4.4.10 | THUMS – Pelvis..... | 76 |
| 4.4.11 | THUMS – Pubic Symphysis..... | 77 |
| 4.4.12 | THUMS – L&R Femur..... | 78 |
| 4.4.13 | Tibia Index (TI) | 81 |
| 4.4.14 | THUMS – Internal Organs Volume and Surface Area | 82 |
| 4.4.15 | THUMS – Spine Deformation..... | 84 |
| 4.4.16 | Comparison with Side Impact and Far Side Impact..... | 86 |
| CHAPTER 5: CONCLUSIONS..... | | 107 |
| APPENDIX A..... | | 111 |
| APPENDIX B..... | | 121 |
| REFERENCES | | 131 |
| ACKNOWLEDGEMENTS | | 133 |

| | |
|---|----|
| Figure 0-1 - Forecast of the number of deaths due to road accidents per 1 million inhabitants in Italy from 2010 to 2025..... | 8 |
| Figure 0-2 - Euro NCAP side impact..... | 9 |
| Figure 0-0-3 - Thesis roadmap..... | 10 |
| Figure 1-1 - 5 stars Euro NCAP review..... | 11 |
| Figure 1-2 – Euro NCAP car sensors..... | 13 |
| Figure 1-3 - Euro NCAP trolley sensors..... | 14 |
| Figure 1-4 - Euro NCAP dummy sensors..... | 14 |
| Figure 2-1 - AE-MDB impactor detail..... | 20 |
| Figure 2-2 - AE-MDB wall impact validation..... | 21 |
| Figure 2-3 - AE-MDB wall impact validation results..... | 21 |
| Figure 2-4 - Real vehicle and FE model of a 2012 Toyota Camry Sedan..... | 23 |
| Figure 2-5 - Details of the model of the vehicle structure..... | 23 |
| Figure 2-6 - Comparison between real and simulate SINCAP test..... | 24 |
| Figure 2-7 - THUMS evolution..... | 26 |
| Figure 2-8 - Details of the THUMS..... | 27 |
| Figure 2-9 - THUMS in standard position..... | 28 |
| Figure 3-1 – Position of the MDB and the car..... | 30 |
| Figure 3-2 - Floor..... | 31 |
| Figure 3-3 - Comparison between full THUMS model and rigid skin model..... | 32 |
| Figure 3-4 – Driver’s seat model..... | 33 |
| Figure 3-5 – Details of the constraint..... | 33 |
| Figure 3-6 – Sitting simulation: first and last step of simulation..... | 34 |
| Figure 3-7 – Detail of the deformed seat cushion..... | 35 |
| Figure 3-8 – PIPER environment model..... | 36 |
| Figure 3-9 - Environment positioning, isometric and section plane view..... | 37 |
| Figure 3-10 - Landmark and joint visualization on PIPER..... | 37 |
| Figure 3-11 - Fixed bones example for higher limb positioning..... | 38 |
| Figure 3-12 - In the figures in the top the isometric and the section view of final position, in the figures in the bottom some details of the hands and the feet positioned..... | 39 |
| Figure 3-13 - Three point seatbelt example..... | 41 |
| Figure 3-14 – Anchors in the FE vehicle model..... | 42 |
| Figure 3-15 – Seatbelt and detail of the mesh of the belt..... | 43 |
| Figure 3-16 - Retractor displacement vs force..... | 44 |
| Figure 3-17 – Comparison between real and FE position on the retractor..... | 45 |

| | |
|--|----|
| Figure 3-18 – Comparison between the real FE position of the D-ring..... | 46 |
| Figure 3-19 - Pretensioner pull in vs time..... | 46 |
| Figure 3-20 - THUMS positioned with the seatbelt model..... | 47 |
| Figure 3-21 - Set of sensors | 48 |
| Figure 3-22 – Head accelerometer | 49 |
| Figure 3-23 – Cross_section_planes: head (green), upper neck (blue), lower neck (red)..... | 50 |
| Figure 3-24 – Thorax and pelvic sensors | 51 |
| Figure 3-25 - Rib cage sensors..... | 52 |
| Figure 3-26 – Internal organs..... | 54 |
| Figure 3-27 – Lower limbs sensors: cross_section_planes (left), accelerometer (right)..... | 55 |
| Figure 4-1 - Isometric view of the impact at t=0ms..... | 56 |
| Figure 4-2 - Isometric view of the impact at t=20ms..... | 56 |
| Figure 4-3 - Isometric view of the impact at t=40ms..... | 57 |
| Figure 4-4 - Isometric view of the impact at t=60ms..... | 57 |
| Figure 4-5 - Isometric view of the impact at t=80ms..... | 57 |
| Figure 4-6 - Isometric view of the impact at t=90ms..... | 57 |
| Figure 4-7 - Front view of the impact at t=0ms | 58 |
| Figure 4-8 - Front view of the impact at t=15ms | 58 |
| Figure 4-9 - Front view of the impact at t=30ms | 58 |
| Figure 4-10 - Front view of the impact at t=45ms | 58 |
| Figure 4-11 - Front view of the impact at t=60ms | 58 |
| Figure 4-12 - Front view of the impact at t=75ms | 58 |
| Figure 4-13 - Front view of the impact at t=90ms | 59 |
| Figure 4-14 - Energy Balance | 60 |
| Figure 4-15 - Energy Ratio | 61 |
| Figure 4-16 - Comparison of velocities | 62 |
| Figure 4-17 - Head Accelerations | 63 |
| Figure 4-18 - HIC window..... | 64 |
| Figure 4-19 - HIC score | 64 |
| Figure 4-20 - Upper neck forces | 66 |
| Figure 4-21 - Lower neck forces..... | 66 |
| Figure 4-22 - Upper neck moments | 67 |
| Figure 4-23 - Lower neck moments..... | 67 |
| Figure 4-24 - Nij AIS 2+..... | 68 |
| Figure 4-25 - Nij AIS 3+..... | 68 |
| Figure 4-26 - Thorax T1 accelerations..... | 69 |
| Figure 4-27 - Thorax T4 accelerations..... | 70 |

| | |
|---|----|
| Figure 4-28 - T12 forces | 71 |
| Figure 4-29 - T12 moments..... | 71 |
| Figure 4-30 - T12 accelerations | 72 |
| Figure 4-31 - Upper thorax deflection | 73 |
| Figure 4-32 - Middle thorax deflection..... | 73 |
| Figure 4-33 - Lower thorax deflection..... | 74 |
| Figure 4-34 - Backplate forces..... | 75 |
| Figure 4-35 - Backplate moments..... | 75 |
| Figure 4-36 - Pelvis accelerations..... | 76 |
| Figure 4-37 - Pubic Symphysis y force..... | 77 |
| Figure 4-38 - Left femur forces..... | 78 |
| Figure 4-39 - Right femur forces | 78 |
| Figure 4-40 - Left femur moments..... | 79 |
| Figure 4-41 - Right femur moments..... | 79 |
| Figure 4-42 - Right vs left femur forces..... | 80 |
| Figure 4-43 - Right vs left moments | 80 |
| Figure 4-44 - Ribcage volume..... | 82 |
| Figure 4-45 - Ribcage surface area | 83 |
| Figure 4-46 - Undeformed spine xz view (left), yz view (right)..... | 84 |
| Figure 4-47 - xz plane deformed spine | 85 |
| Figure 4-48 - yz plane deformed spine | 85 |
| Figure 4-49 - Comparison resultant head accelerations | 86 |
| Figure 4-50 - Comparison rotational x accelerations | 87 |
| Figure 4-51 - Comparison rotational y accelerations | 87 |
| Figure 4-52 - Comparison rotational z accelerations | 88 |
| Figure 4-53 - Comparison resultant rotational accelerations | 88 |
| Figure 4-54 - Comparison T1 x accelerations..... | 89 |
| Figure 4-55 - Comparison T1 y accelerations..... | 89 |
| Figure 4-56 - Comparison T1 z accelerations | 90 |
| Figure 4-57 -- Comparison T12 y accelerations..... | 90 |
| Figure 4-58 - Comparison T12 x forces..... | 91 |
| Figure 4-59 - Comparison T12 y forces..... | 91 |
| Figure 4-60 - Comparison T12 x moments | 92 |
| Figure 4-61 - Comparison T12 y moments | 92 |
| Figure 4-62 - Comparison upper thorax deflections | 93 |
| Figure 4-63 - Comparison middle thorax deflections | 93 |
| Figure 4-64 - Comparison lower thorax deflections | 94 |

| | |
|---|-----|
| Figure 4-65 - Viscous criterion AIS 2-3 | 94 |
| Figure 4-66 - Comparison backplate x forces | 95 |
| Figure 4-67 - Comparison backplate y forces | 95 |
| Figure 4-68 - Comparison backplate y moment..... | 96 |
| Figure 4-69 - Comparison backplate z moment | 96 |
| Figure 4-70 - Comparison pelvis x accelerations..... | 97 |
| Figure 4-71 - Comparison pelvis y accelerations..... | 97 |
| Figure 4-72 - Comparison pelvis z accelerations | 98 |
| Figure 4-73 - Comparison pubic symphysis y forces..... | 99 |
| Figure 4-74 - Comparison right femur total forces | 100 |
| Figure 4-75 - Comparison right femur total moments | 100 |
| Figure 4-76 - Comparison left femur total forces | 101 |
| Figure 4-77 - Comparison left femur total moments..... | 101 |
| Figure 4-78 - Comparison right upper tibia total forces..... | 102 |
| Figure 4-79 - Comparison right upper tibia total moments..... | 102 |
| Figure 4-80 - Comparison right lower tibia total forces..... | 103 |
| Figure 4-81 - Comparison right lower tibia total moments..... | 103 |
| Figure 4-82 - Comparison left upper tibia total forces..... | 104 |
| Figure 4-83 - Comparison left upper tibia total moments..... | 104 |
| Figure 4-84 - Comparison left lower tibia total forces..... | 105 |
| Figure 4-85 - Comparison left lower tibia total moments..... | 105 |
| Figure 4-86 - Tibia index risk curve | 106 |
| | |
| Appendix A 1- Right lung volume..... | 111 |
| Appendix A 2 - Right lung surface area..... | 111 |
| Appendix A 3 - Left lung volume | 112 |
| Appendix A 4 - Left lung surface area..... | 112 |
| Appendix A 5 - Heart volume..... | 113 |
| Appendix A 6 - Heart surface area..... | 113 |
| Appendix A 7 - Pancreas volume..... | 114 |
| Appendix A 8 - Pancreas surface area | 114 |
| Appendix A 9 - Spleen volume | 115 |
| Appendix A 10 - Spleen surface area..... | 115 |
| Appendix A 11 - Liver volume | 116 |
| Appendix A 12 - Liver surface area..... | 116 |
| Appendix A 13 - Stomach volume..... | 117 |
| Appendix A 14 - Stomach surface area..... | 117 |

| | |
|---|-----|
| Appendix A 15 - Large intestine volume | 118 |
| Appendix A 16 - Large intestine surface area..... | 118 |
| Appendix A 17 - Small intestine volume | 119 |
| Appendix A 18 - Small intestine surface area..... | 119 |
| Appendix A 19 - Abdomen volume | 120 |
| Appendix A 20 - Abdomen surface area..... | 120 |
| | |
| Appendix B 1 - Head y_acceleration | 121 |
| Appendix B 2 - Head x_acceleration | 121 |
| Appendix B 3 - head z_acceleration | 122 |
| Appendix B 4 - Upper neck x_force | 122 |
| Appendix B 5 - Upper neck y_force | 123 |
| Appendix B 6 - Upper neck z_force | 123 |
| Appendix B 7 - Upper neck total_force | 124 |
| Appendix B 8 - Upper neck x_moment | 124 |
| Appendix B 9 - Upper neck y_moment | 125 |
| Appendix B 10 - Upper neck z_moment..... | 125 |
| Appendix B 11 - Upper neck total_moment | 126 |
| Appendix B 12 - Lower neck x_force..... | 126 |
| Appendix B 13 - Lower neck y_force..... | 127 |
| Appendix B 14 - Lower neck z_force..... | 127 |
| Appendix B 15 - Lower neck total_force..... | 128 |
| Appendix B 16 - Lower neck x_moment..... | 128 |
| Appendix B 17 - Lower neck y_moment..... | 129 |
| Appendix B 18 - Lower neck z_moment | 129 |
| Appendix B 19 - Lower neck total_moment..... | 130 |

Preface

Introduction

Side impact crash injuries are one of the principal causes of fatality on streets, a study of Insurance Institute for Highway Safety (IIHS) said that in 2017, 25% of the death on road accidents were caused in a side impact scenario [1] [2]. The main cause of fatal injury in these cases are the thorax damage, responsible for nearly 60% of deaths [3]. These facts remark the importance of the study of this case scenario and the development of new and modern active/passive security device. The development of the NCAP program, in that sense, it was a great effort for the evaluation of the new automobile designs for performance against various safety threats with a standard procedure [4]. The main problem of the NCAP programme however, is the high expense of each test since the vehicle tested is no more usable (up to 4 cars needed for an assessment by Euro NCAP) [5]. To solve this problematic and have a better understanding of the injury mechanisms, Finite Element models are used to reproduce the real case scenario. The Human Body Models in this regard were a huge step on the increasing of the quantity and accuracy of data related to human response to any kind of stress, including crash situations, so much so that currently they are able to provide a more realistic response than the normal dummy used in a real crash test [6]. With all these instruments today, it's possible to simulate, with a fair accuracy, different impact crash and analyse a massive quantity of data. Thanks to all the continue evolving of the road security field, the number of fatalities is decreasing every year. The instruments used in this thesis are just an example of why it was possible to achieve all this.

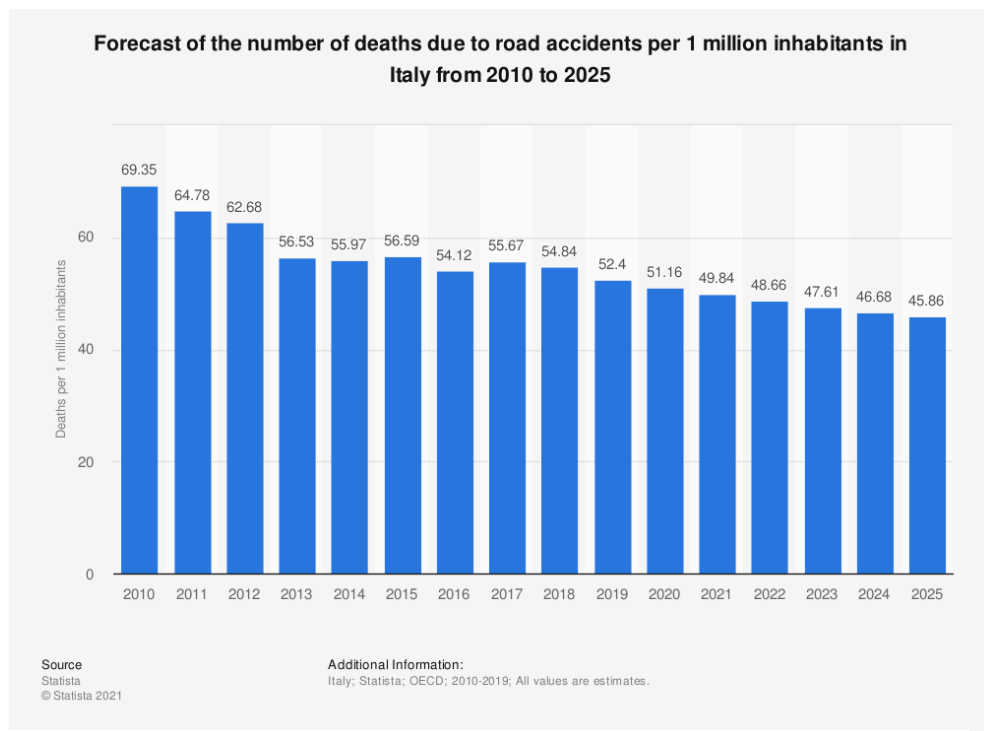


Figure 0-1 - Forecast of the number of deaths due to road accidents per 1 million inhabitants in Italy from 2010 to 2025

Purpose

The aim of this thesis is the simulation of a side impact crash with a longitudinal offset from the R point with a moving deformable barrier, using a Finite Element simulation. This type of crash test is not regulated by Euro NCAP, which, however, provides among the various cases of crash, the side impacts. It has been chosen therefore to refer to the protocol of Euro NCAP regarding all the phase of recreation of the crash with the difference of the point of impact of the MDB. A Human Body Model, able to simulate the reaction of a real body in crash scenario, was used in the simulation. Through some Injury Criteria, which will be discussed later, we are able to have a clear idea of the severity of the injury of the occupant. At the end a comparison between the side impact and the case with offset is made. For the realization of the car model was used a 2012 Toyota Camry provided by the Center for Collision Safety and Analysis (CCSA). The impact object used, following the setting of an Euro NCAP test, is a moving deformable barrier based on NHTSA's Moving Deformable Barrier according to FMVSS 214 Regulations and developed by Livermore Software Technology Corporation (LSTC). The HBM used is the Total Human Model for Safety (THUMS) developed by Toyota. All the simulations were realized using LS-DYNA Finite Element explicit code.

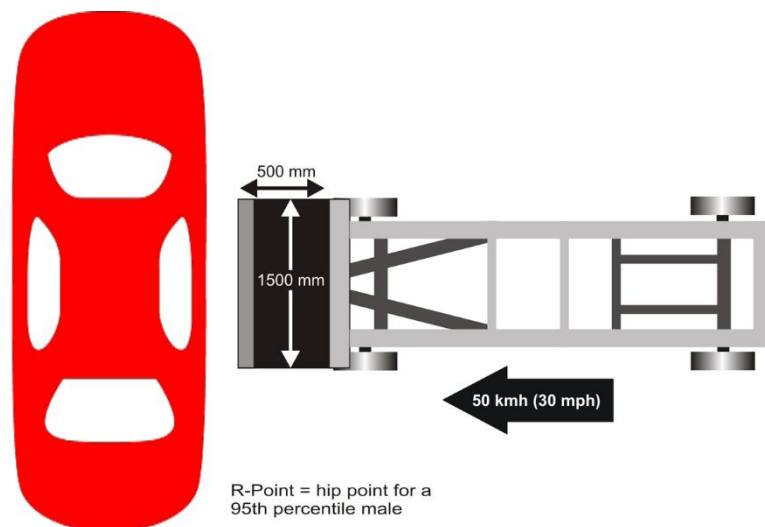


Figure 0-2 - Euro NCAP side impact

Roadmap

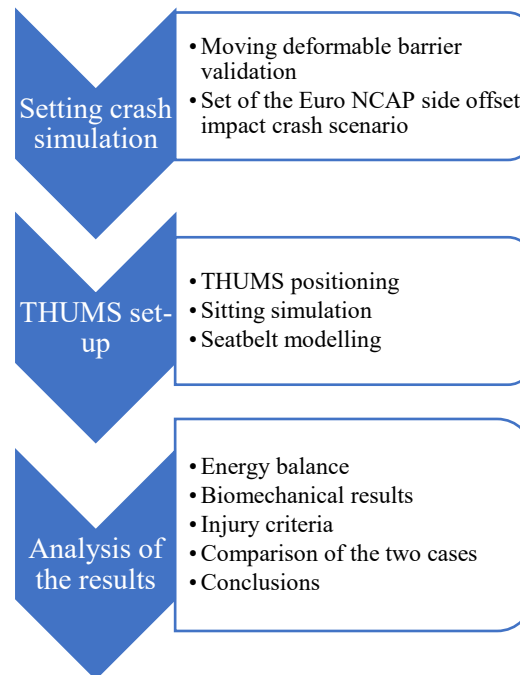


Figure 0-0-3 - Thesis roadmap

First of all, it was necessary to validate the Moving Deformable Barrier through the documentation provided by LSTC [7]. After this step an Euro NCAP full simulation without the occupant was performed. Due to this first big effort most of the parameters for the FE simulation were set.

In order to include the driver in the model simulation some steps are necessary. The THUMS must be positioned in the standard driving position, following the Euro NCAP standard, using the PIPER Tool. Then the car environment needs some implementation. A sitting simulation, to simulate the real deformation of a normal driver seat, and a seatbelt model were provided in order to complete and launch a full simulation. The final considerations are made analysing the data obtained and with the help of the Injury Criteria.

Chapter 1: Literature Review

1.1 Euro NCAP

1.1.1 Introduction

The European New Car Assessment Programme (Euro NCAP) is a European voluntary car safety performance assessment programme based in Leuven (Belgium) and founded in 1996.

It was created by the Swedish Road Administration, the Fédération Internationale de l'Automobile and International Consumer Research & Testing, backed by 14 members, and motoring & consumer organisations in several EU country. The project came to life after the release of the New Car Assessment Program (NCAP), introduced in 1979 by the US National Highway Traffic Safety Administration (NHTSA), where Euro NCAP took most inspiration.

Euro NCAP have provided several standard tests in order to evaluate the safety system adopted by the main constructors. With a five stars review of many parameters the consumer can understand the safety value of the vehicle [4] [5].



Figure 1-1 - 5 stars Euro NCAP review

The tests are not mandatory for the constructors, in fact the car models are chosen by the same Euro NCAP or sponsored by the manufactures, however, the value of Euro NCAP reports is recognised worldwide. This increases the competitiveness of the market in the security field and raises the safety

standards. With over then 1800 new car tested the Euro NCAP is one of the most relevant voices in the automotive field of security.

In this work the simulation will be set according to the Euro NCAP procedure of a side impact crash test.

1.1.2 Side impact testing protocol

Side impact crashes are the second cause of death in car accidents, mainly for injuries of the chest and the head. This is caused by the massive energy generated in a car crash and the thinness of the side part of the car, where the door has to absorb an high amount of kinetic energy remaining in restricted constrains of deformation. A lot of safety systems were implemented by the constructors to ensure protection to the driver, torso airbags are one of the examples of this breakthrough. Euro NCAP have developed a standard protocol to rate the safety of the side protections of manufactures [8].

The Euro NCAP's standard includes a dummy, with several sensors, and a moving deformable barrier that is thrown against the vehicle at 50 ± 1 Km/h speed. The direction of impact is perpendicular to side of the car and pointed on the R-point, a parameter provided by the constructor, with a tolerance of ± 25 mm. The barrier has to be certified by Euro NCAP and respects some manufacture constrains. The weight it's supposed to be 950 ± 20 Kg with a wheelbase of 3000 mm for example. More details about the barrier construction and validation will be given in the next chapter.

Previously the crash test some settings of the vehicle and the dummy as to be done.

- The car's tank as to be fill on the 90% of his capacity and all the others liquid containers as to be at full capacity.
- Measure the front and rear axle weights and determine the total weight of the vehicle. This weight is the "unladen kerb mass" of the vehicle.
- Measure and record the ride heights of the vehicle at all four wheels.

After this procedure an object with a mass of the dummy (80Kg) have to be placed in the driver seat and a 100Kg mass as to be added in the rear compartment and the same measurements of before as to be repeat.

With all these data's collection the final setting of the vehicle is realized. A mass of the equivalent of the weight of the dummy (80Kg) is positioned on the driver seat and the vehicle have to respect

some checks. The vehicle mass can differ to the reference weight of a maximum of 1% and the axels loads can differ to the previous measurements with a tolerance of 5% for each parameter.

The FE vehicle used in this simulation respect the Euro NCAP requirements and no validation had to be necessary in this work.

Now the dummy has to be positioned. Following the Euro NCAP legislation the dummy has to respect some constraints describe as follow:

- The torso of the dummy has to be positioned as close as possible to the driver seat and to the H-point.
- The hands are supposed to be in contact with the steering wheel at a position of quarter to three.
- The left foot, since in the model a footrest is not provide, has to be positioned parallel to the floor in a rest position.
- The right foot is positioned on the undepressed acceleration pedal, with the heel as far forwards as possible and in contact with the floor. The right foot should overlap the accelerator pedal with at least 20mm.

After this crucial step the seatbelt can be placed and the test is ready to start.

1.1.3 Sensors Euro NCAP legislation on the side impact

Before the positioning of the dummy the implementation of the sensors has to be done in order to collect all the parameters necessary to the evaluation of the safety of the vehicle.

On the car an acceleration sensor is placed to measure the lateral acceleration on the unstruck B-post.

| Location | Parameter | Minimum Amplitude | No of channels |
|-----------------------------------|---------------------|--------------------------|-----------------------|
| B-Post (unstruck) | Acceleration, A_y | 150g | 1 |
| Total Channels per Vehicle | | | 1 |

Figure 1-2 – Euro NCAP car sensors

The trolley has to be placed an accelerometer on the Center of Gravity in order to measure the acceleration of impact A_y .

| Location | Parameter | Minimum Amplitude | No of channels |
|----------------------------|---------------------|-------------------|----------------|
| Trolley C of G | Acceleration, A_y | 150g | 1 |
| Total Channels per Trolley | | | 1 |

Figure 1-3 - Euro NCAP trolley sensors

The dummy has to be implemented with some sensors as well described in the following table.

| Location | Parameter | Minimum Amplitude | No of channels |
|-----------------------------------|------------------------------|-------------------|----------------|
| Head | Accelerations, $A_x A_y A_z$ | 250g | 3 |
| Shoulder | Forces, $F_x F_y F_z$ | 8kN | 3 |
| Thorax T1 | Accelerations, $A_x A_y A_z$ | 200g | 3 |
| Thorax T12 | Acceleration, A_y | 200g | 1 |
| Ribs - Upper Middle Lower | Acceleration, A_y | 700g | 3 |
| | Deflection, D_{nb} | 90mm | 3 |
| Abdomen - Front Middle Rear | Forces, F_y | 5kN | 3 |
| | | | |
| Backplate | Forces, $F_x F_y$ | 5kN | 4 |
| | Moments, $M_y M_z$ | 200Nm | |
| T12 | Forces, $F_x F_y$ | 5kN | 4 |
| | Moments, $M_x M_y$ | 300Nm | |
| Pelvis | Accelerations, $A_x A_y A_z$ | 150g | 3 |
| Pubic Symphysis | Force, F_y | 20kN | 1 |
| Femurs (L & R) | Forces, $F_x F_y F_z$ | 22kN | 6 |
| | Moments, $M_x M_y M_z$ | 350Nm | 6 |
| Total Channels per Dummy | | | 43 |
| 1 x ES-2 | | | 43 |

Figure 1-4 - Euro NCAP dummy sensors

At the end of this procedure the sensors implemented are 45.

1.2 Injury criteria

1.2.1 Introduction

Injury criteria have been developed to address the mechanical responses of crash test dummies in terms of risk to life or injury to a living human. The criteria have been derived from experimental efforts using human surrogates where both engineering parameters and injury consequences are observed and the most meaningful relationship between forces/motions and resulting injuries are determined using statistical techniques. Frequently criteria are developed, based on extensive analysis, for one size dummy (an adult) and these criteria are applied and translated to other size dummies (for example child) through a scaling process. This technique overcomes the influence of geometrical and material differences between experimental subject and the subject of interest assuming that are scale model of each other and that their property vary by relatively simple mathematical relationship. In this section, the main Injury Criteria are introduced [9].

1.2.2 Head Injury Criteria (HIC)

The Head Injury Criteria (HIC) is one of the most widely used to calculate the damage suffered by the head. It is computed as [10]:

$$HIC_{36} = (t_2 - t_1) \left(\left(\frac{1}{t_2 - t_1} \right) \int_{t_1}^{t_2} a_r dt \right)^{2.5}$$

Where:

- a_r is the head resultant acceleration
- 36 is the length of the corresponding time interval

The measurement value of the head acceleration are filtered according to CFC 1000.

1.2.3 Neck Injury Criteria (Nij)

The Neck Injury Criteria (Nij) propose critical limits for all four possible modes of neck loading, tension or compression combined with flexion forward or rearward. It is computed as [10]:

$$Nij = \frac{F_Z}{F_{int}} + \frac{M_y}{M_{int}}$$

Where:

- F_Z is the axial load
- F_{int} is the critical value used for normalization
- M_y is the bending moment
- M_{int} is the critical value used for normalization

The measured values of the tensile force and compression force are filtered with CFC 600.

1.2.4 Tibia Index (TI)

The Tibia Index (TI) takes into account the axial force and the bending moment to which the tibia undergoes. It is computed as [10]:

$$TI = \left| \frac{M_R}{(M_C)_R} \right| + \left| \frac{F_Z}{(F_C)_R} \right|$$

Where:

- $M_R = \sqrt{(M_x)^2 + (M_y)^2}$
- F_Z is the axial compression in z-direction
- $(M_C)_R$ is the critical bending moment
- $(F_C)_R$ is the critical compression force in z-direction

The measured value of the bending moment and axial force are filtered with CFC 600.

1.2.5 Viscous Criterion (VC)

The Viscous Criterion (VC) is used for the chest area, one of the most suffered area of the body during the side impact and assesses the risk of injury of the soft tissue injury due to a crush mechanism. In the side impact case, it considers the rib deflection. It is computed as [10]:

$$VC = \text{Scaling factor} \frac{Y_{CFC180}}{Def_{konst}} \frac{dY_{CFC180}}{dt}$$

Where:

- *Scaling factor* is function of the dummy type used in the simulation
- *Y* is the rib deflection
- $\frac{dY_{CFCxxx}}{dt}$ is the velocity of deformation
- *Defconst* is the dummy constant that is equal to the depth or width of half of the rib cage of the dummy used in the simulation

The measured values used were filtered with CFC 180.

Chapter 2: Finite Element models

2.1 Introduction

In the side impact crash simulation several FE models are involved. These models used the Finite Element Method (FEM) to predict the real behaviour of the component. To achieve this level various tests, static and dynamic, has to be done in order to adjust the parameters of the model. The predictive accuracy of the model can be obtained comparing the outcome of the simulation with real data obtained in a controlled experiment. All the models used in this work have carried out this validation process and can predict with fair accuracy the behaviour of a real crash.

In the side impact crash scenario three main FE models are involved:

- A mobile deformable barrier (MDB) model, the impact object of this test, that will be through to the car at a velocity of 50Km/h.
- A car model, a 2012 Toyota Camry, that will host the HBM during the crash.
- A Human Body Model (HBM), that will be housed inside the cabin and, through different sensors collocated inside the model, will provide the injury level due to the crash impact.

In the following will be provided a brief description of the models involved in this work of thesis.

2.2 Advanced European Movable Deformable Barrier model

The movable deformable barrier consists of two parts: a trolley and an impactor. The impactor consists of six single blocks of aluminium honeycomb, which have been processed in order to give a progressively increasing level of force with increasing deflection. An additional single element is attached of 60mm depth to the front of the lower row of blocks. Front and rear aluminium plates are attached to the aluminium honeycomb blocks [11] [12].

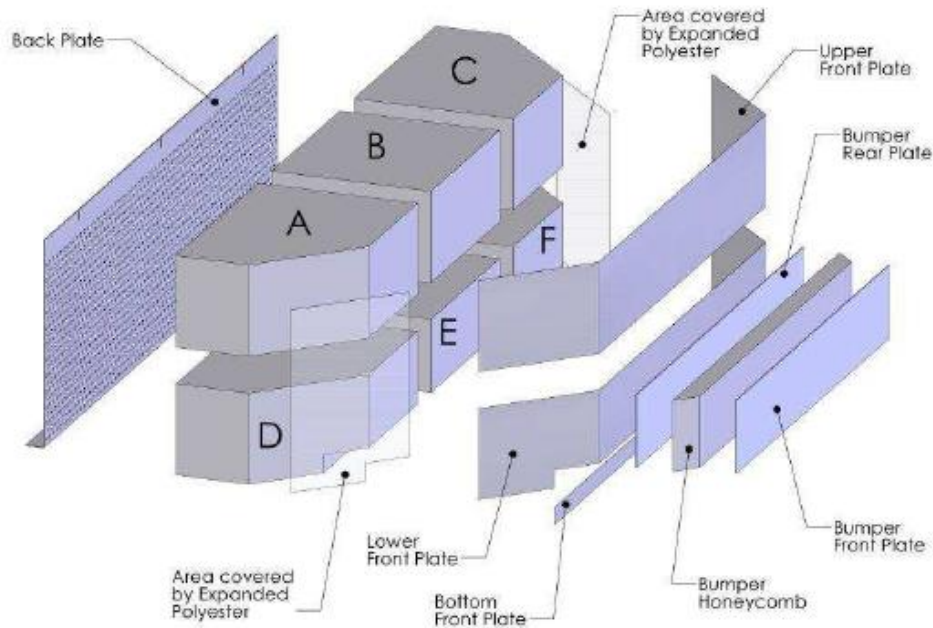


Figure 2-1 - AE-MDB impactor detail

In this thesis a FE model of the AE-MDB is provided. The mobile deformable barrier has been developed by Livermore Software Technology Corporation (LSTC). The model is based on the Advanced European Movable Deformable Barrier Version 1.0 specification, released on 26th February, 2013. The MDB is made mainly by shell elements and recreate the real behaviour.

Some validations have to be made to ensure the validity of the model. In particular it was simulated a front impact against a rigid wall at 35Km/h in order to verify that the force-displacement graph fit with one provided by LSTC.

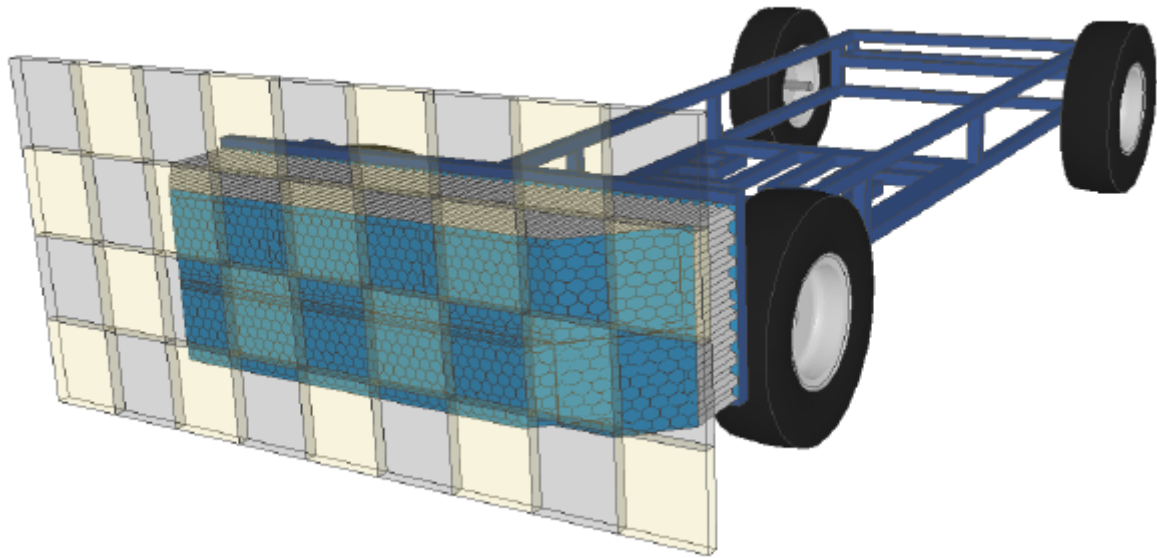


Figure 2-2 - AE-MDB wall impact validation

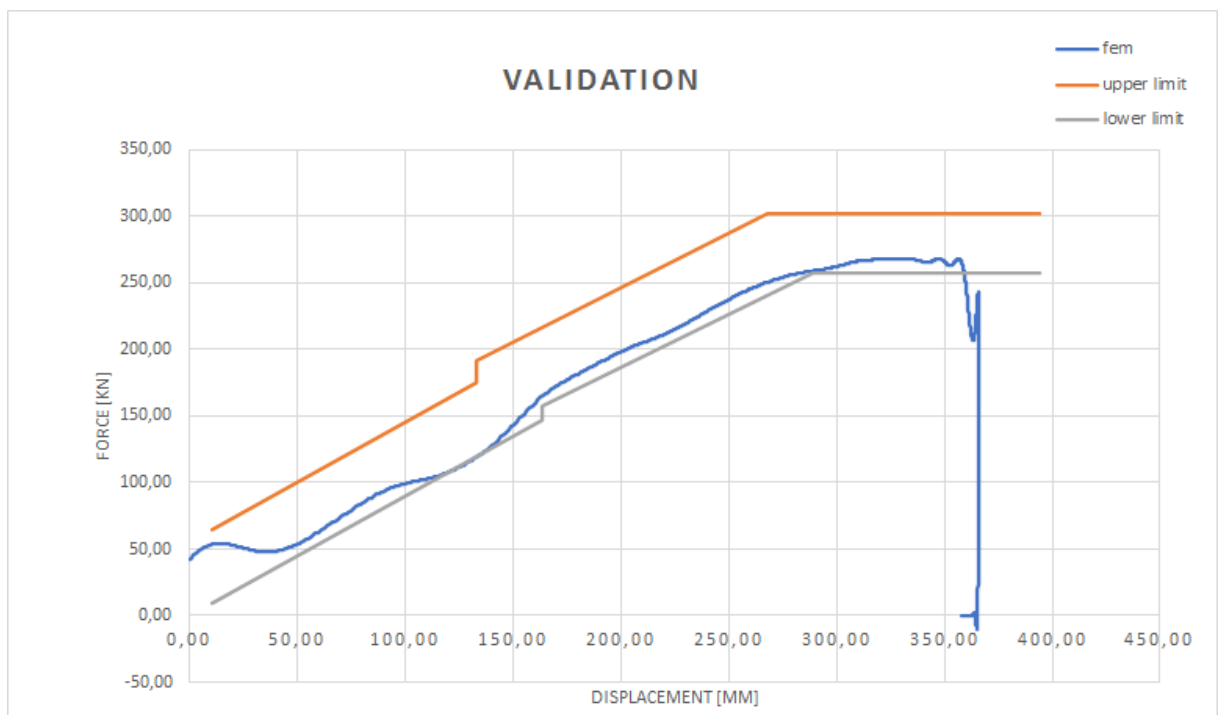


Figure 2-3 - AE-MDB wall impact validation results

As can be seen from the diagram on figure 2.3 the validation of the model results sufficient because the blue curve that shows the results of the simulation is between the given limits.

The model provided by LSTC is set for the validation so it include a *ae-mdb_version_R1.0_wall.k* and a *ae-mdb_version_R1.0_floor.k*, they has to be deleted from the *ae-mdb_version_R1.0_main.k* file.

Through the keyword **RIGIDWALL_PLANAR_FINITE* will be created a new floor in the main file for all the model used, this procedure will be described in the next chapter.

The MDB model is ready for the simulation.

2.3 2012 Toyota Camry model

This model is computer representation of a 2012 Toyota Camry mid-size passenger sedan for use in crash simulations. It was developed through a reverse engineering process by Center for Collision Safety and Analysis (CCSA) researchers under a contract with the Federal Highway Administration [13] [14].



Figure 2-4 - Real vehicle and FE model of a 2012 Toyota Camry Sedan

The reverse engineering process systematically disassembled the vehicle part by part as in past efforts.



Figure 2-5 - Details of the model of the vehicle structure

Each part was catalogued, scanned to define its geometry, measured for thicknesses, and classified by material type. All data was entered into a computer file and then each part was meshed to create a computer representation for finite element modelling that reflected all of the structural and mechanical features in digital form. Material data for the major structural components was obtained from manufacturer specifications or determined through coupon testing from samples taken from

vehicle parts. The material information provided appropriate stress and strain values for the analysis of crush behaviour or failures in crash simulation.

The model was validated against several full-scale crash tests, include the side impact crash test but following the American side impact NCAP standard (SINCAP), different from the Euro NCAP for the velocity and the direction of impact of the mobile deformable barrier. In the figure below the comparison between the real crash and the simulate one.

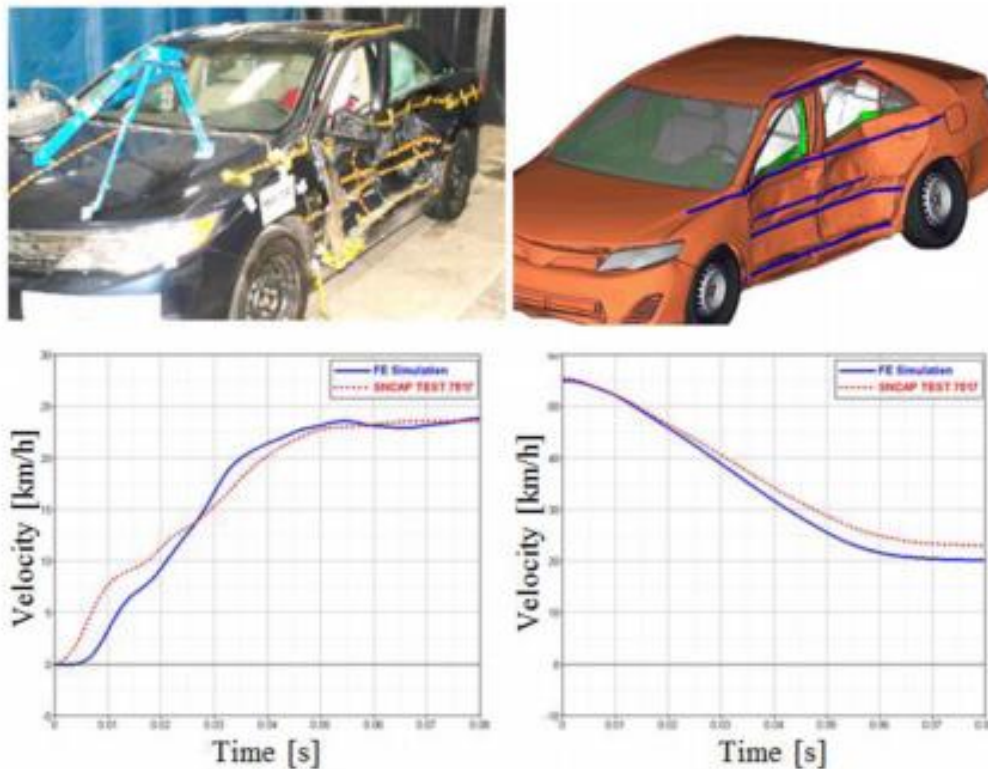


Figure 2-6 - Comparison between real and simulate SINCAP test

Reasonable correlations were obtained as it can be seen from the graph with a CORA rating of 0.92 for the vehicle velocity time history and 0.87 for the barrier kinematics. A side impact test with the same velocity and direction of impact of the Euro NCAP was also accomplished but no technical time history data was accessible from the conducted test [15].

The resulting Finite Element vehicle model has 2.25 million elements. It includes details of the structural, drivetrain, as well as the interior components allowing for integration of occupant (dummy) models in the simulations.

The model was provided set for a NHTSA NCAP frontal full-width crash test, which mean a frontal impact against a rigid wall at 35 mph (56.327 Km/h). Due to this reason a few changes have to be made.

- On the model the keyword `*INITIAL_VELOCITY` has to be deleted because in the Euro NCAP the impacted vehicle is firm.
- The unit of measure has to be change in according to the HBM model and the trolley so the unit of measure were changed from mm/ton/s to mm/kg/ms.
- We need to include the car model in the main file created before through the keyword `*INCLUDE`.

The car is ready to be set for the simulation.

2.4 Human Body model

2.4.1 Introduction

The Human Body Model (HBM) [16] is a Finite Element (FE) model of a human body created to replicate its biomechanics response of several cases. For the creation of the model a comparison between cadavers and FE model in many types of impact has been made in order to obtain a precise simulation of the real behaviour. The complexity and the fidelity of the model allow engineering to overcome the limitations of a common dummy and simulate more realistic and complicate scenarios that otherwise would be difficult or impossible to analyse. Using an HBM every human movement can be reach and it can be positioned in impossible ways compared to a dummy. This allowed to use this kind of models to study the behaviour of the body in a lot of fields, from sport to aerospace. The implementation of more precise and specific sensors allows a more accurate analysis of the response and the development of new injuries criteria like the Peak Virtual Power method (PVP) [17].

In this thesis an HBM model called THUMS, developed by Toyota Motor Corporation and Toyota Central R&D Labs., Inc., is provided. The acronym THUMS stands for To-tal Hu-man Mod-el for Safe-ty and was the first virtual human body software when it launched in 2000. Several versions were provided during the years and from January 2021 the last version is freely available.

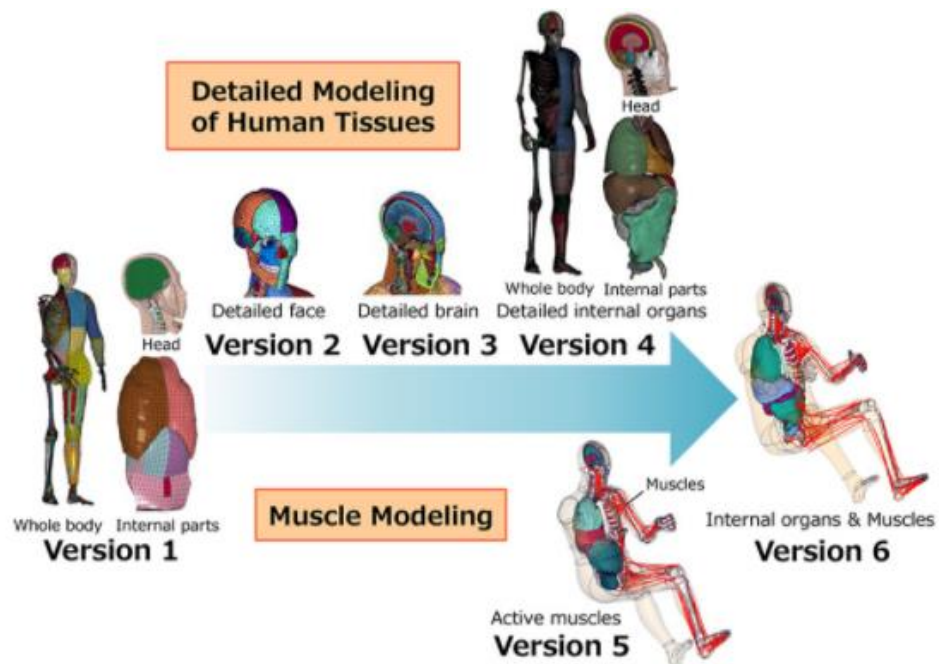


Figure 2-7 - THUMS evolution

For the side impact simulation, a size an adult male (AM50%ile) with a height of 175cm and a weight of 77 kg is provided. The models include detailed head (face, skull, brain, and spinal cord), the skeleton, internal organs (heart, stomach, liver, etc.), and air cavities (including the lung). The model provided was obtained through a high-resolution CT scanning process in order to digitize the interior of the body and to generate precise geometrical data for each model part. The HBM recreate the anatomical features of each organ, tissue, and bones in a human body, associating the proper material properties to each body part as reported in literature. Therefore, the model can simulate brain and internal organ injury at a tissue level, as well as skeletal fractures and ligamentum injuries. The complexity of the THUMS is such as to be able to simulate the involuntary muscular movements of the human body. The model contains approximately 760,000 nodes and 1.9 million elements.

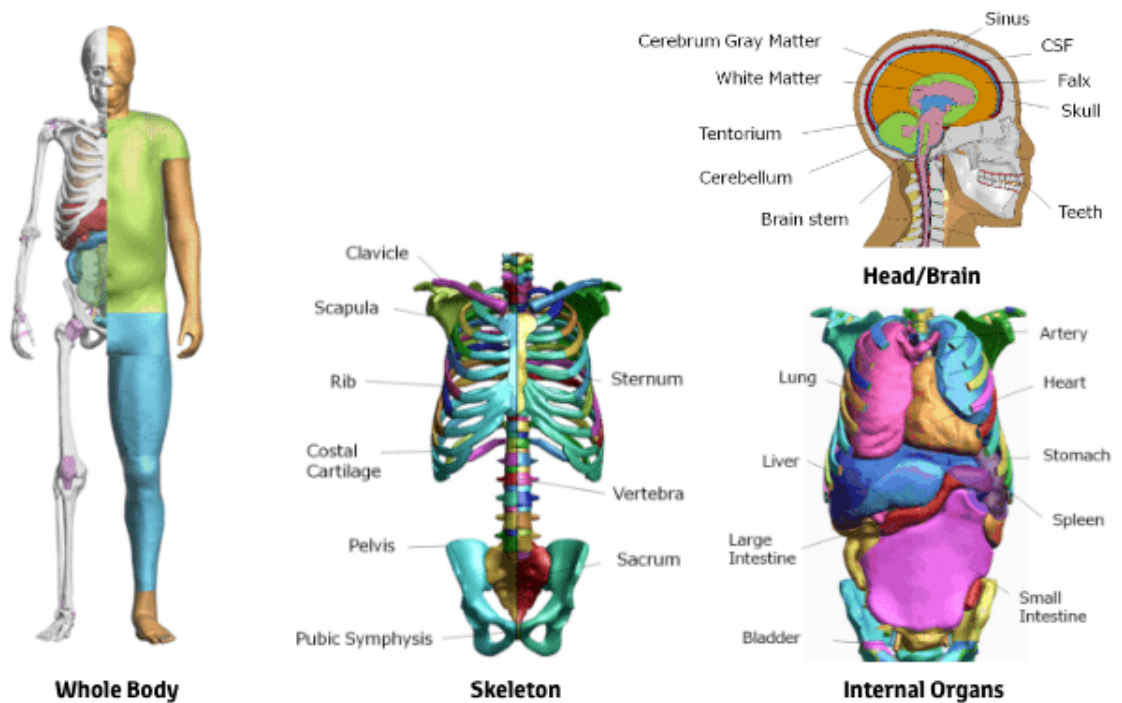


Figure 2-8 - Details of the THUMS

The model is provided in a standard position configuration as it can be seen from the figure 2.9.

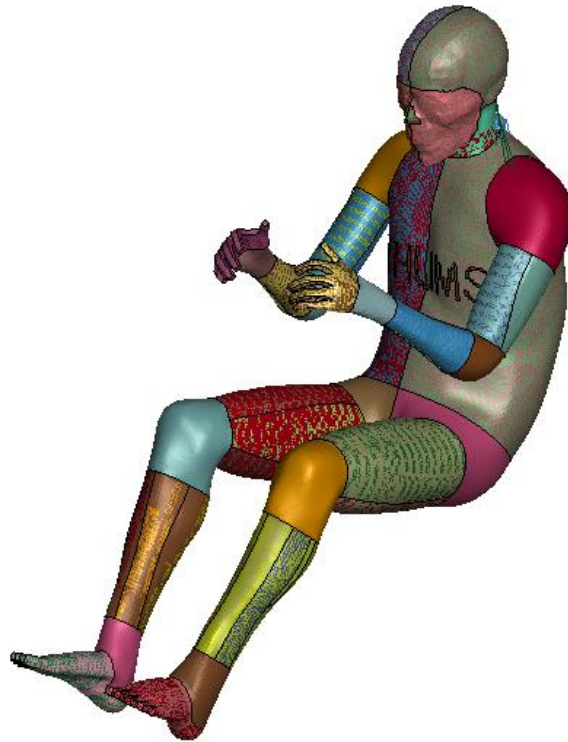


Figure 2-9 - THUMS in standard position

The model requires a set and simulation positioning through the PIPER software. The procedure will be explained in the next chapter in the details.

Chapter 3: Pre-simulation process

3.1 Setting crash simulation

3.1.1 Introduction

The aim of a FE simulation is to simulate in the best possible way the reality of the crash test, to do this is important following the standard and rules set by Euro NCAP in the setting of the simulation environment. The critical points that require particular attention are:

- the definition of the trolley's position and velocity
- the definition of the contacts
- the definition of the controls

3.1.2 Description of the simulation settings

As said before, this type of crash is not regulated by Euro NCAP because this test is not carried out. However, in order to set the simulation, parameters that are as similar as possible to the standards were used.

The trolley is aligned to the front axle and strikes perpendicularly to the left side of the car, as you can see in the figure 3.1. This position of the moving deformable barrier was decided in such a way that it could be easily replicated later with other tests with different cars. This choice makes it possible to differentiate from the standard side crash test and see a different behaviour of the vehicle after the impact. The correct position of the barrier is reached in LS-PP translating and rotating the MDB with the option *Transform* in *EleTol*.

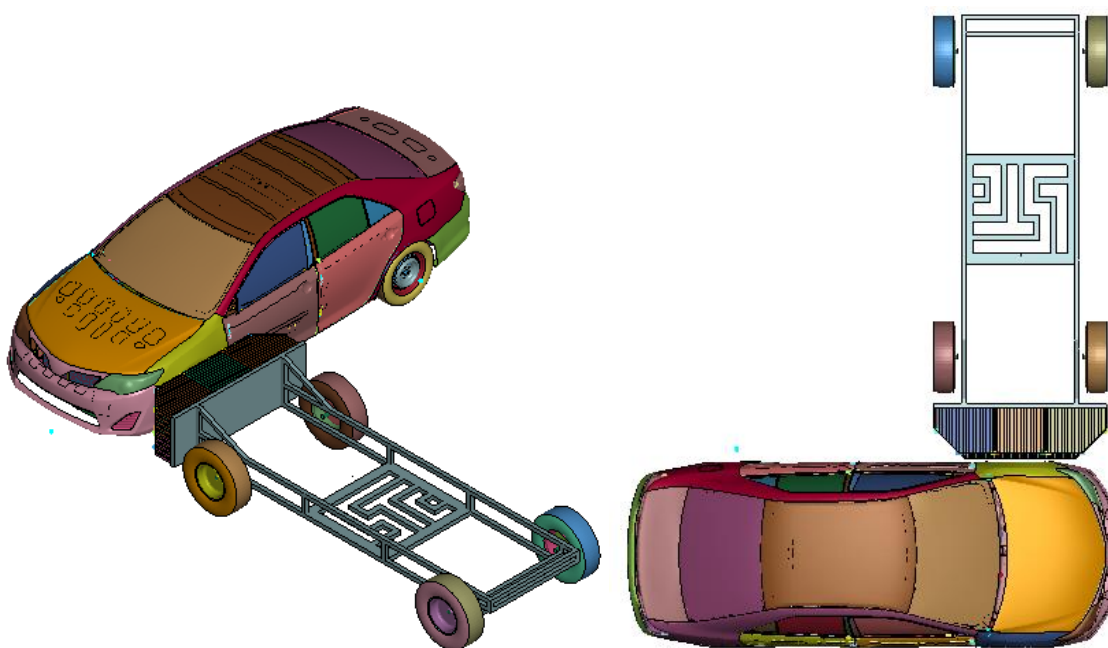


Figure 3-1 – Position of the MDB and the car

Following the required standards, the car is stationary while it is the moving deformable barrier that impacts it with a fixed speed. The barrier's speed is 50 km/h. After some tests on LS-PP, it was decided to set the initial velocity of the barrier by means of a set of nodes that includes the whole deformable barrier. It is important to be consistent with the units of measurement.

The simulation contains many contact definitions because it is complex and there are different aspect and different parts to consider, nevertheless some of them are already defined in the initial FE model of the vehicle and the MDB. The contact between the deformable barrier and the vehicle must be defined, to do this the keyword `*CONTACT_AUTOMATIC_SURFACE_TO_SURFACE` is recommended by LS-DYNA. Two sets of segments for the definition of the contact have been created, one of the car and the other on the barrier. On LS-PP, in the keyword's card, the segment set of the car is defined as slave and that of the barrier as master. This choice was made after some tests to improve the behaviour during the impact.

It is now necessary to create a floor that will recreate the interaction between the wheels and the ground, to do this the keyword `*RIGIDWALL_PLANAR_FINITE` is used. A high friction coefficient of 0.9 has been chosen to simulate the optimal situation of tire grip. For the planar dimension it's required to consider also the possible translation of the vehicle after the impact. The floor created on LS-PP is visible in the figure 3.2.

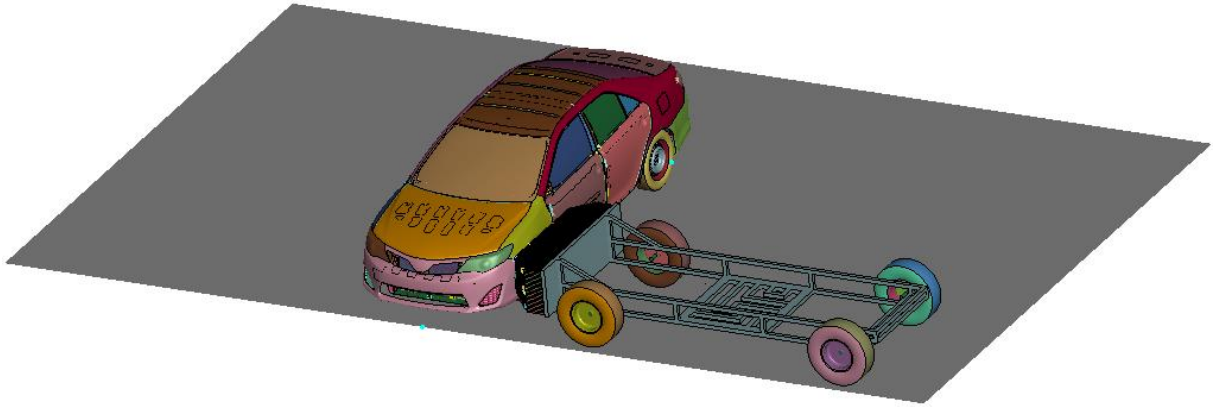


Figure 3-2 - Floor

Another important aspect that needs to be set in order to create the simulation in the correct way are the controls. Controls have been added to improve some feature of the simulation. It has been added the *CONTROL_ENERGY in order to visualize the trend of the hourglass energy and to understand from these data if the simulation results are acceptable. To have more accurate simulations it has been added also the *CONTROL_CONTACT card that has been used to specify some parameter as the initial penetration and the contacts between rigid bodies, this control card allows to improve the definitions of contact given previously. It is necessary at this point to fix the duration of the simulation, it has been seen from other works focused always on the crash test simulations that the peak of acceleration on the driver is always previous 100ms. This term of duration is therefore fixed through the *CONTROL_TERMINATION card. The full set of controls useful to have accurate results is listed:

- *CONTROL_ACCURACY
- *CONTROL_BULK_VISCOSITY
- *CONTROL_CONTACT
- *CONTROL_CPU
- *CONTROL_ENERGY
- *CONTROL_HOURLASS
- *CONTROL_OUTPUT
- *CONTROL_SHELL
- *CONTROL_SOLID
- *CONTROL_SOLUTION
- *CONTROL_TERMINATION
- *CONTROL_TIMESTEP

3.2 Sitting simulation

3.2.1 Introduction

When an occupant sits inside a vehicle, the seat deforms in its soft part like the cushion due to the weight of the person. In order to represent in the best of the ways the reality it is necessary therefore to carry out a sitting simulation. What is obtained at the end of the simulation is a deformed seat under the static load of the HBM will be later included in the model previously described of the car. This practice allows not to have penetrations and a better behaviour between the body and the seat.

3.2.2 Description of the process

This simulation requires the following models to be run:

- HBM model:
because of the high computational cost due to the great detail of the HBM, simplification can be made to the model. It can be assumed with a very good approximation that the deformation of the HBM is practically negligible in this type of simulation. Therefore, starting from the original model of the HBM, the parts corresponding to the skin are selected and exported with their section and material properties. Once a new subsystem has been created, *MAT_RIGID is assigned to each part, thus creating a model containing only rigid skin. In the following figure 3.3 you can see the HBM model before and after this operation.

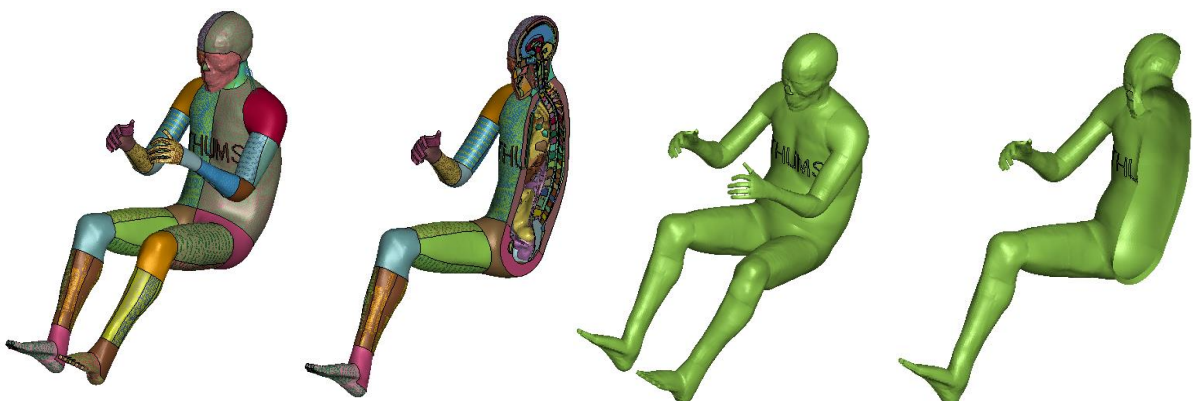


Figure 3-3 - Comparison between full THUMS model and rigid skin model

- Driver's seat:
the FE model of the undeformed driver seat is exported from the FE car model, creating a new subsystem.



Figure 3-4 – Driver's seat model

In order to carry out this simulation, the seat has to be fixed in the space, so rotational and translational degrees of freedom are locked by the command `*BOUNDARY_SPC_SET`. In particular, these constraints are applied to the seat fastening points as shown in the figure 3.5.

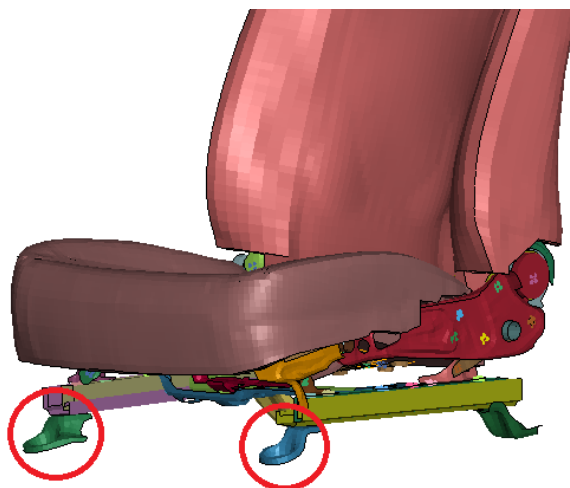


Figure 3-5 – Details of the constraint

The movement of the HBM is given by the keyword `*BOUNDARY_PRESCRIBED_MOTION_RIGID` with a fixed displacement of 50 mm in x positive direction and 80 mm in z negative direction as in the practice in automotive companies so as to deform the seat cushions.

The keyword `*CONTACT_AUTOMATIC_SURFACE_TO_SURFACE` is the one suggested to define the contact between the skin and the seat with a friction coefficient of 0.6.

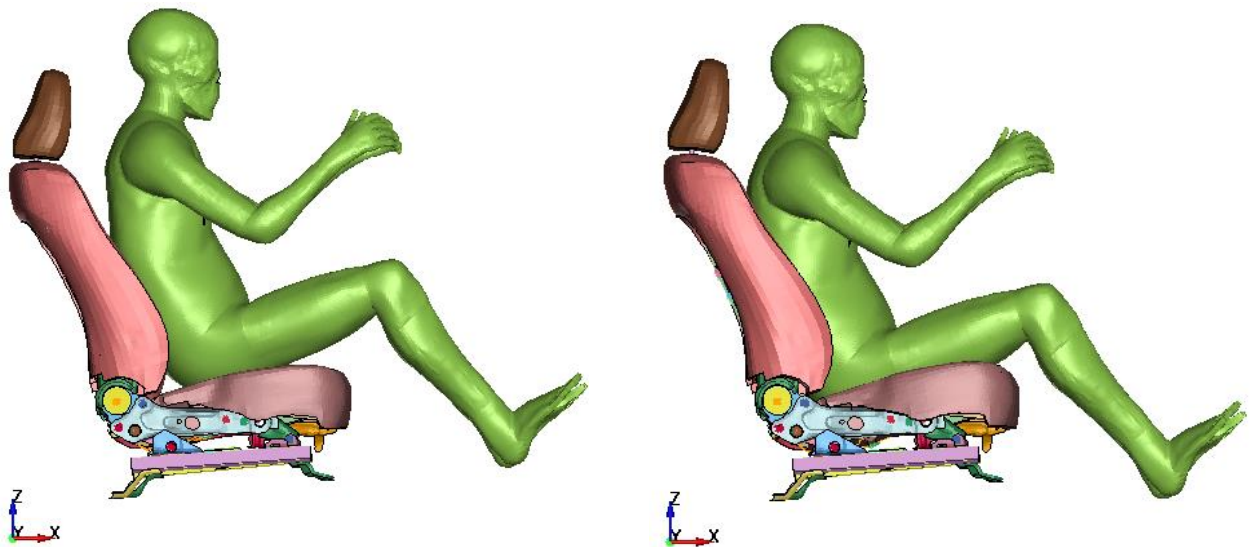


Figure 3-6 – Sitting simulation: first and last step of simulation

At the end of the simulation, a deformed driver's seat is exported and the model is included in the FE car model.

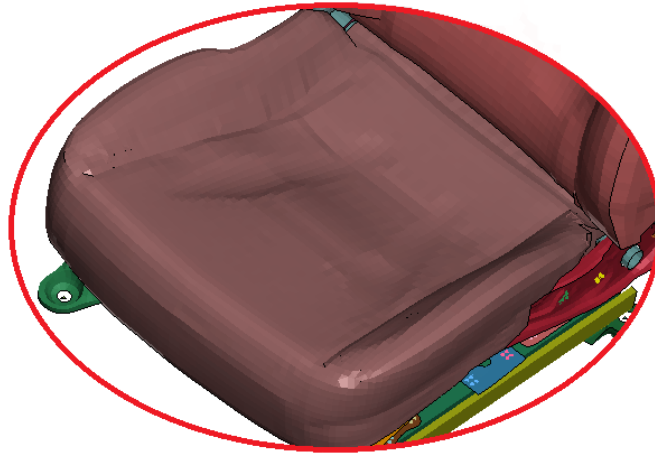


Figure 3-7 – Detail of the deformed seat cushion

3.3 THUMS positioning

3.3.1 Introduction

In this section the positioning procedure will be explained.

The positioning of the THUMS was made in order to respect the standard procedure of a Euro NCAP side impact procedure described in the 1.1.2 chapter. For the positioning process two software were used, PIPER software and LS-DYNA. The PIPER software can be used to help to position the Human Body Models for impact. It has been tested with several models during the development phase (including some from the GHBMC and THUMS families). The route to follow for positioning is as follows:

1. Positioning of the THUMS through the PIPER software functionality
2. Creation of a script for the positioning simulation on LS-DYNA
3. Simulation with LS-DYNA

3.3.2 Positioning through PIPER software

The first step is to create and include a simplify environment model of the inside of the vehicle focusing on the driving position and with the introduction of the deformed seat previously created.

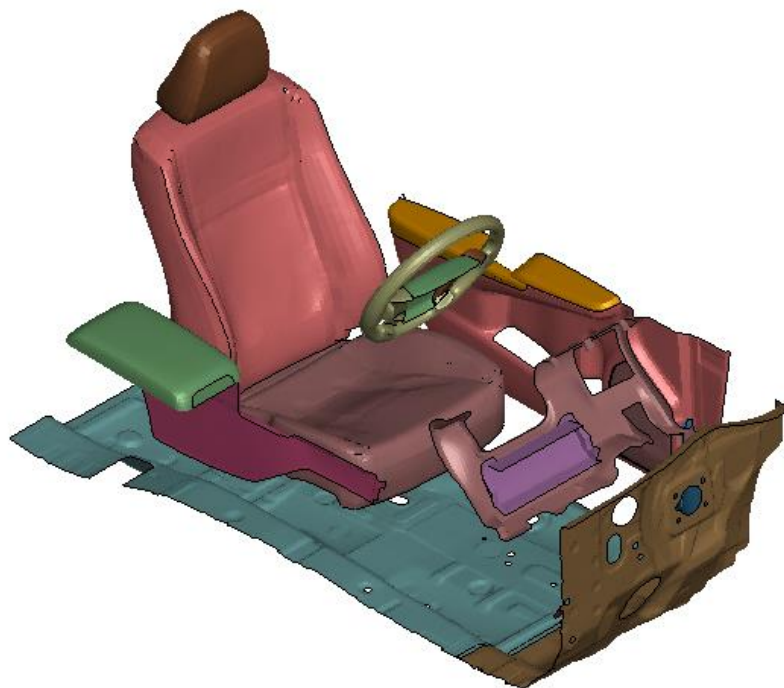


Figure 3-8 – PIPER environment model

This model will help the user in the positioning of the HBM. The environment created is show in the figure 3.8.

The environment model is imported in the PIPER graphical user interface and the THUMS must be fitted in it respecting the Euro NCAP standard. The result should be as in the figure 3.9.

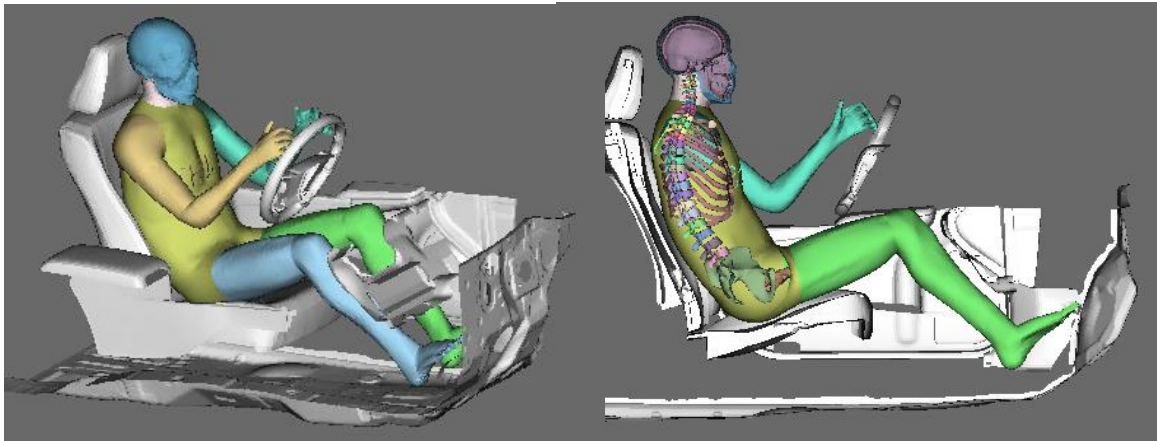


Figure 3-9 - Environment positioning, isometric and section plane view

The positioning of the THUMS was made mainly using 2 features of PIPER, the *landmark* positioning, and the *joint* positioning.

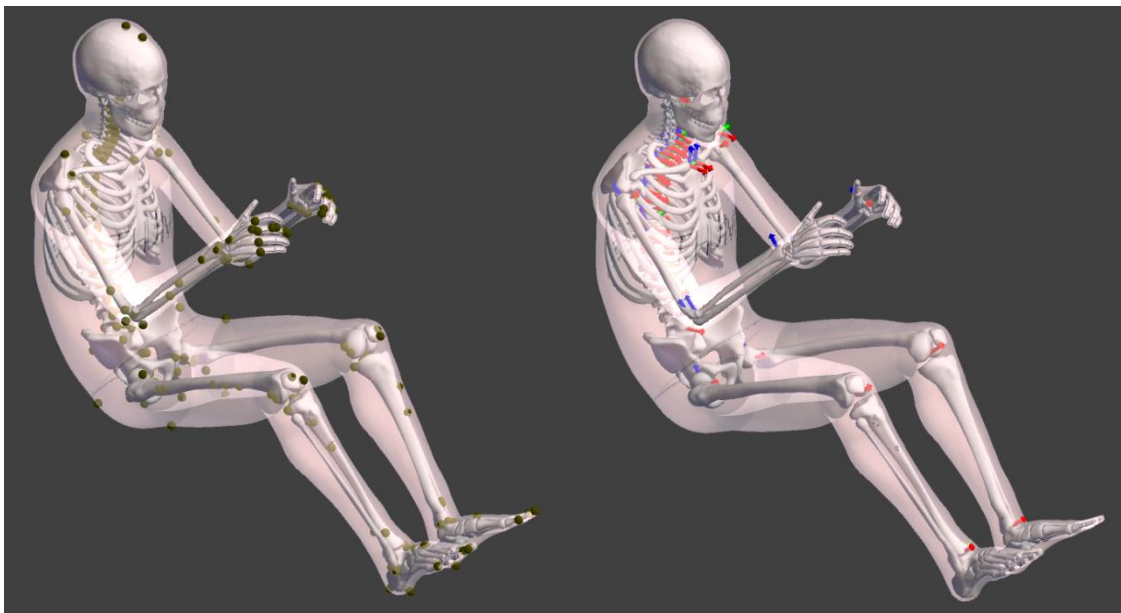


Figure 3-10 - Landmark and joint visualization on PIPER

The model has in fact several landmarks in order to identify the critical points for the positioning and joint to ensure the rotation of the parts up to their functional biological limit.

After the rotation of a joint or the movement of a landmark the *control* feature must be run in order to simulate the movement. In this phase the entire model will adapt to the single movement. A particular care has to be made on the control, check the *auto stop* mode and uncheck the *collision* mode. The first stops the positioning when the landmark goal is reach (otherwise the script is continuing write), the second one is useless because eventual penetration verification are not needed because the final simulation will be performed with another software.

The feature *fixed bones* were used to fix some portions of the body during the positioning of every main region of the body. This was done to not influence the complete positioning of some parts with the general movement of the model due to a single movement.



Figure 3-11 - Fixed bones example for higher limb positioning

The procedure started with the positioning of the lower limb and then moving to the higher limb. After iterative steps, the correct position of the model was reach following the Euro NCAP standard.

To be able to use the model, however, a simulation of the positioning must be made with a FE solver. A script file must be made in order to set the FE simulation. This is provided through the *scripting* feature, where, after saving the history of the positioning through the *update* function a few files for the simulation are obtained:

- *CURVE.k*
- *ele_beam.k*
- *main.k*
- *motion.k*
- *nodeset_PIPER.k*
- *noeuds_extr_beam.k*

Including on the *main.k* file the main file of the THUMS the simulation can be run. The results after having run LS-DYNA are the following.

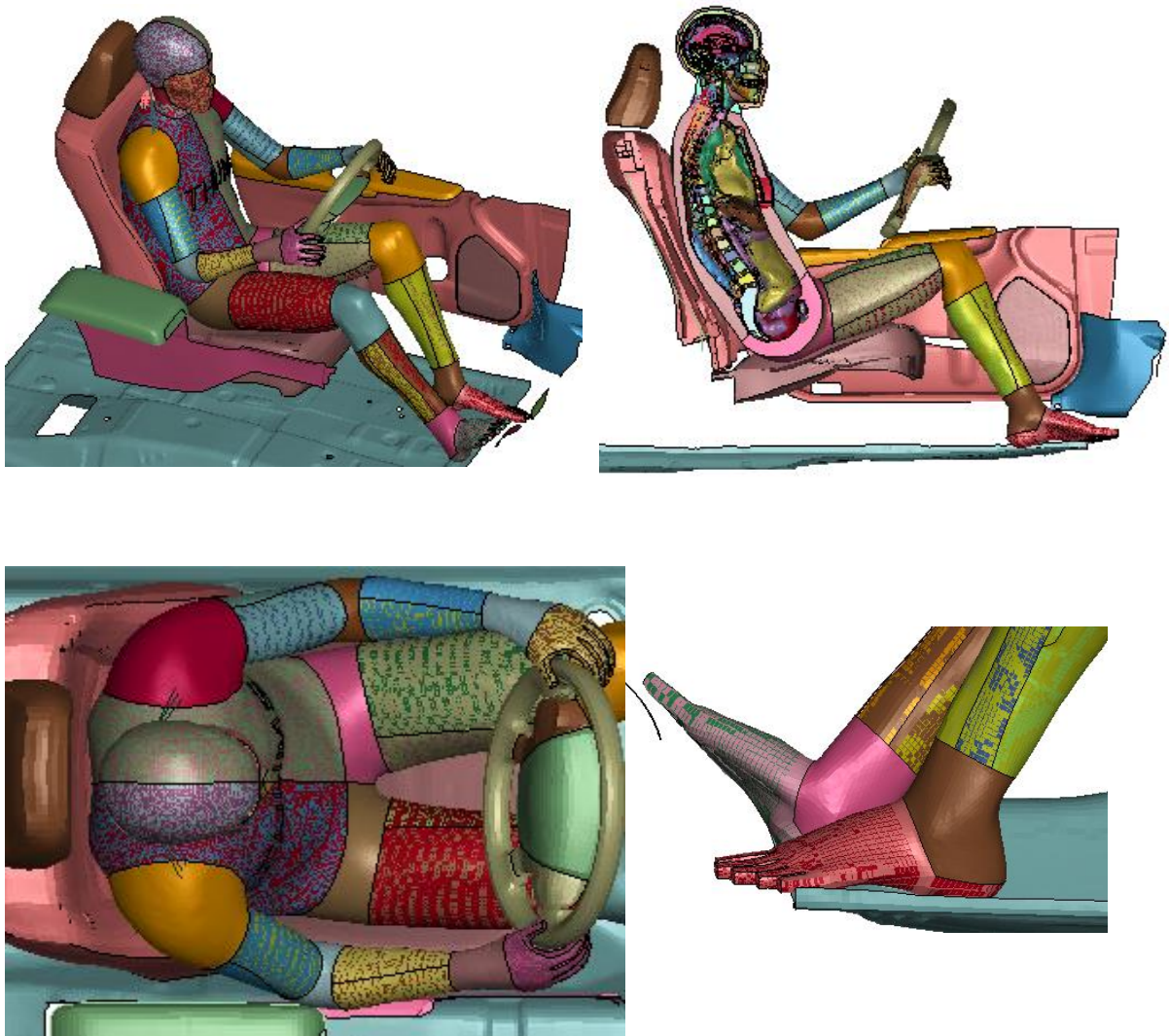


Figure 3-12 - In the figures in the top the isometric and the section view of final position, in the figures in the bottom some details of the hands and the feet positioned

As can be seen from the figure the positioned THUMS respect the requirement of the Euro NCAP dummy positioning described in the chapter 1.1.2.

The model of the THUMS was then included in model of the car and accurately located. To ensure proper interaction between the dummy and the vehicle interior, new contact definitions must be defined. A `*PART_SET` of the driver's seat was created and a keyword `*CONTACT_AUTOMATIC_SURFACE_TO_SURFACE` was added on the model. In the same way the contacts between the THUMS and the parts around it, which the dummy might hit during the impact, such as steering wheel and the dashboard, are defined.

3.4 Seatbelt modelling

3.4.1 Introduction

One component that has not yet been addressed is the seatbelt. These are explicitly required by the Euro NCAP protocol in which it is stated that the driver is secured on his/her seat during the crash test. This component is not present in the initial FE vehicle model, so it must be created. To do this, the HBM must first be placed in the correct position inside the car. The whole routine to create the seatbelts is done on LS-PP [18] [19].

3.4.2 Seatbelt routine

The belt chosen for the simulation is a three-point-seatbelt composed by:

- B-pillar belt
- Shoulder belt
- Lap belt

A simple example of a three point seatbelt is shown in figure 3.13.

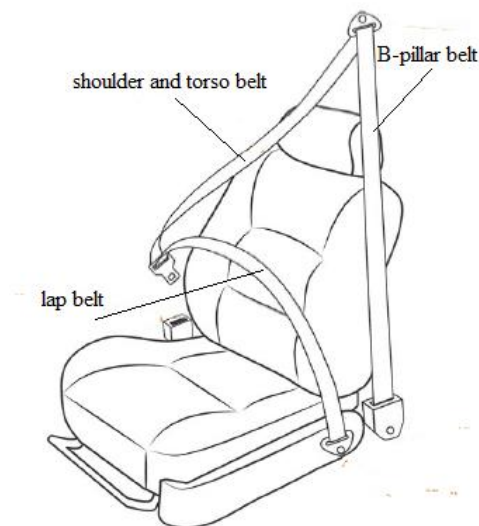


Figure 3-13 - Three point seatbelt example

Each one of these belts is created independently, so in the end the whole will be made up of different parts. The belt can be shaped in different ways depending on where they are located and

on their function. The first belt to be created is the B-pillar belt, this is modelled as a segment belt, i.e. with 1D elements, it can be done this way because this belt does not interact with the dummy and therefore reduces the computational weight. The other two belts are instead modelled with a mixed structure, in which there are 2D elements that allow a more realistic interaction with the body of the occupant. In order to create the seatbelt some FE models are necessary:

- The driver's seat previously deformed
- THUMS positioned
- The vehicle structure used by the belt as anchors

The anchors are those parts of the vehicle to which belts pass or are connected and they are:

- D-rings
- The point in which the belt is fixed to the frame
- The point in which the belt comes out from the retractor

The exported parts useful for the belt definition are shown in the figure 3.14.

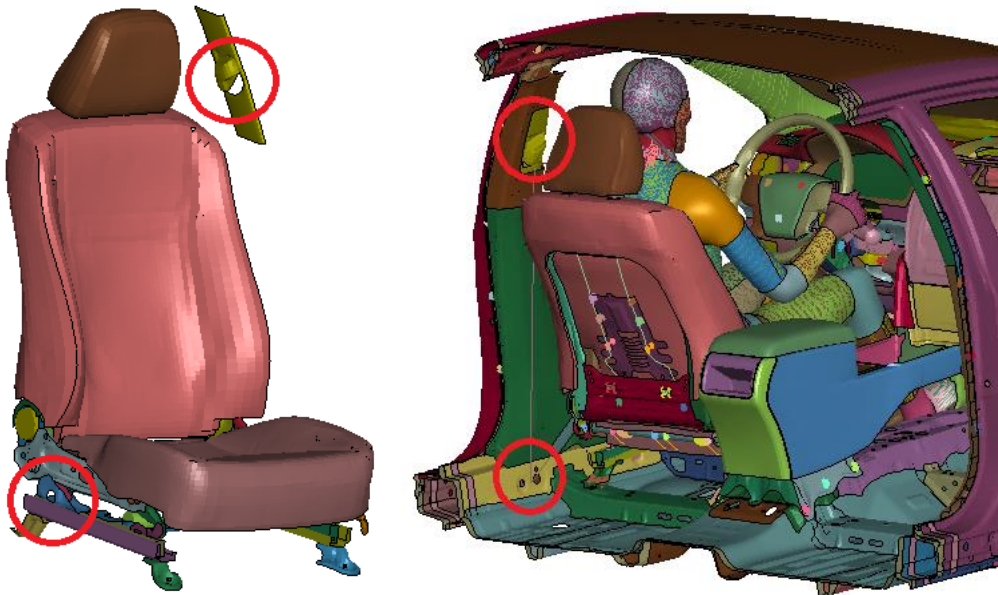


Figure 3-14 – Anchors in the FE vehicle model

There is a routine for creating belts on LS-PP. Through the *Occupant Safety* and using the *Seatbelt Fitting* command these can be modelled. To be able to do this, it is necessary to create sets of segments on the parts of the THUMS involved in each belt in order to wrap them precisely around the body.

Once the segment sets have been created, a set of points must be specified for each belt to create it. It is very important that the end and the start points of two consecutive belts are the same to

ensure that they work. The result of this process is visible in figure 3.15. The interface that opens with the command *Seatbelt Fitting* can be used to define a number of parameters such as the number of elements in the belt or its width. A triangular mesh has been used by default on LS-PP as can be seen in figure 3.15.

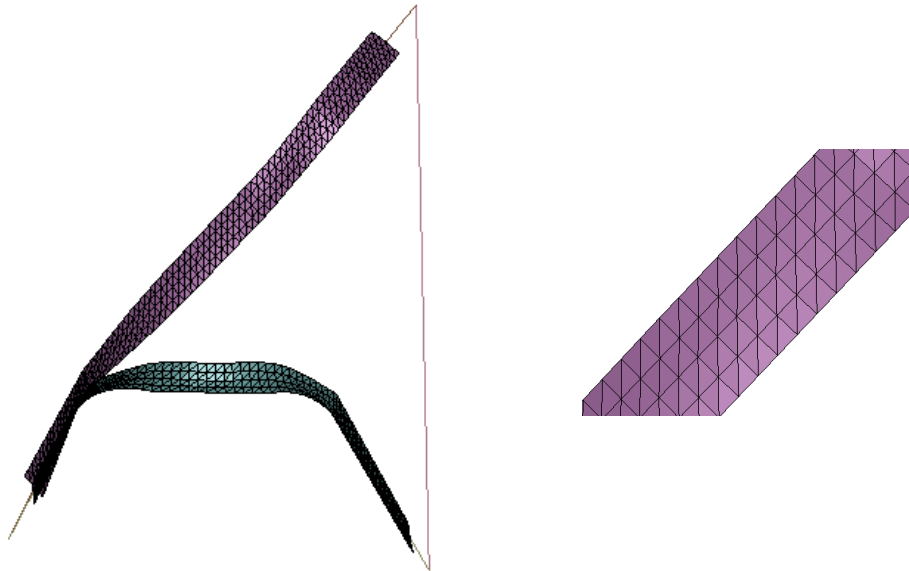


Figure 3-15 – Seatbelt and detail of the mesh of the belt

After this routine has been carried out, the material and section property must be assigned to the belts [20], these are assigned manually. After the belts have been created, it is necessary to define some elements that are present in the real vehicle but absent in the FEM one:

- Retractor
- D rings
- Pretensioner
- Sensor

Since these elements were not present in the model, they were placed by observing the inside of the real car with photos.

3.4.3 Retractor

The device of the retractor applies a counteracting torque with the help of a spring to the spooling of the seatbelt. This ensures continuous tension on the belt and avoids any possible slack. When the vehicle is involved in an accident, a locking mechanism is triggered either by the deceleration of the car or the seatbelt movement. When the retractor is “locked-up”, some amount of belt can still be spooled out according to a force-deflection curve visible in figure 3.16.

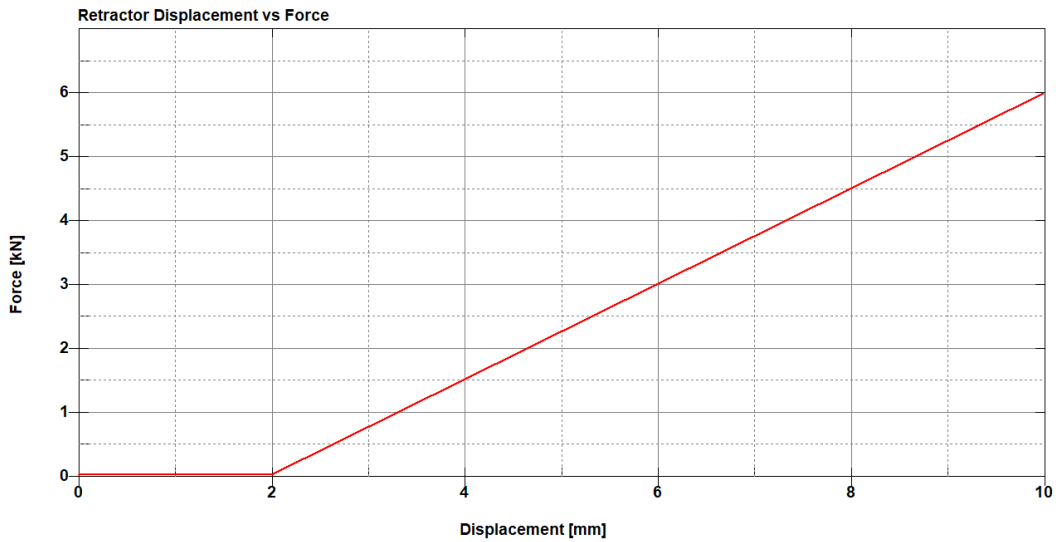


Figure 3-16 - Retractor displacement vs force

This element is placed in the lower part of the B-pillar, this element is created with the keyword *ELEMENT_SEATBELT_RETRACTOR, in this card it is necessary defining the retractor node: a node in which the element is located. It is important that the node coincides with the one chosen for the creation of the belt. A parameter that can be set is the time delay, which is set to zero as a first approximation and indicates the time that elapses between the activation of the sensor and that of the retractor. The position of the retractor is visible in figure 3.17.

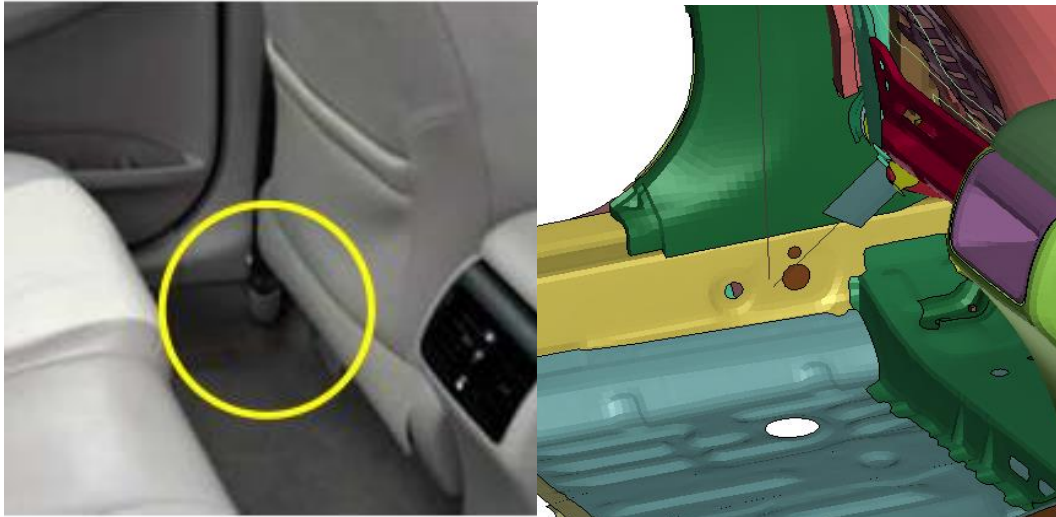


Figure 3-17 – Comparison between real and FE position on the retractor

3.4.4 D-rings

The seatbelt models, previously described, define the three sections of the entire belt, but to reproduce the seatbelt loop, it is required that these segments behave as a single component. The d-rings allow the belt to slide, they are defined with the keyword `*ELEMENT_SEATBELT_SLIPRING`. This keyword represents the seatbelt loop in these locations and in the LS-DYNA code, it allows for the elements in proximity of the anchor to pass through the loop and continue their movement. In this card you have to define a node (the slipping node) on the fixed structure and two seatbelt elements that have that node coincident. One D-ring is present at the top of the B-pillar and the second one in the buckle area. For the second, an existing rigid part of the seat was chosen. The comparison between the real and the simulated D-ring is shown in Figure 3.18.



Figure 3-18 – Comparison between the real FE position of the D-ring

3.4.5 Pretensioner

The pretensioner has the role of tighten the belt in case of an event of crash in order to move the occupant in a more optimal crash position. This element is created with the keyword `*ELEMENT_SEATBELT_PRETENSIONER`, type 5, the *pyrotechnic retractor*, was chosen. A delay time of zero is set as a first approximation, It represents the time interval from sensor activation to pretensioner activation. The card required a definition of the pull in vs time curve, this is shown in figure 3.19, it has a rapid response to approximate the pyrotechnic behaviour.

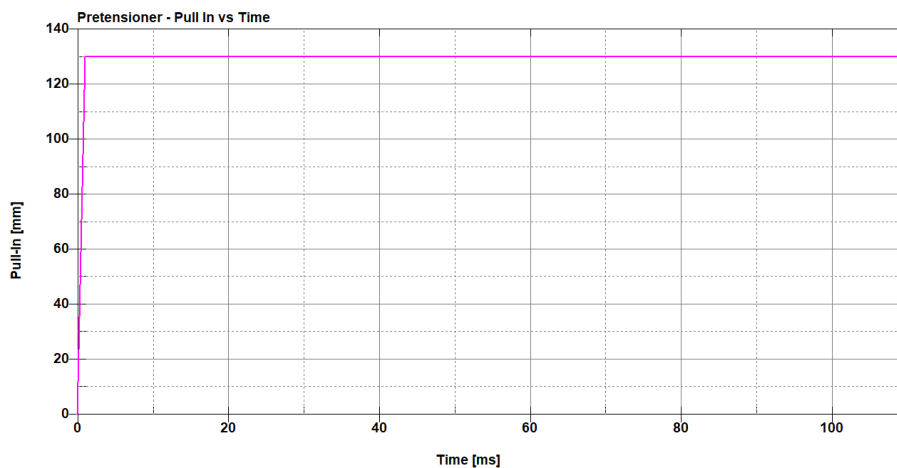


Figure 3-19 - Pretensioner pull in vs time

3.4.6 Sensors

Both the retractor and the pretensioner need a sensor to start working. The sensors are created with the keyword *ELEMENT_SEATBELT_SENSOR, different strategies can be used as triggers. In the case of the retractor a time delay of 1ms for the sensor to send the signal has been chosen. This value range for the pretensioner is instead between 10ms and 30ms but specific values are not available from automotive companies, because of this, following LSTC guidelines it has been chosen a value of 13ms.

The figure 3.20 shows the final result after all the above operations have been carried out.



Figure 3-20 - THUMS positioned with the seatbelt model

3.5 Set-up of the sensor

In order to obtain biomechanical results from the performed crash test simulation, it is necessary to include in the THUMS model a series of sensors that are required by the above-mentioned protocol. In fact, the THUMS developed by Toyota Motors Corporation, actually, does not have a pre-installed set of sensors as reported [21] “users need to specify the entities for output such as nodes, elements, materials and cross section, in order to output data such as acceleration, velocity, displacements, forces, stress, strain and energy”.

In this work, an existing example of sensors system, made for previous activities by Germanetti [22] [23] has been used. Some modifications have been implemented in order to better comply with the Euro NCAP requirements for the dummy outputs. The additional components are needed to register the loading during the side impact in specific areas such as: shoulder, upper neck, lower neck, pelvis and lower limbs. In Figure 3.21, the complete set of accelerometers and load sensors is shown.

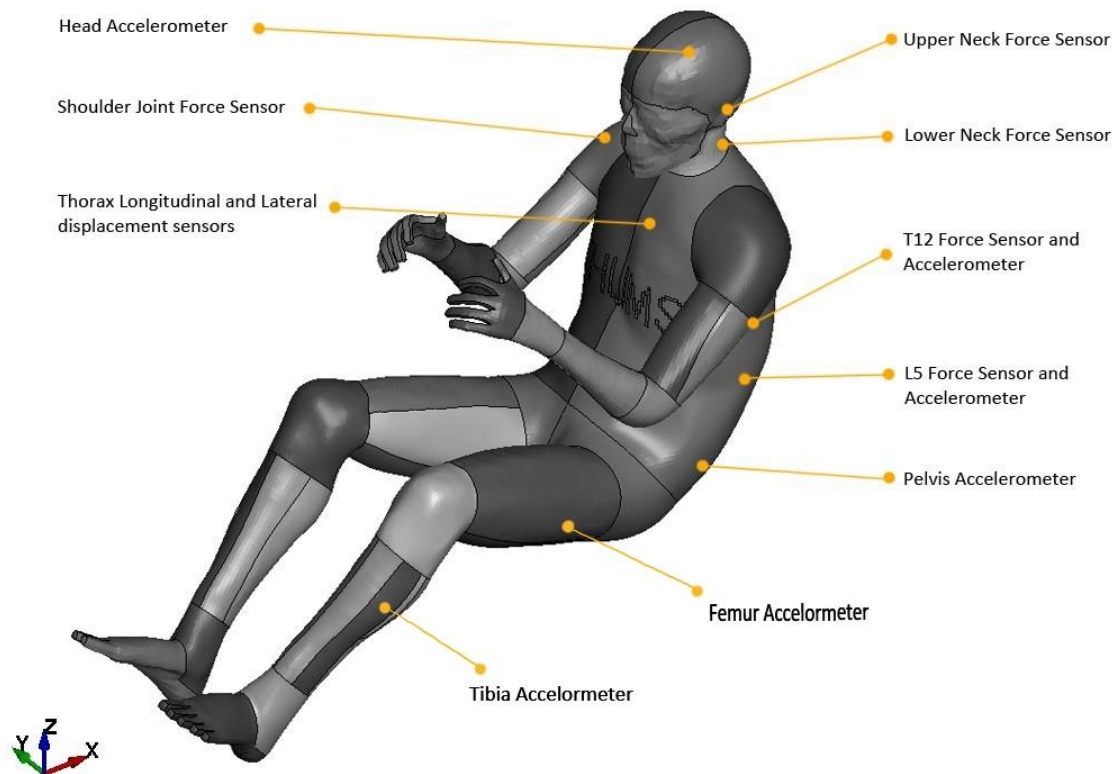


Figure 3-21 - Set of sensors

3.5.1 Head sensor

The model is equipped with a sensor able to record the head accelerations in the three degrees of freedom in space. For a proper implementation inside the THUMS, a small part of the brain visible in Figure 3.22, the *third ventricle left*, has been converted to rigid and an accelerometer has been connected to this. This process is necessary since the implementation of such sensor in LS-DYNA through the keyword `*ELEMENT_SEATBELT_ACCELEROMETER`, requires a rigid element to which being attached. However, in the conversion, the thickness and density properties of the components of interest are not changed. Doing so does not change the total weight of the HBM and the minimum necessary variations are applied on the overall model. This method provides a more stable and cleaner accelerometer signal than other solutions.

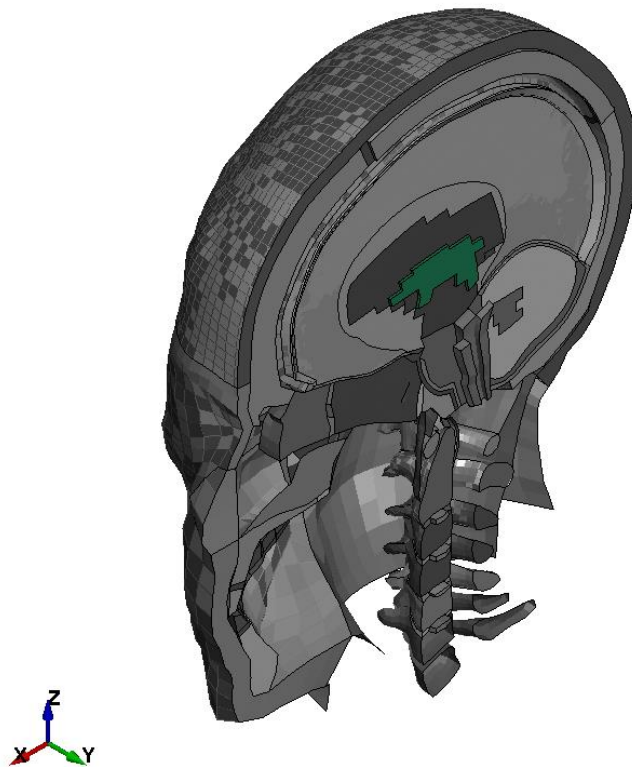


Figure 3-22 – Head accelerometer

3.5.2 Neck sensors

It is important to specifically evaluate the behaviour of the neck, even if the Euro NCAP protocol does not prescribe its control, because this area of the body is subjected to high loads during a side impact. Two different sections are monitored: the upper neck and the lower neck and the same strategies for implementing the sensors are adopted in both areas. Load sensors are modelled by using the keywords `*DATABASE_CROSS_SECTION_SET` in order to define load cells being on the C1 vertebrae and the C7 vertebrae, and `*DATABASE_CROSS_SECTION_PLANE` for defining planes crossing the upper area of the neck and the lower area of the neck as it is visible in Figure 3.23. It is important to remind that the planes defined previously are referred to specific parts, i.e., head, C1 vertebrae and C7 vertebrae. These sensors record both the loads transmitted through the neck and the moment to which it is subject.

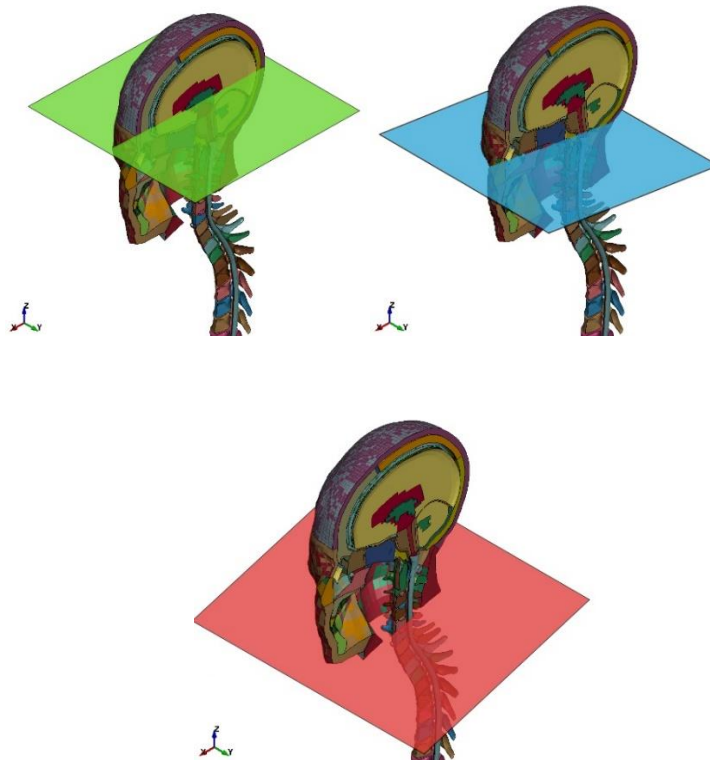


Figure 3-23 – Cross_section_planes: head (green), upper neck (blue), lower neck (red)

3.5.3 Thorax and pelvis sensors

Multiple sensors are positioned in the thorax for describing the upper part of the body. Two accelerometers are positioned in vertebrae T12 and L5 defined similarly to the one present in the head: the vertebrae are converted to rigid and the sensor is defined on these nodes. On those same vertebrae load sensors are also modelled. 1D discrete elements have been connected in the lateral direction between shoulder ribs, upper thorax ribs, middle thorax ribs, lower thorax ribs, upper and lower abdominal ribs in the lateral direction. These elements are useful to measure the displacement and rotation. Additionally, a load sensor is also positioned at the meeting point of the iliac crests in the Symphysis for measuring the lateral forces transmitted by the pelvis. Figure 3.24 shows their disposition and anchorage points on the THUMS.

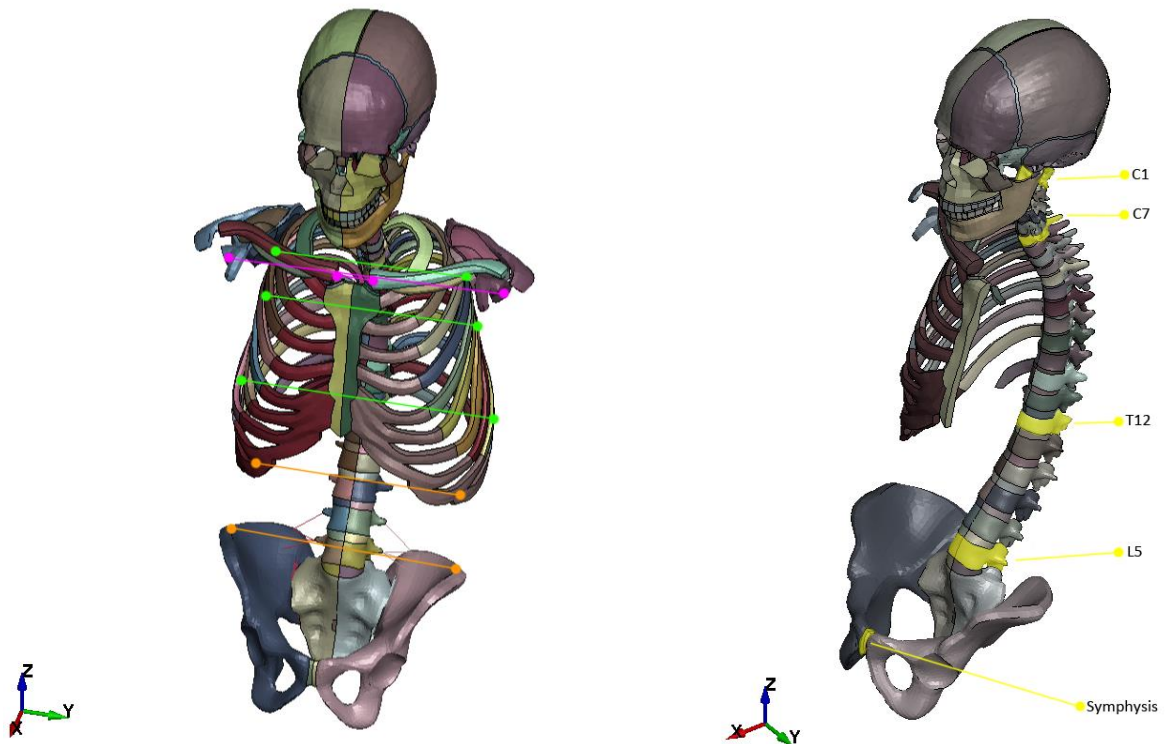


Figure 3-24 – Thorax and pelvic sensors

3.5.4 Rib cage sensor

Despite not being required by the Euro NCAP protocol, it is possible in order to analyse in detail the deformation of the thorax and of the spine, to position markers on ribs and vertebrae so that it is possible to visualize instant by instant the deformation of the thorax circumference or the spine alignment. *DATABASE_HISTORY_NODES_ID cards are used to define these markers set and they monitor:

- Cervical Vertebrae
- Thorax Vertebrae
- Lumbar Vertebrae
- Chest Ribs: 4 chest bands have been defined at different height, as can be seen in figure 3.25.

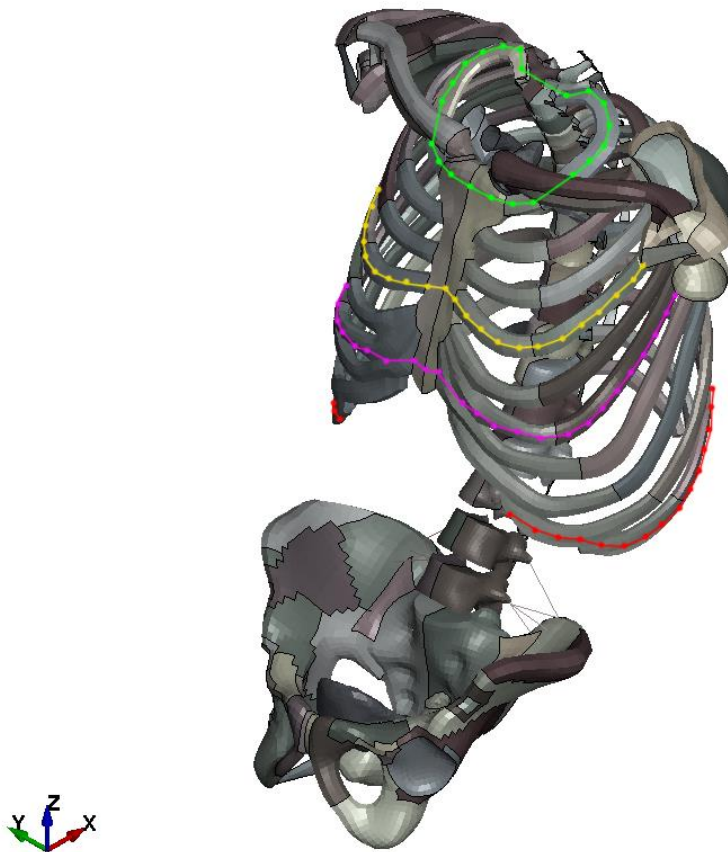


Figure 3-25 - Rib cage sensors

3.5.5 Internal organs volume sensor

The high detail provided by the THUMS model, instead of the rigid dummies, allows to further analyse the possible injuries occurring to the human body model during an accident beyond what prescribed the Euro NCAP protocol since by nature, it has been designed to regulate the use of a real dummy, the WorldSID to be more specific. Specific sensors have been modelled for analysing the behaviour of the internal organ by using *AIRBAG_SIMPLE_PRESSURE_VOLUME keywords. These LS-DYNA cards are able to provide data on the change in volume of a closed surface and its normalized surface variation. In this work the organs groups taken into consideration for further analysis are:

- Ribcage: Enclosed surface of Pleura and Diaphragm
- Right Lung: Enclosed surface of Right Pleura Visceralis (green)
- Left Lung: Enclosed surface of Left Pleura Visceralis (orange)
- Heart: Enclosed surface of Pericardium
- Pancreas: Enclosed surface of Pancreas
- Spleen: Enclosed surface of Spleen
- Liver: Enclosed surface of Liver
- Stomach: Enclosed surface of Stomach (red)
- Small Intestine: Enclosed surface of Small Intestine (yellow)
- Large Intestine: Enclosed surface of Large Intestine (purple)
- Abdomen: Enclosed surface of Peritoneum and Diaphragm

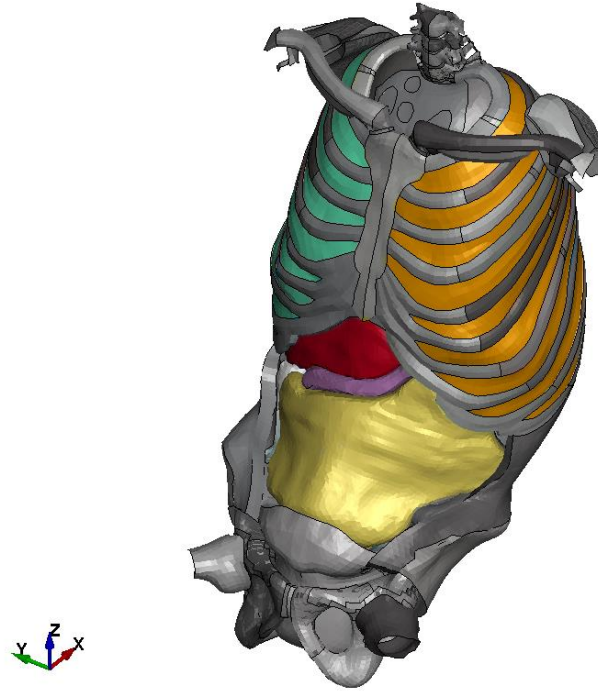


Figure 3-26 – Internal organs

3.5.6 Lower limbs

Following the protocol, data from the lower limbs must be analysed. In order to obtain these results, some *CROSS_SECTION_PLANE were inserted on both right and left femur and tibia as was done previously on the neck. To obtain the accelerations, *SEATBELT_ACCELEROMETER on rigid cubes, already implemented in previous work [22], are used. They are shown in figure 3.27.

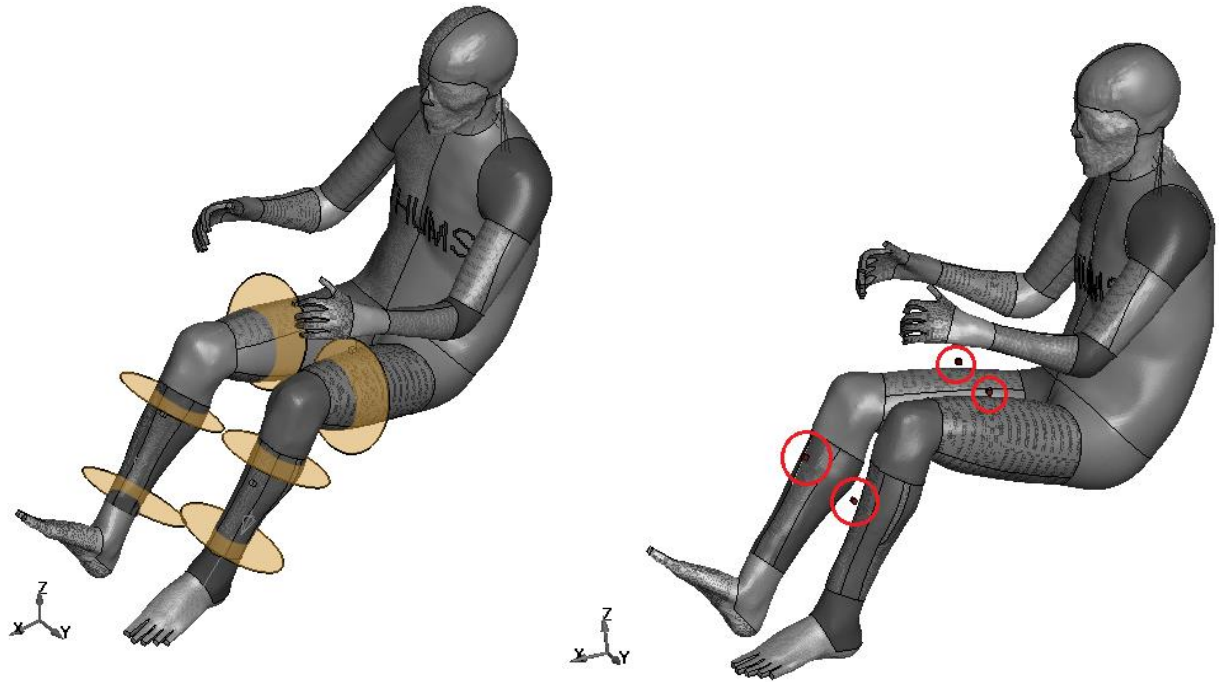


Figure 3-27 – Lower limbs sensors: cross_section_planes (left), accelerometer (right)

Chapter 4: Results

4.1 Overview

Once all steps have been done and the model is complete, the impact simulation can be launched. This is launched through the HPC project of Politecnico di Torino, a powerful tool furnished by the Politecnico that correspond in calculation resources and technical support for academic and didactic research activities using centre systems. The main two cluster used in this work of thesis are the Legion and Hactar cluster. The simulation required 31 hours to be completed with 64 cores on 2 nodes. The memory used is around 25 Gb. In figures 4.1-4.6 isometric views of the impact are shown and in figures 4.7-4.13 front view of the impact in section are presented.

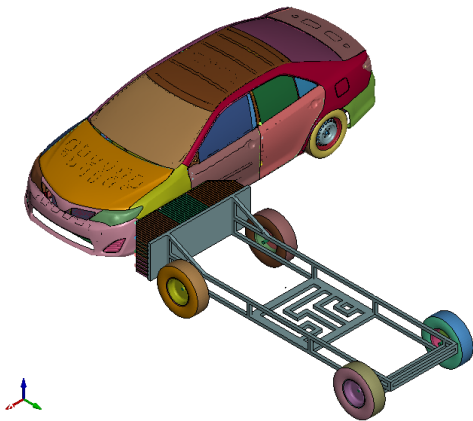


Figure 4-1 - Isometric view of the impact at $t=0ms$

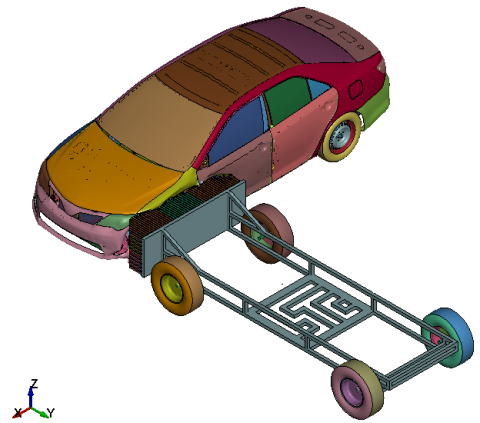


Figure 4-2 - Isometric view of the impact at $t=20ms$

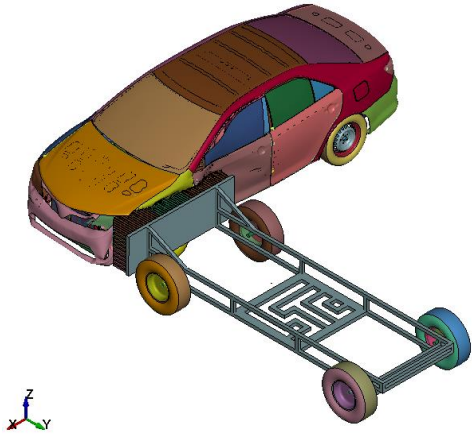


Figure 4-3 - Isometric view of the impact at $t=40ms$

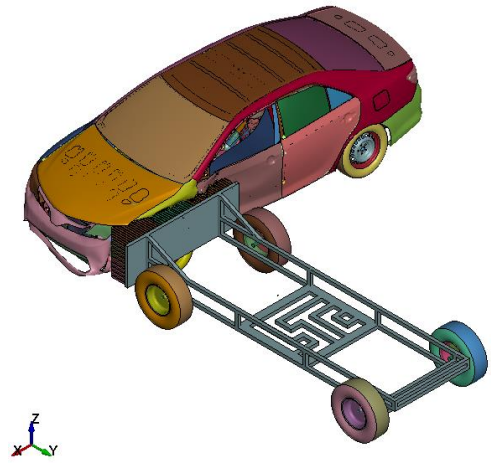


Figure 4-4 - Isometric view of the impact at $t=60ms$

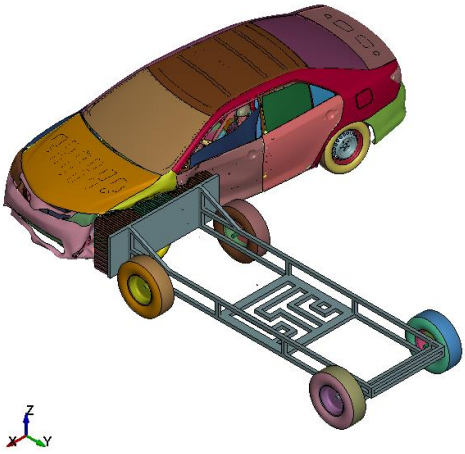


Figure 4-5 - Isometric view of the impact at $t=80ms$

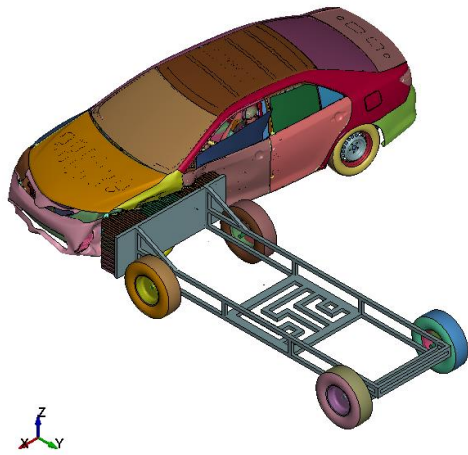


Figure 4-6 - Isometric view of the impact at $t=90ms$



Figure 4-7 - Front view of the impact at t=0ms



Figure 4-8 - Front view of the impact at t=15ms



Figure 4-9 - Front view of the impact at t=30ms



Figure 4-10 - Front view of the impact at t=45ms



Figure 4-11 - Front view of the impact at t=60ms



Figure 4-12 - Front view of the impact at t=75ms

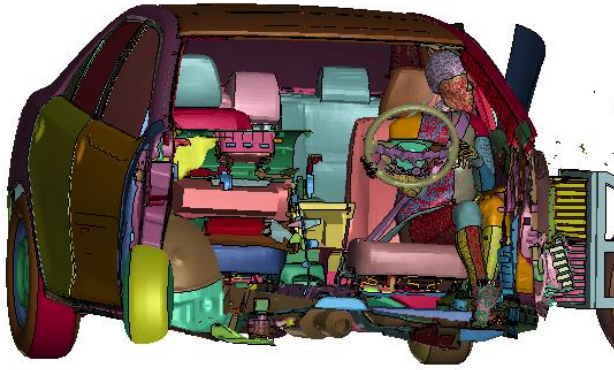


Figure 4-13 - Front view of the impact at $t=90ms$

In the following the results of the simulation will be presented, in particular:

- Energy analysis
- Car and trolley sensor analysis
- THUMS sensor analysis
- Injury criteria

4.2 Energy balance

The energy balance takes into account different energy components such as:

- Total energy
- Kinetic energy
- Internal energy
- External energy
- Sliding interface energy
- Hourglass energy

The energy balance is a good indicator of a success of the simulation without numerical errors. Unexpected trends are symptoms of possible problems or errors. Energies are plot in figure 4.14.

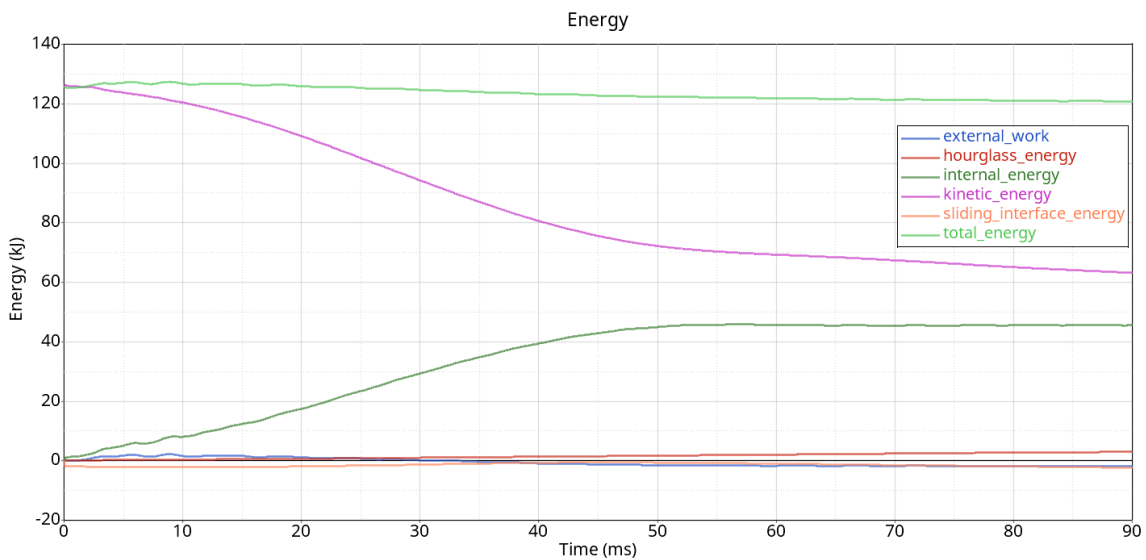


Figure 4-14 - Energy Balance

A slight variation in total energy of about 5% can be seen, but it remains within acceptable limits, which is probably due to small errors in the contacts. The trends of the kinetic and internal energy are correct. The hourglass energy, a value that is correlated to the zero energy mode of deformation that produce zero strain and no stress, is under the 10% of the total energy as indicated by the LS-Dyna guidelines. An important parameter to be checked is the energy ratio, define as:

$$e_{ratio} = \frac{E_{tot}}{E_{tot}^{\circ} + W_{ext}}$$

In which:

E_{tot} = total energy

E_{tot}° = initial total energy

W_{ext} = external work

This should be close to the unit value to get a good simulation. It is shown in the figure 4.15.

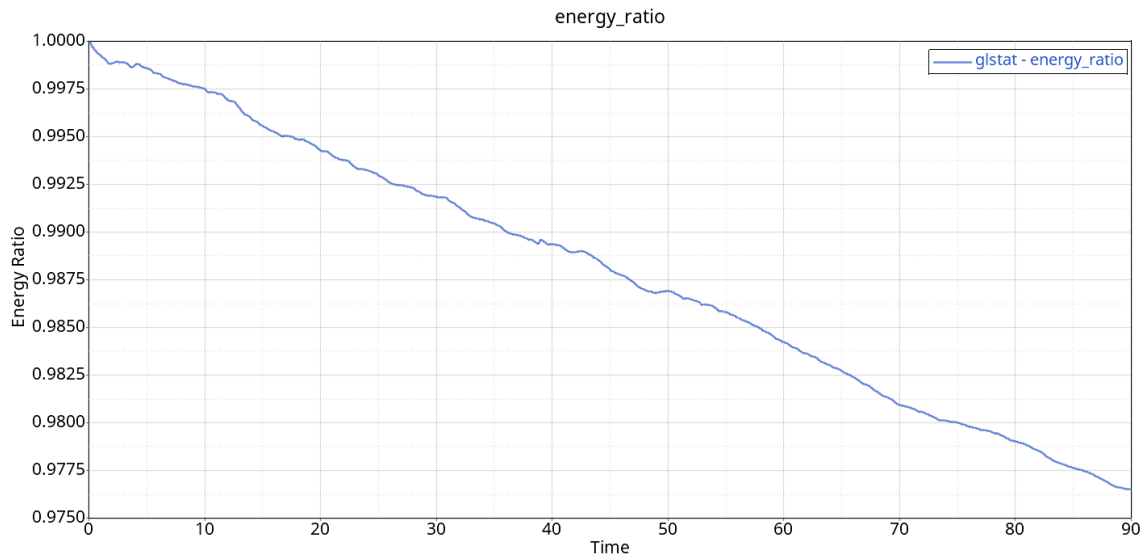


Figure 4-15 - Energy Ratio

It can be seen that the variation of the energy ratio is about 2.5% that is within an acceptable range of error.

4.3 Car and trolley sensor analysis

The figure 4.16 shows the velocity curves of the AE-MDB and of the Toyota Camry obtained from accelerometers, one placed on the MDB carriage and one on the vehicle chassis.

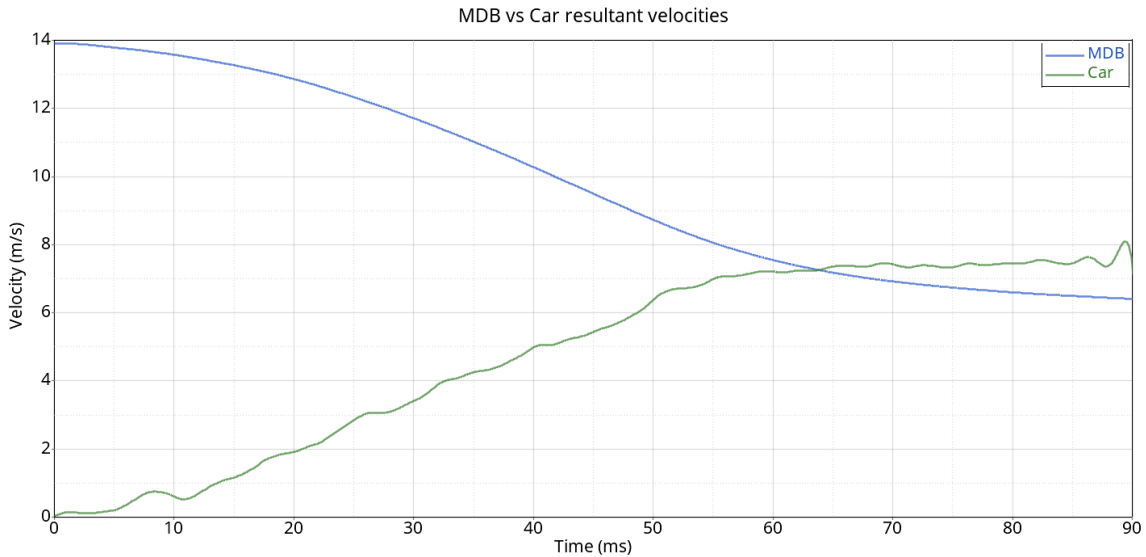


Figure 4-16 - Comparison of velocities

As can be seen from the graph, the deformable barrier starts at a speed of 13.9 m/s or 50 km/h, as indicated by the Euro NCAP normative. The speed then decreases immediately after impact with the stationary car just as we would expect. The vehicle instead has an opposite behavior as it starts from a standstill but after the impact it gains speed. From the simulation it can be seen that the vehicle undergoes a rotation around the vertical axis.

4.4 THUMS sensor analysis

In this chapter, the biomechanical results of the accelerometers installed on the THUMS and described in the previous chapter will be analysed. The results were all filtered with SAE 180 filter.

4.4.1 THUMS – Head

Head acceleration is an important parameter to investigate because it is closely related to the severity of the accident. As the head is the most delicate part of the body, it is important to check these results. According to Euro NCAP normative, accelerations along the three axes are plotted in figure 4.17.

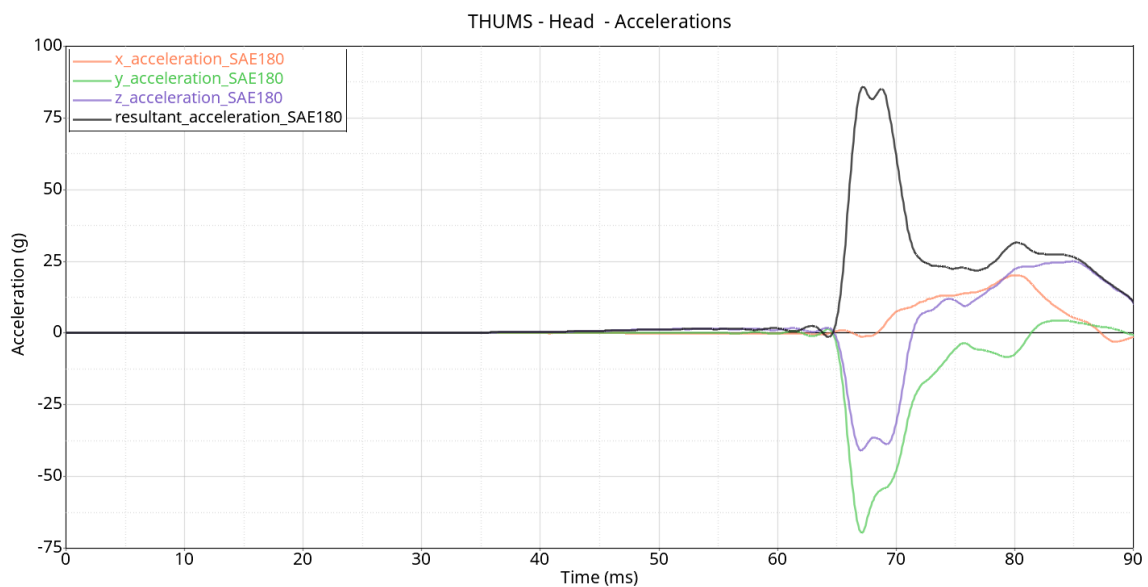


Figure 4-17 - Head Accelerations

As can be seen from the figure 4.17 the head undergoes a high acceleration especially in y direction that is the direction of the impact. The head has a peak of acceleration of 88g.

4.4.2 Head Injury Criteria (HIC)

The Head Injury Criteria (HIC) is then calculated as previously described in chapter 1.2.2. The window taken into account is of 36 ms as suggested by Euro NCAP normative. The HIC_{36} calculated in this simulation is 220 in the range of time between 66ms and 70ms, as visible in figure 4.18. In order to correlate the value of HIC with the possibility of injury of the driver, the set of curves developed by Prasad and Mertz in figure 4.7 are used.

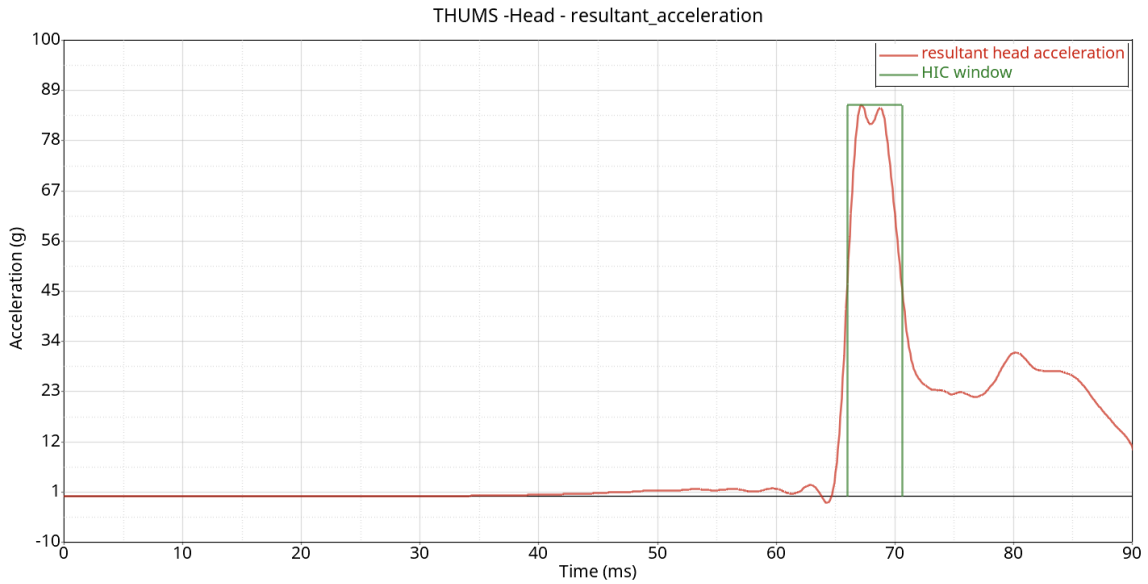


Figure 4-18 - HIC window

INJURY PROBABILITY VS HIC

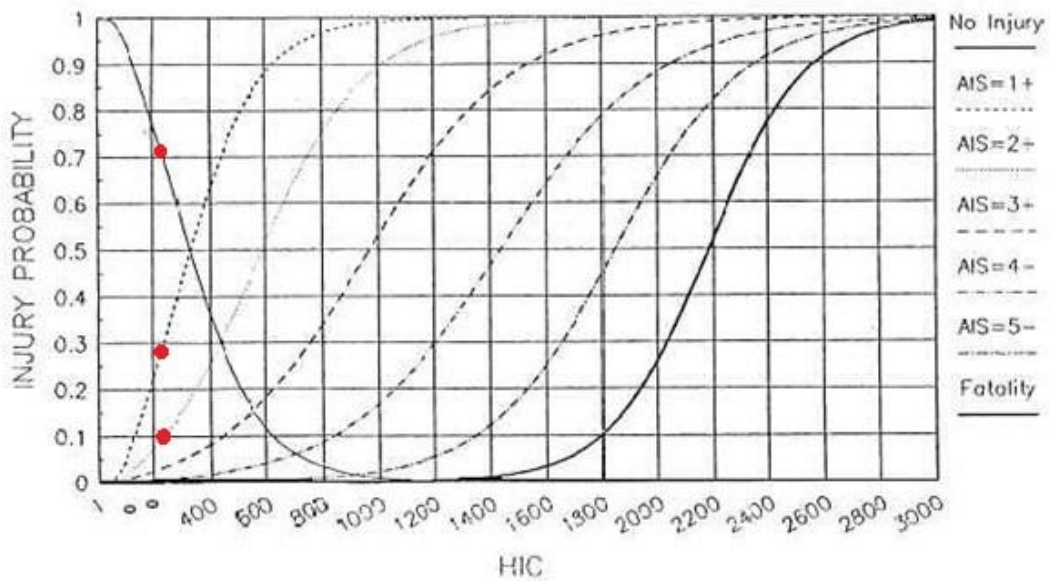


Figure 4-19 - HIC score

Results

Graphically it can be seen as a HIC of 220 corresponds to a 71% of percentage of no injuries of the driver, a 28% of probability of AIS 1 that means a minor injury. An HIC of 220 corresponds also 10% of probability of AIS 2 or a major injury suffered by the driver.

4.4.3 THUMS - Neck

The Euro NCAP normative does not require checking the signals obtained from the neck, but this may be of interest because, looking at the pictures of the collision, there seems to be a significant flexion of the neck. This is a delicate part of the body as an accident damage could lead to a serious injury to the driver. The graphs of forces (figures 4.20, 4.21) and moments (figures 4.22, 4.23) to which the neck is subjected are reported. Two sections of the neck are considered, described in chapter 3.4.4.

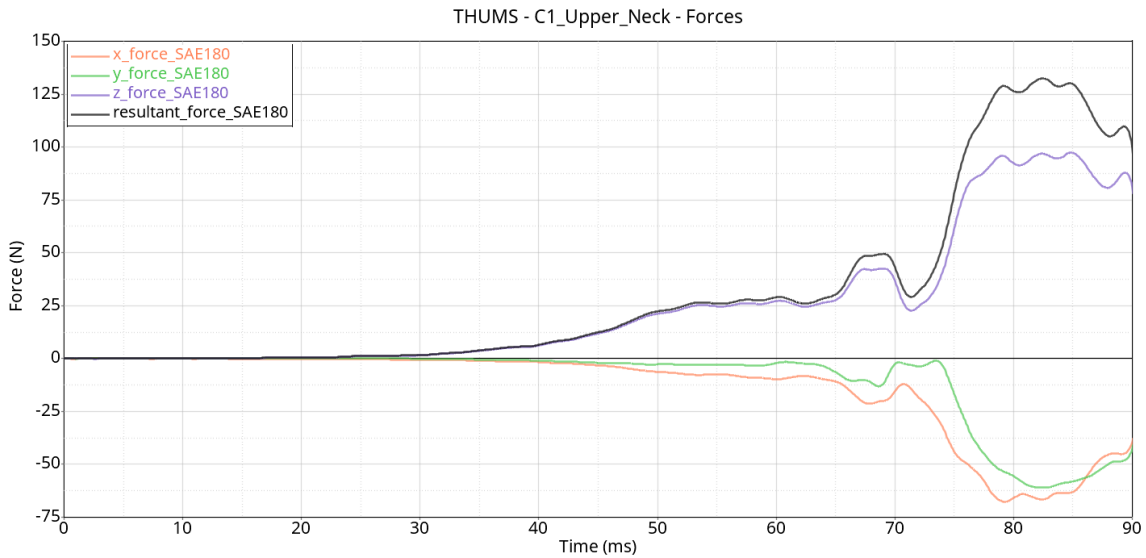


Figure 4-20 - Upper neck forces

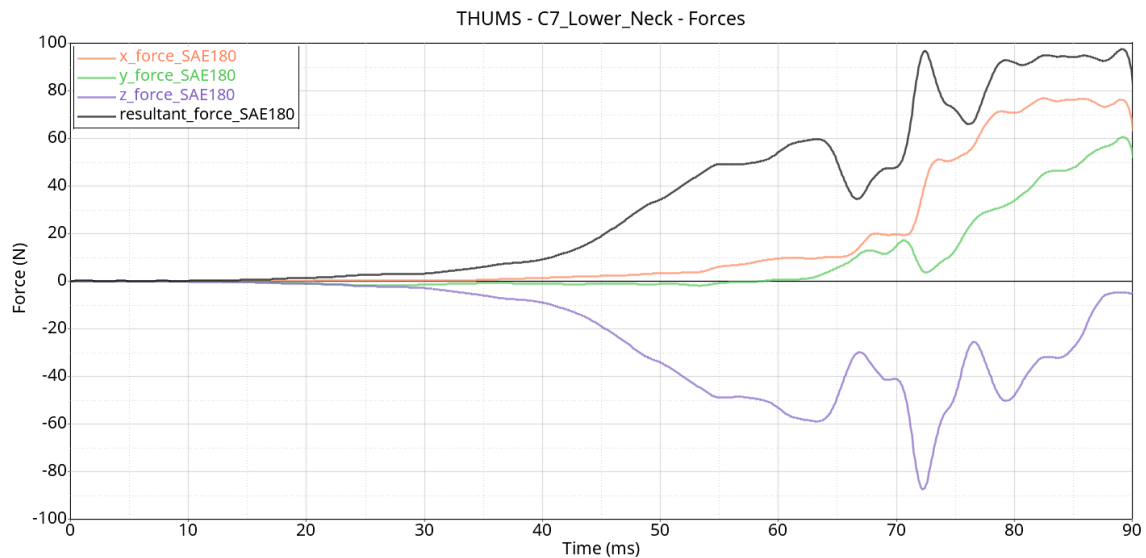


Figure 4-21 - Lower neck forces

Results

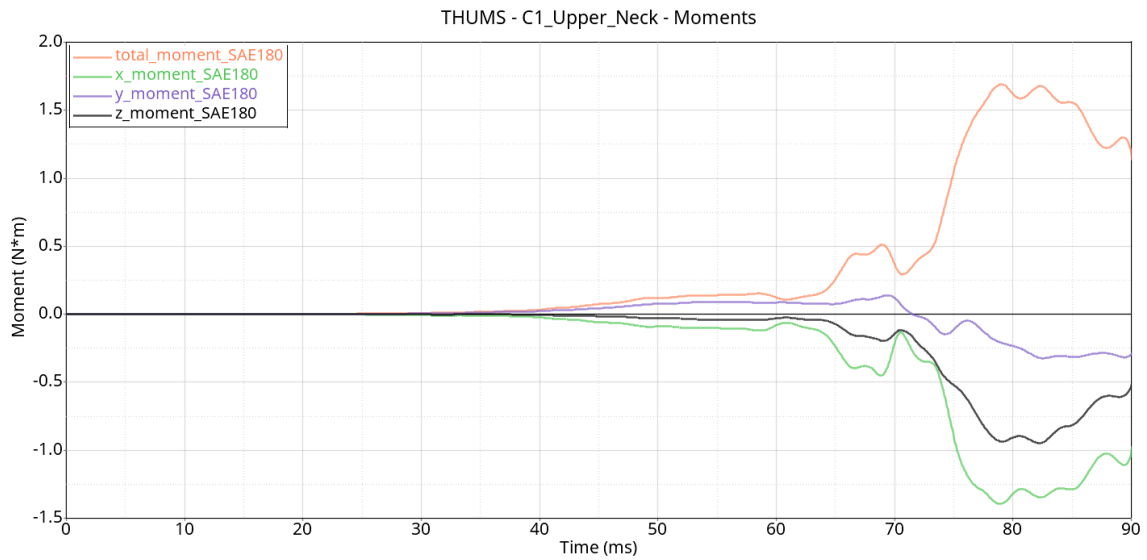


Figure 4-22 - Upper neck moments

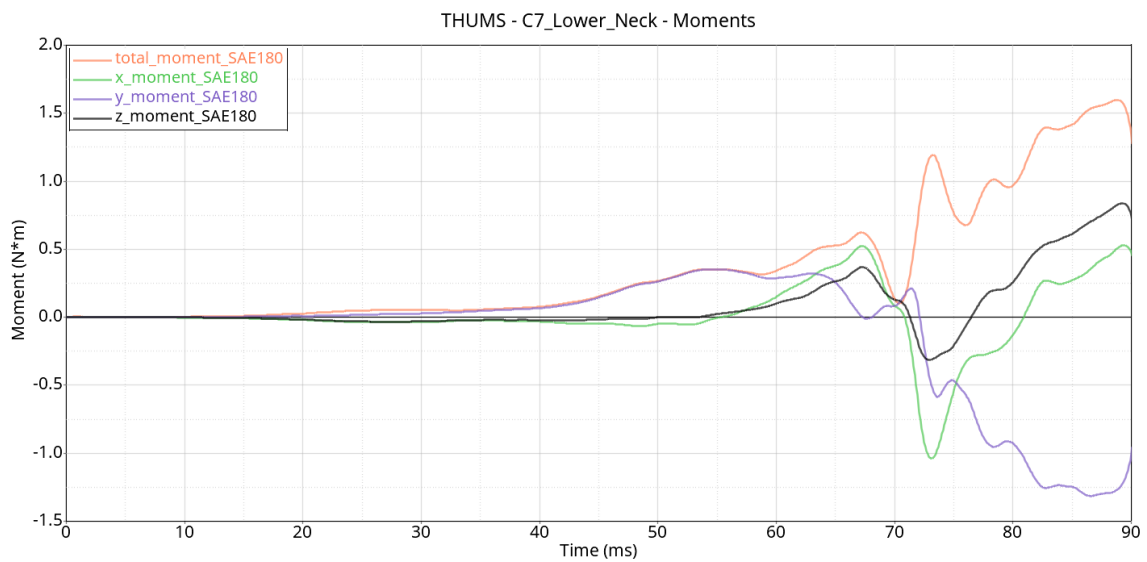


Figure 4-23 - Lower neck moments

From the biomechanical results shown above it can be seen that the section of the neck named 'upper neck' is the most stressed.

4.4.4 Neck Injury Criteria

The Neck Injury Criteria is calculated as described previously in chapter 1.2.3. To do this, the data from the most stressed section of the neck is used. The N_{ij} obtained is equal to 0.02 and it is in the quadrant of tension-extension, while the N_{ij} calculated on the lower section of the neck is equal to 0.018 and it is in the quadrant of compression-extension.

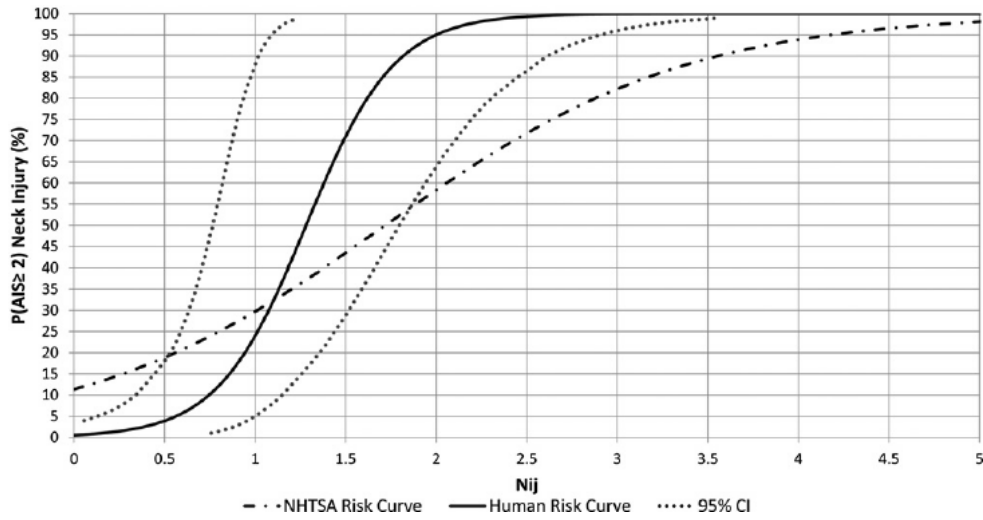


Figure 4-24 - N_{ij} AIS 2+

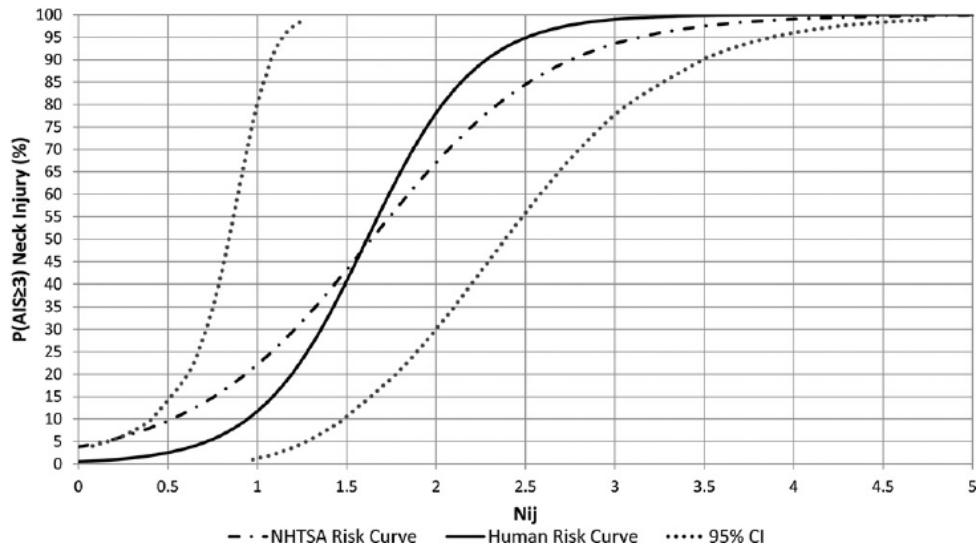


Figure 4-25 - N_{ij} AIS 3+

With a N_{ij} equal to 0.02 the risk of an injury at a level higher than AIS 2 is practically null [24], in spite of the bending of the neck in the images of the impact.

4.4.5 THUMS – Thorax T1

According to the Euro NCAP normative the accelerations of the T1 vertebra are plotted in figure 4.26.

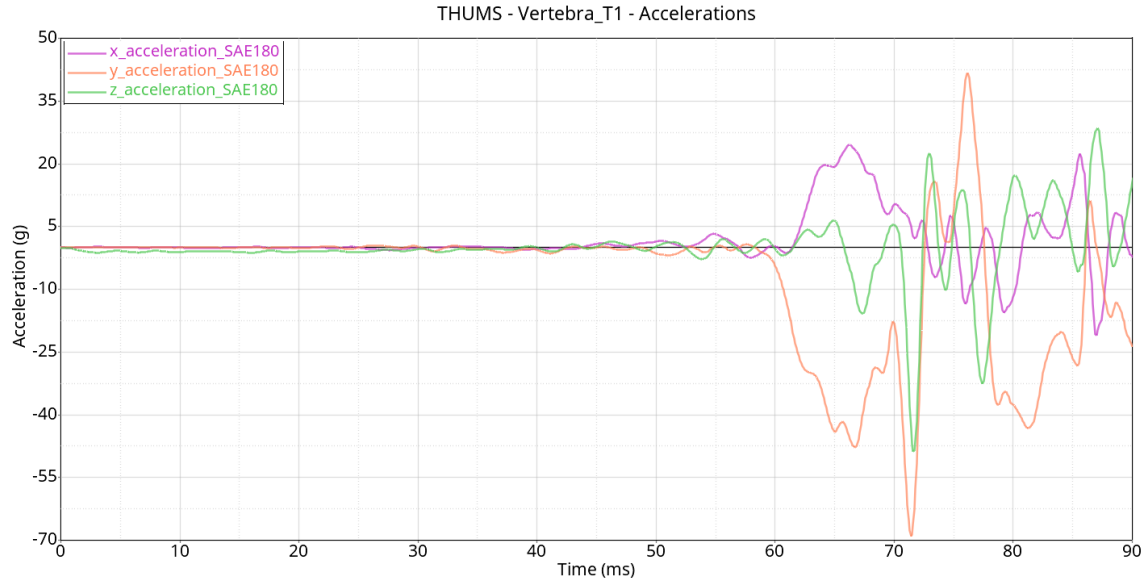


Figure 4-26 - Thorax T1 accelerations

The T1 vertebra is subjected to a peak of 69g of acceleration in the direction of the impact.

4.4.6 THUMS – Thorax T4

Accelerations are not explicitly required by the Euro NCAP normative but are useful for understanding the behaviour of the thorax of the THUMS, as this is one of the body parts most at risk in a side impact. Accelerations are shown in figure 4.27.

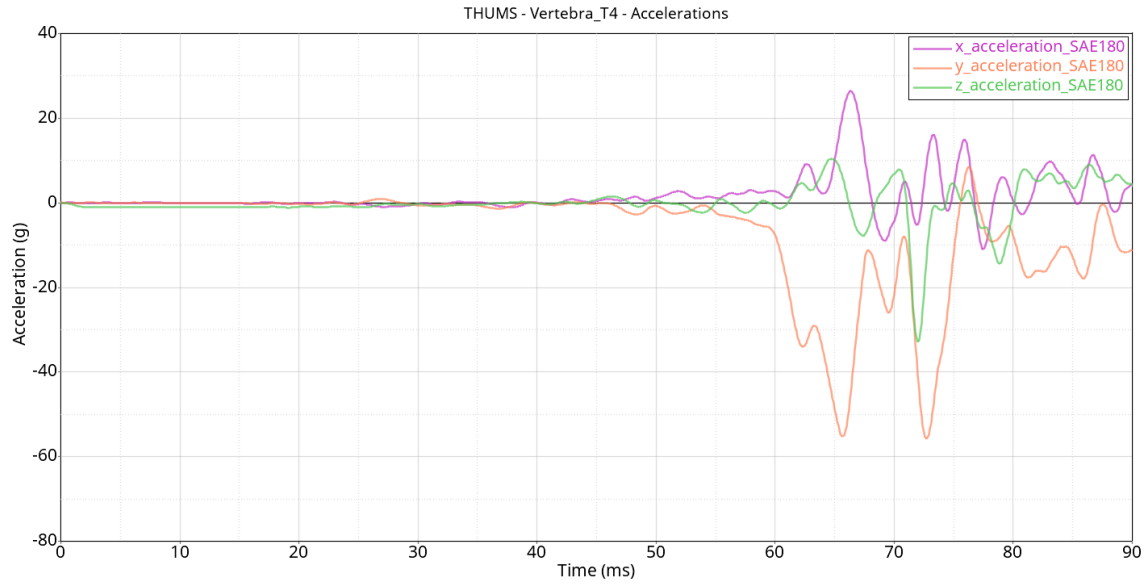


Figure 4-27 - Thorax T4 accelerations

4.4.7 THUMS – Thorax T12

With respect to the T12 vertebra, following the requirements of the standard, forces along the x and y axes and moments on x and y are studied. The normative also requires acceleration along the y direction.

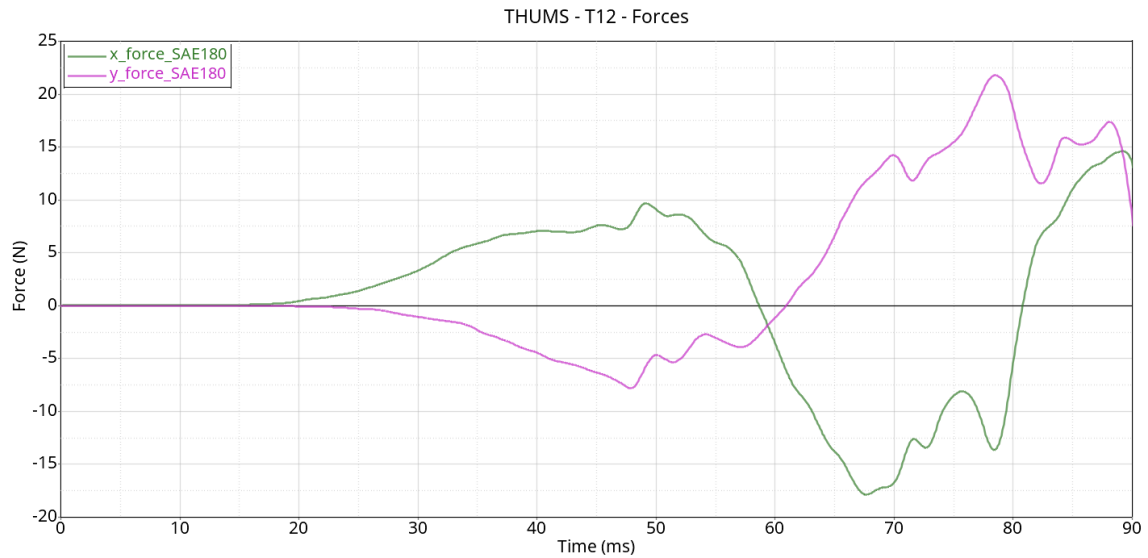


Figure 4-28 - T12 forces



Figure 4-29 - T12 moments

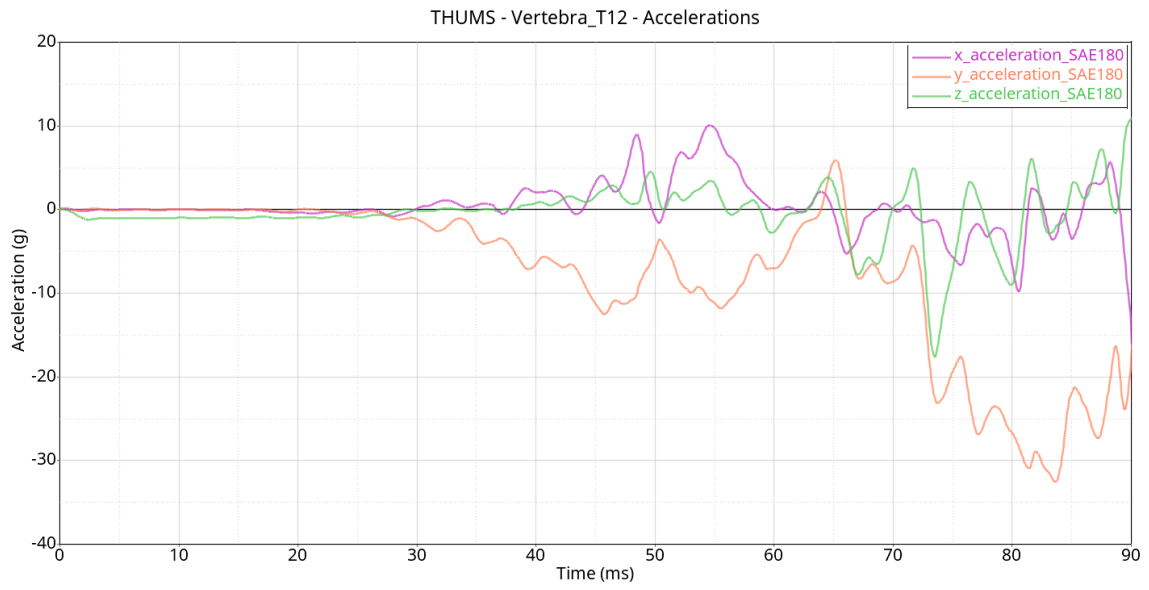


Figure 4-30 - T12 accelerations

4.4.8 THUMS – Ribs

Following the Euro NCAP normative the acceleration of the ribs along the direction of impact and their deflections are plotted. Ribs at different heights (upper thorax, middle thorax, lower thorax) as defined in chapter 3.4.6 are studied.

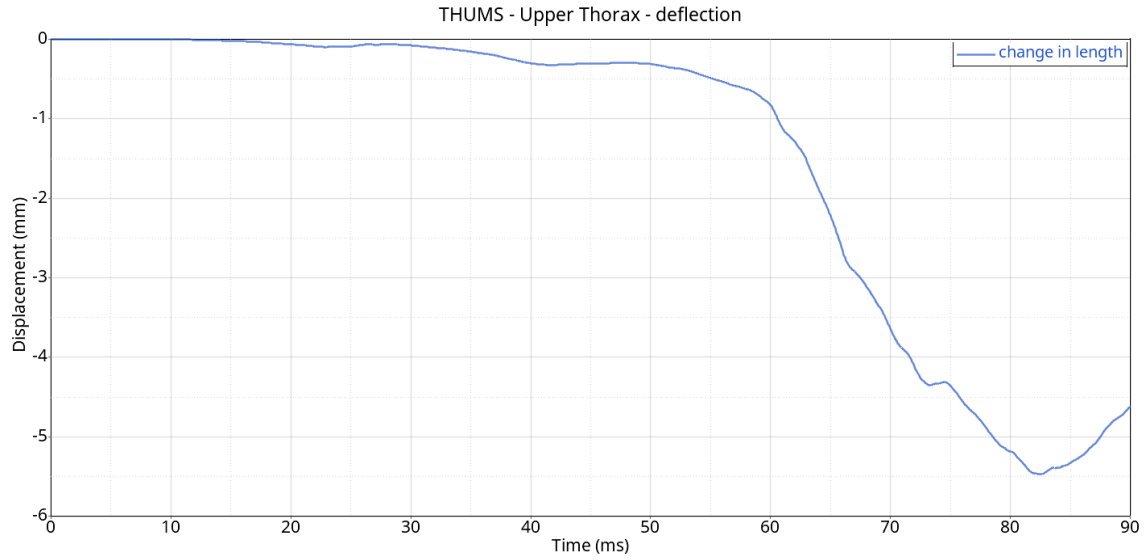


Figure 4-31 - Upper thorax deflection

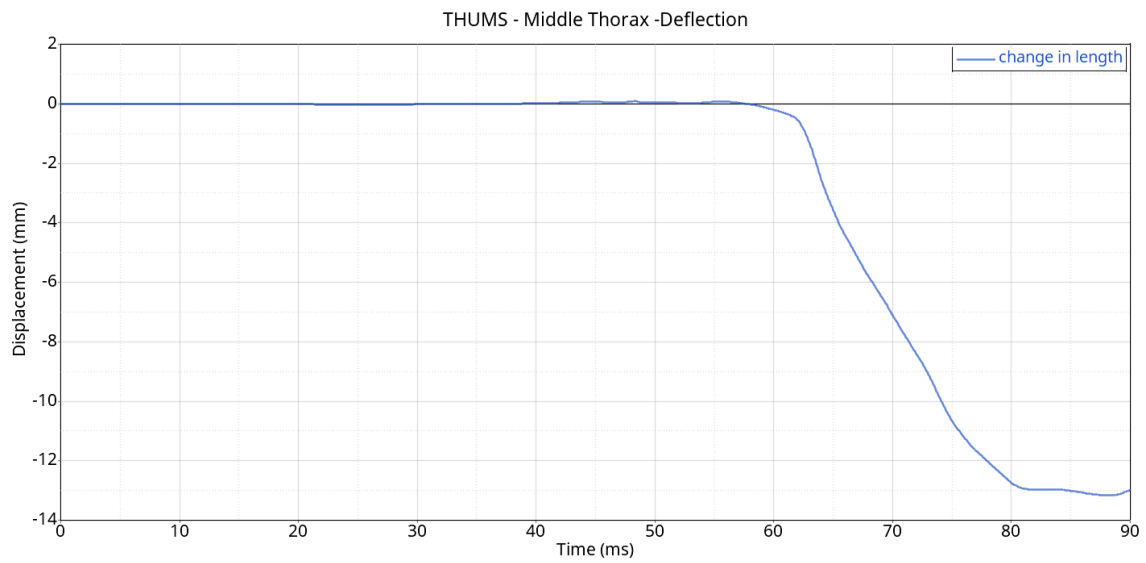


Figure 4-32 - Middle thorax deflection

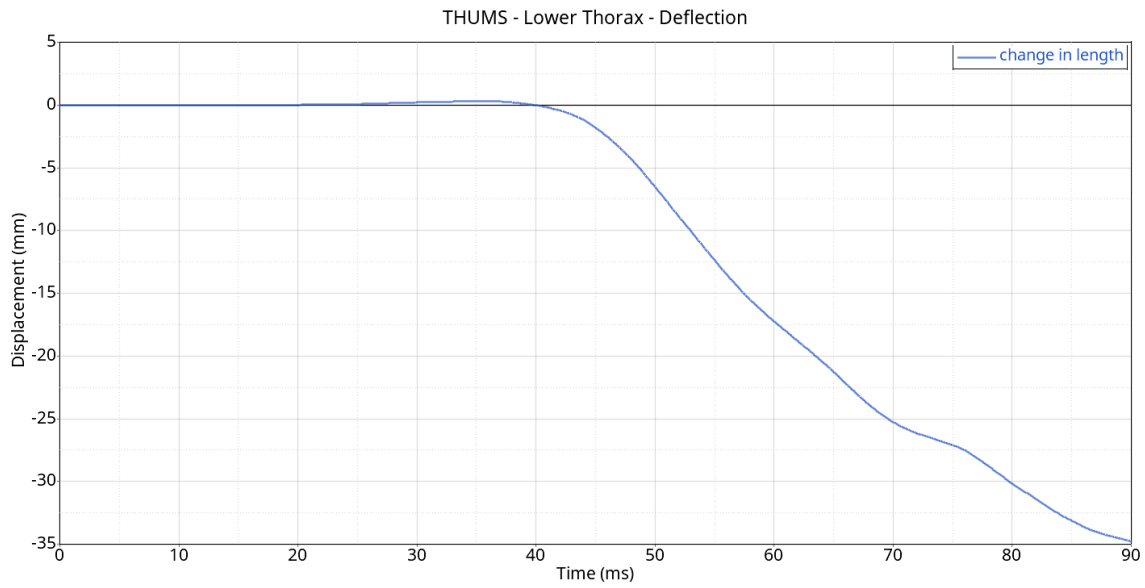


Figure 4-33 - Lower thorax deflection

As can be seen from the figure 4.33, it is evident that the lower thorax, corresponding to the 9th rib, is the part of the ribcage that is subjected to the greatest compression of 35mm. The thorax is a part of interest in the study of a lateral crash test because, according to the literature, it is one of the most affected parts in this type of impact.

4.4.9 THUMS – Backplate

According to Euro NCAP normative, the forces of the backplate along x and y axes and the moment along y and z axes are plotted in figures 4.34, 4.35.

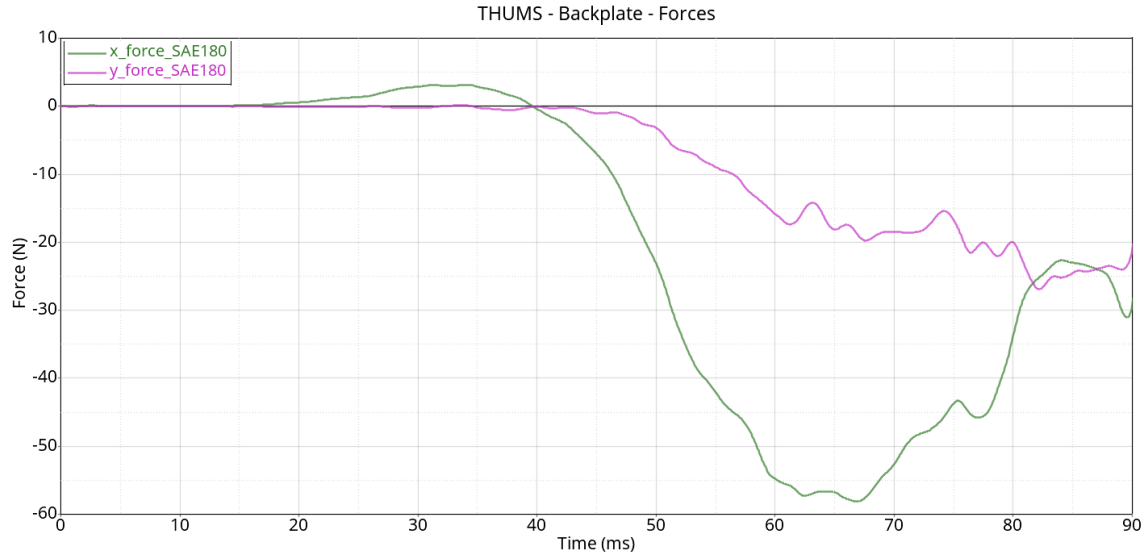


Figure 4-34 - Backplate forces

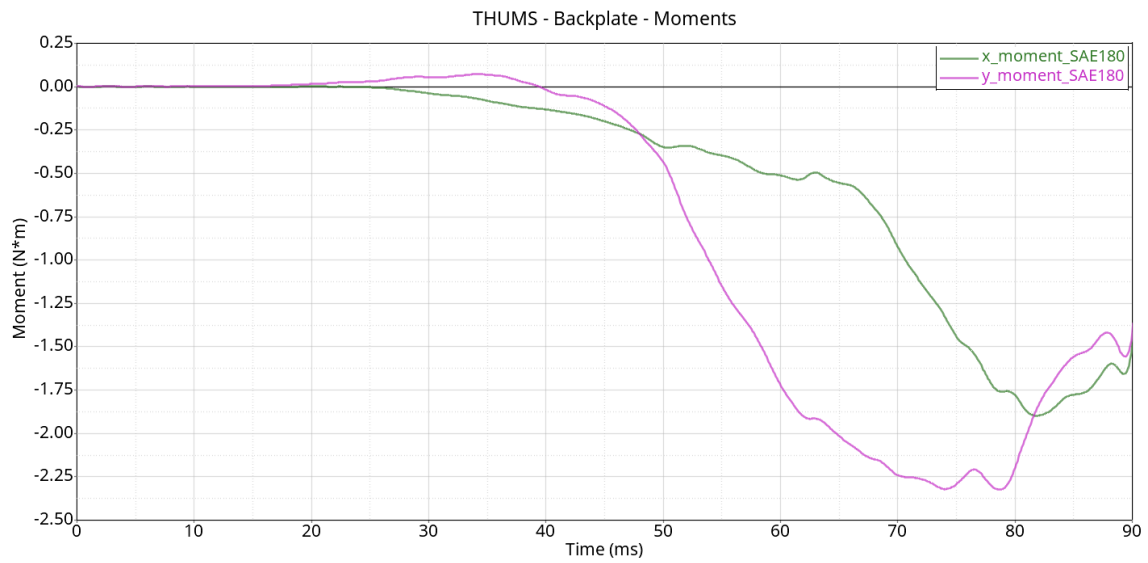


Figure 4-35 - Backplate moments

4.4.10 THUMS – Pelvis

Following the Euro NCAP normative, the accelerations to which the pelvis is subjected are plotted in the figure 4.36.

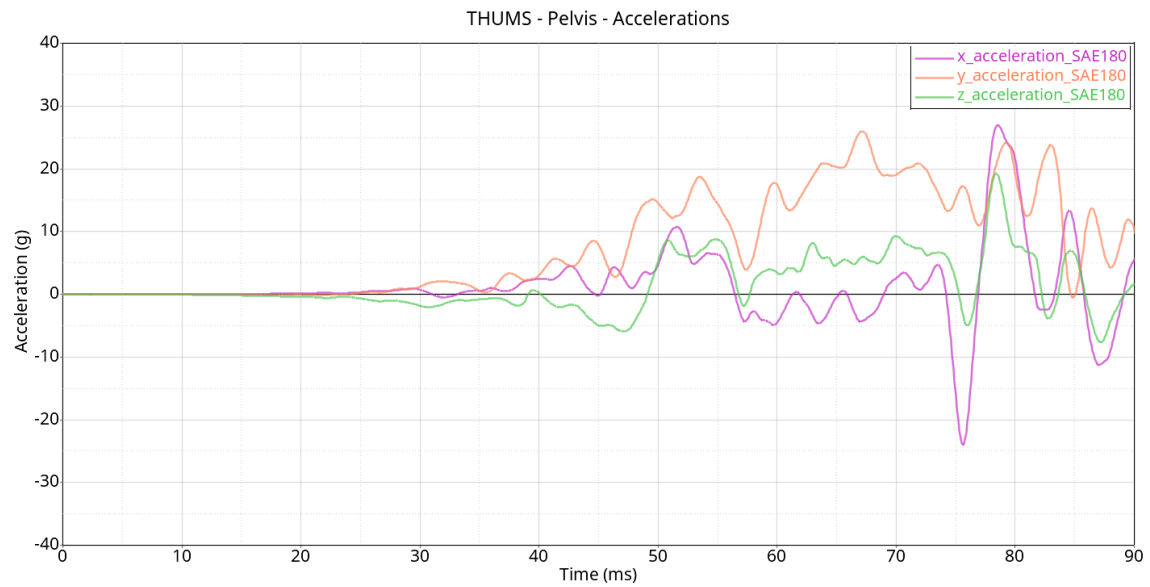


Figure 4-36 - Pelvis accelerations

4.4.11 THUMS – Pubic Symphysis

According to the Euro NCAP normative, the force in the direction of the impact is studied. The y force to which the pubic symphysis is subjected is plotted in figure 4.37.

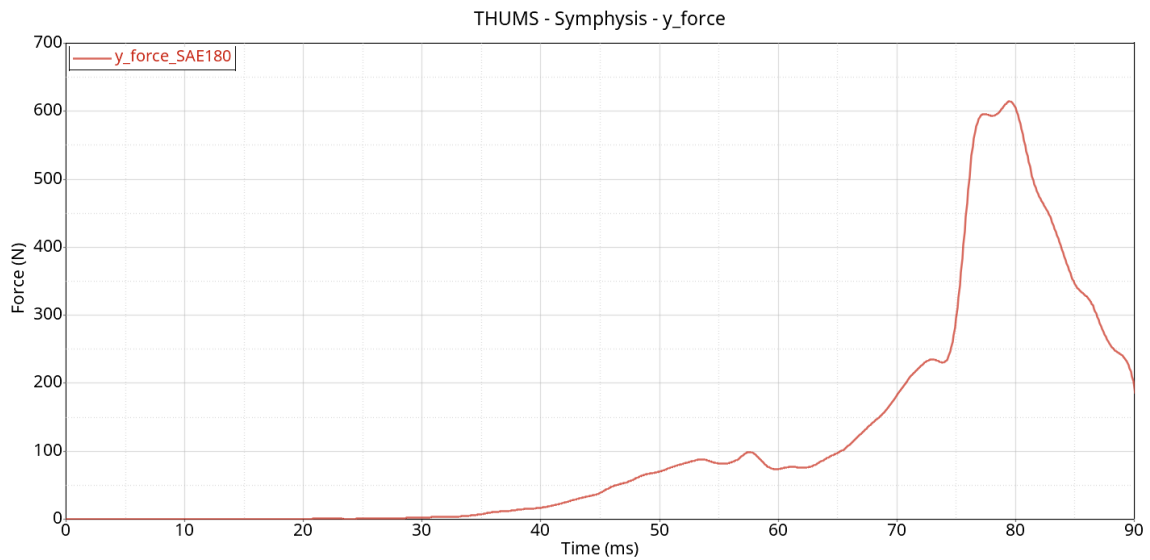


Figure 4-37 - Pubic Symphysis y force

The peak of the force along the direction of the impact is around 615N, because of this high value this leads it to be an interested part in this type of impact.

4.4.12 THUMS – L&R Femur

Following the Euro NCAP normative, the moments and the forces on the femurs of the THUMS are studied. It is also interesting to make a comparison between the right and the left side. The comparison of total forces and moments acting on the right and left femur are shown in the figures 4.42-4.43.

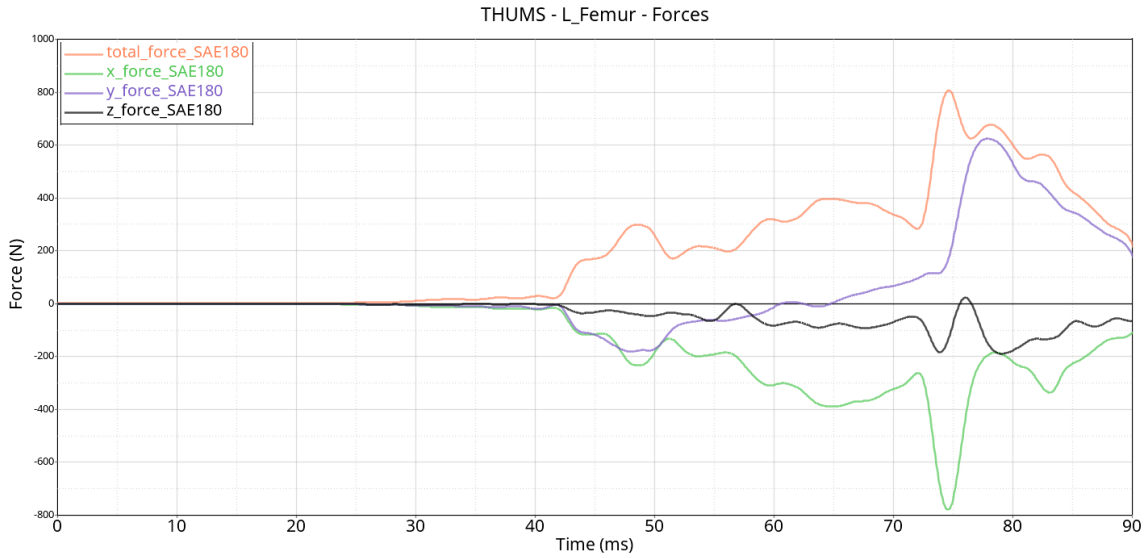


Figure 4-38 - Left femur forces

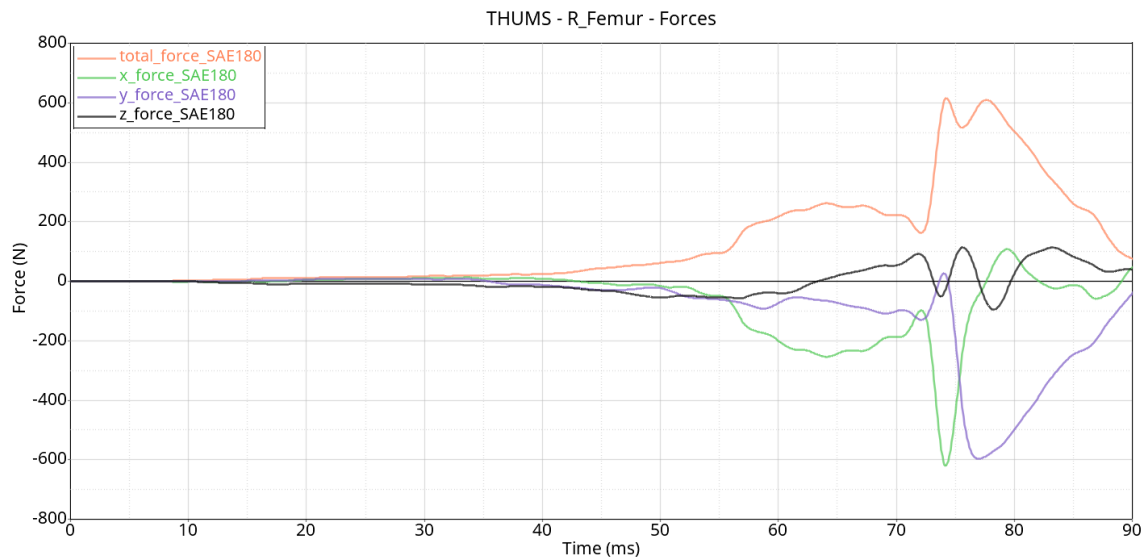


Figure 4-39 - Right femur forces

Results

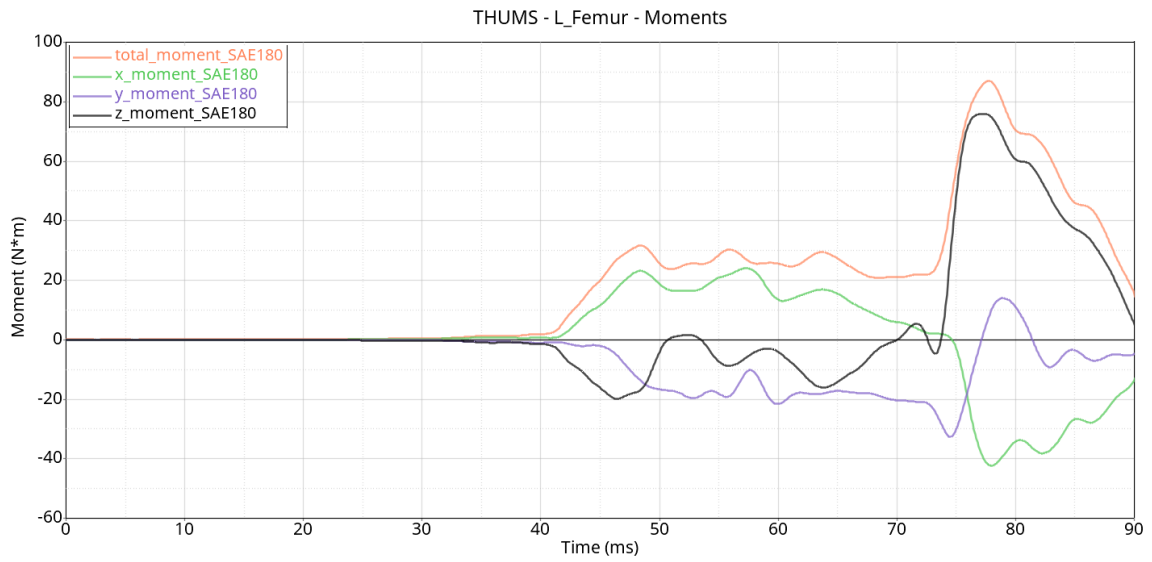


Figure 4-40 - Left femur moments

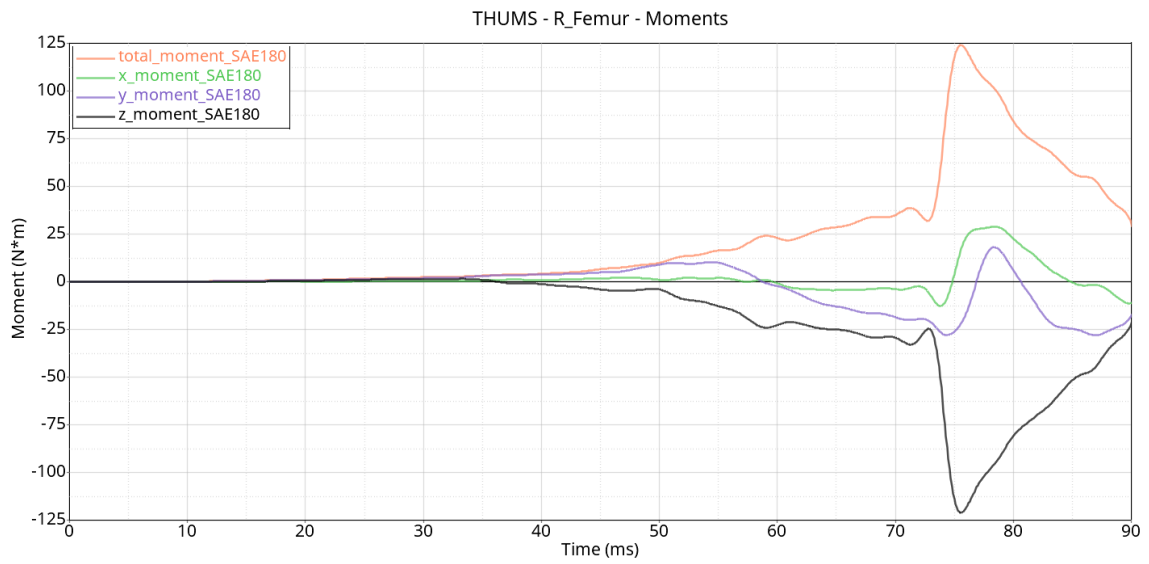


Figure 4-41 - Right femur moments

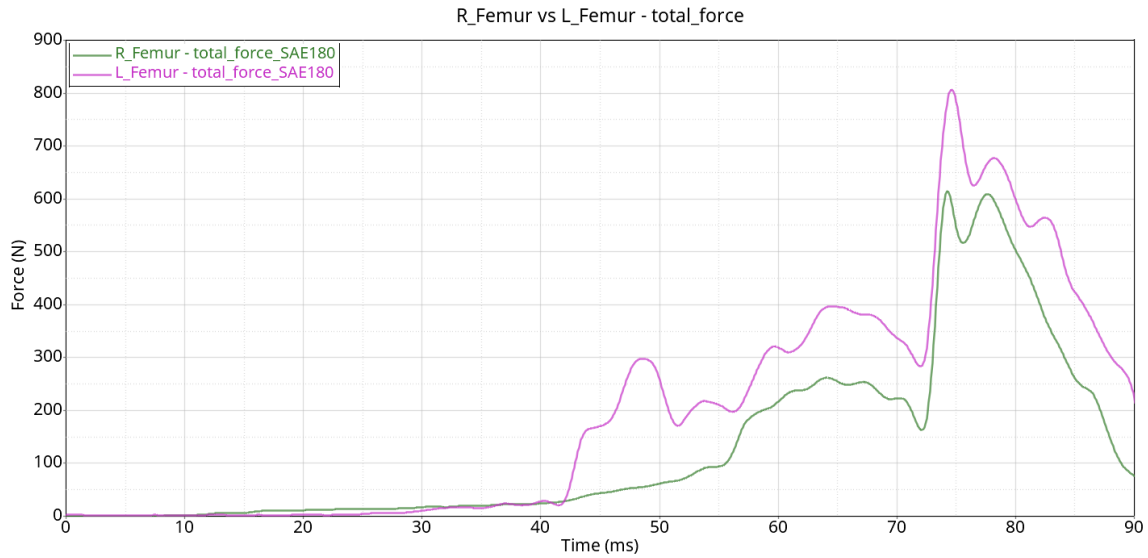


Figure 4-42 - Right vs left femur forces

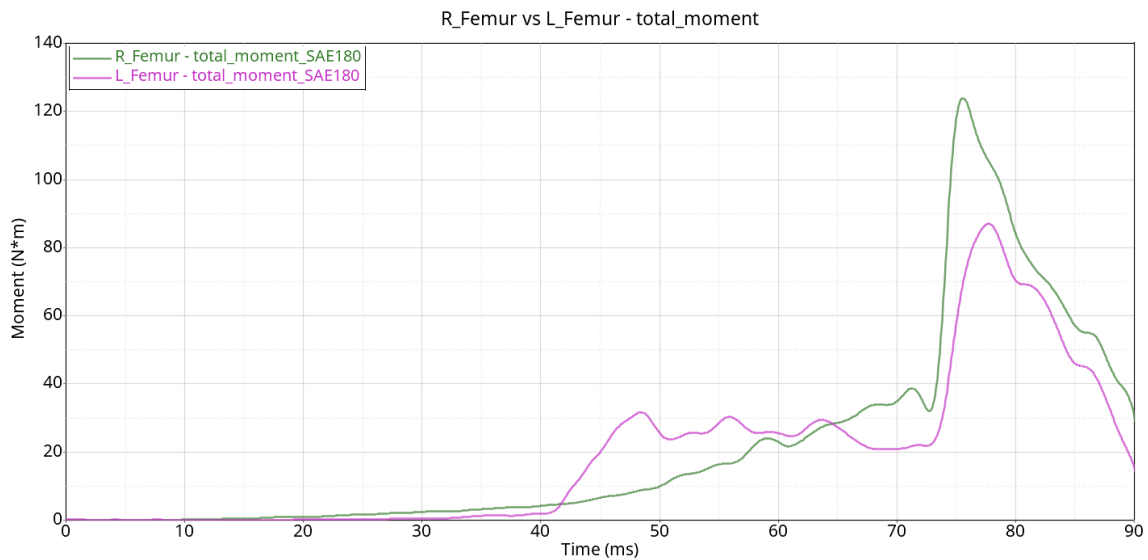


Figure 4-43 - Right vs left moments

It is possible to see from the comparison of forces between the right and left femur in figure 4.42, that it is clear that the left femur is subjected to a greater force than the right one, with a peak of about 810N, making it very stressed. This is because the left femur is closer to the point of impact. On the other hand, if the moments to which they are subjected are analysed, as it is possible to see in the figure 4.43 the right one undergoes a much higher moment with a peak of about 125 Nm. This is explained because the right femur suffers a second hit by bumping into the left leg.

4.4.13 Tibia Index (TI)

The Tibia Index is then calculated as describe in chapter 1.2.4. The critical bending moment result equal to 225Nm, instead the critical force 39kN. The tibia index is then obtained taking into account the worst case between right and left tibia, it results equal to 0.152. The plots of forces and moments of the sections of the tibia are reported as a comparison with the side crash in the chapter 4.4.16. As suggested by Mertz [25] an injury is unlikely when $TI < 1$.

4.4.14 THUMS – Internal Organs Volume and Surface Area

The THUMS sensor set allowed to obtain the volume and the surface area of defined organs through the keyword *AIRBAG_SIMPLE_PRESSURE_VOLUME as described in chapter 3.5. The organs analysed in this thesis are the lungs, the heart, the pancreas, the spleen, the liver, the stomach, the intestine. These organs are enclosed in two larger regions: the ribcage and the abdomen. In this section these two areas are studied in terms of variations of volume and area and the results are shown in figures 4.44, 4.45. The complete reports with the data on each organ mentioned above are given in the Appendix A. Although these results are not currently used in normative standards, in the future they may be useful for the definition and application of new injury criteria. The study of these areas is important because the literature shows that these parts of the body are the most affected and most damaged in a side impact crash scenario.

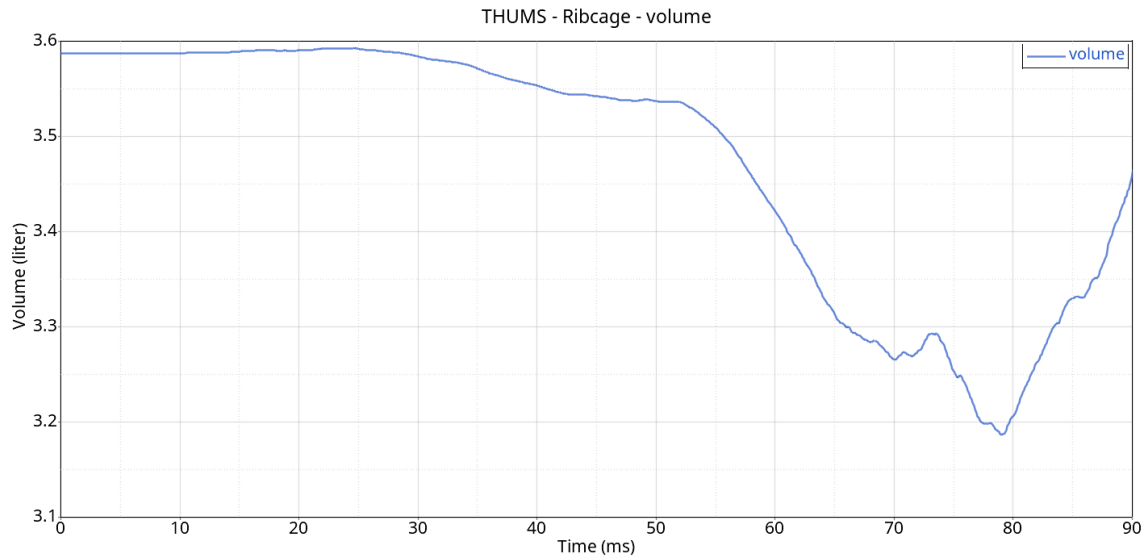


Figure 4-44 - Ribcage volume

Results

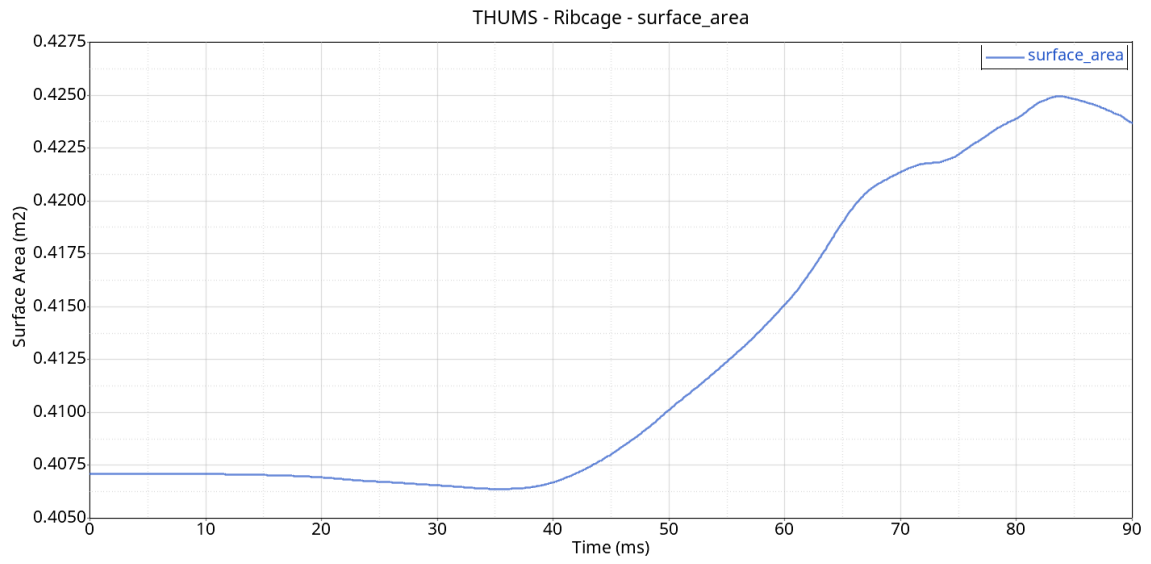


Figure 4-45 - Ribcage surface area

4.4.15 THUMS – Spine Deformation

Through the keyword *DATABASE_NODOUT and markers applied to each vertebra of the spine it is possible to observe how it deforms during the impact in the tree plane coordinates. The figure 4.46 shows the spine in the xz e yz planes at rest. The following figures 4.47, 4.48 show the spine projected in the same planes at sample of time: 0ms, 15ms, 30ms, 45ms, 60ms, 75ms, 90ms.



Figure 4-46 - Undeformed spine xz view (left), yz view (right)

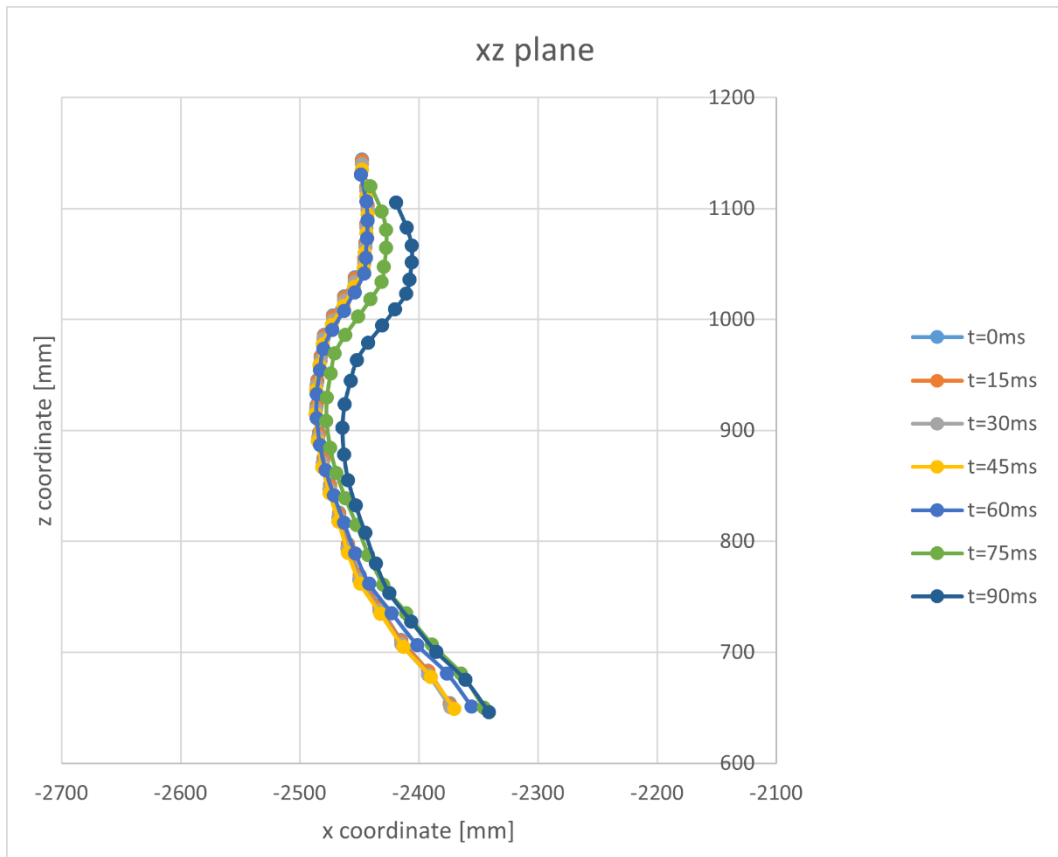


Figure 4-47 - xz plane deformed spine

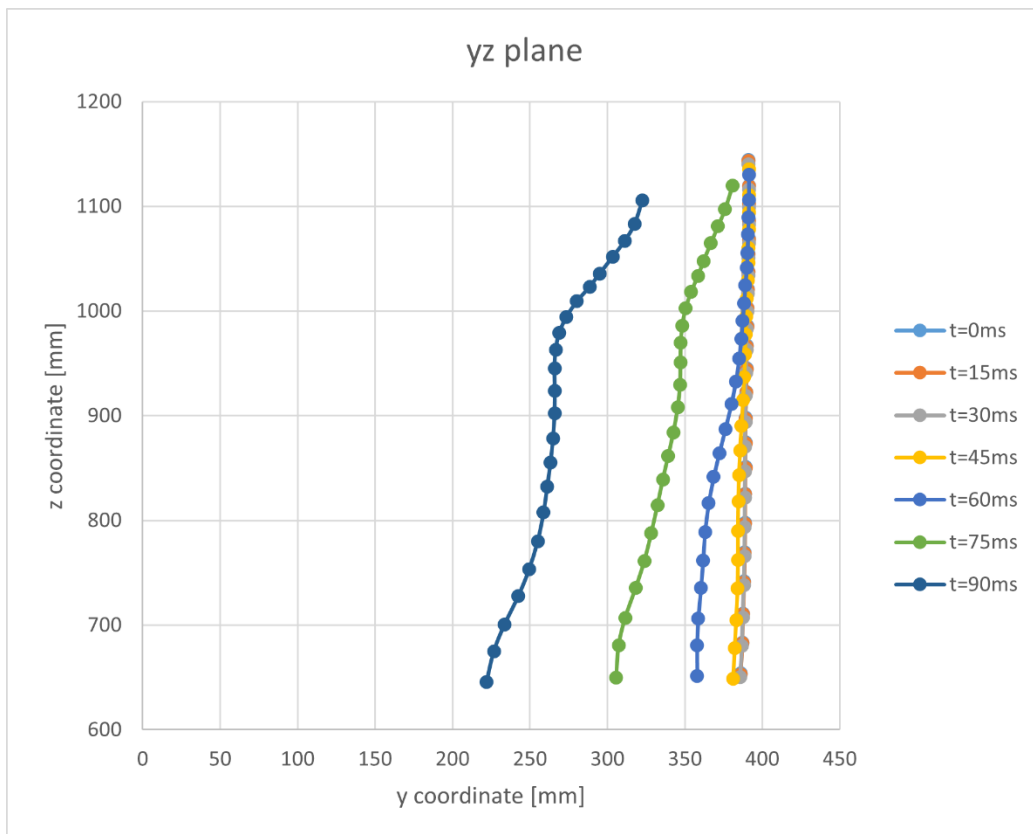


Figure 4-48 - yz plane deformed spine

4.4.16 Comparison with Side Impact and Far Side Impact

In this chapter, a comparison is made between the crash test with offset just studied and the one developed by F. Garelli [26], i.e. a side crash test standardised by Euro NCAP and the far side crash test studied by P. Assandri [27]. The biomechanical results obtained from the three simulations will be compared. Only the far side data concerning the head and the torso will be compared because these are the ones required by the normative for this type of impact. The data obtained in the case of the far side is over an interval of 180ms in order to be able to see the large displacement by the driver during the impact. In this chapter the main results according to Euro NCAP standard are proposed, for the sake of completeness, complementary data comparing the various parameters analysed in the various directions are included in Appendix B.

Head

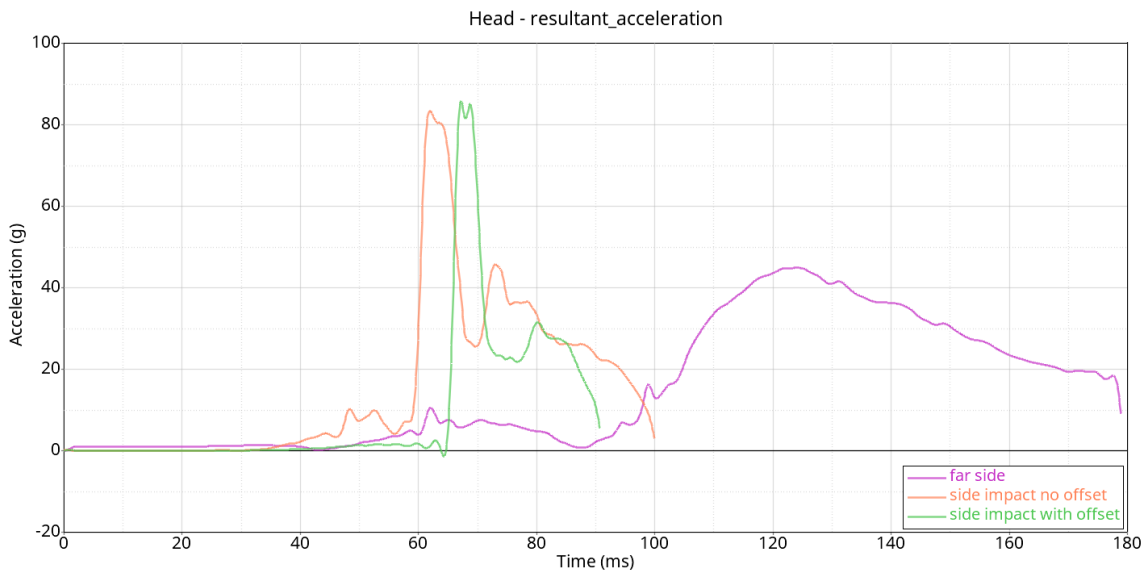


Figure 4-49 - Comparison resultant head accelerations

The comparison shows that in the case with offset the head undergoes greater acceleration but for a shorter time interval, so HIC is equal to 220 but lower than the case without offset which is 314. While in the case of the far side HIC is equal to 183. This last type of impact result to be less dangerous than the other ones for the head. The HIC values are reported in table 1.

Table 1 - Comparison of HIC values

| | with offset | no offset | far side |
|-----|-------------|-----------|----------|
| HIC | 220 | 314 | 183 |

Rotational accelerations

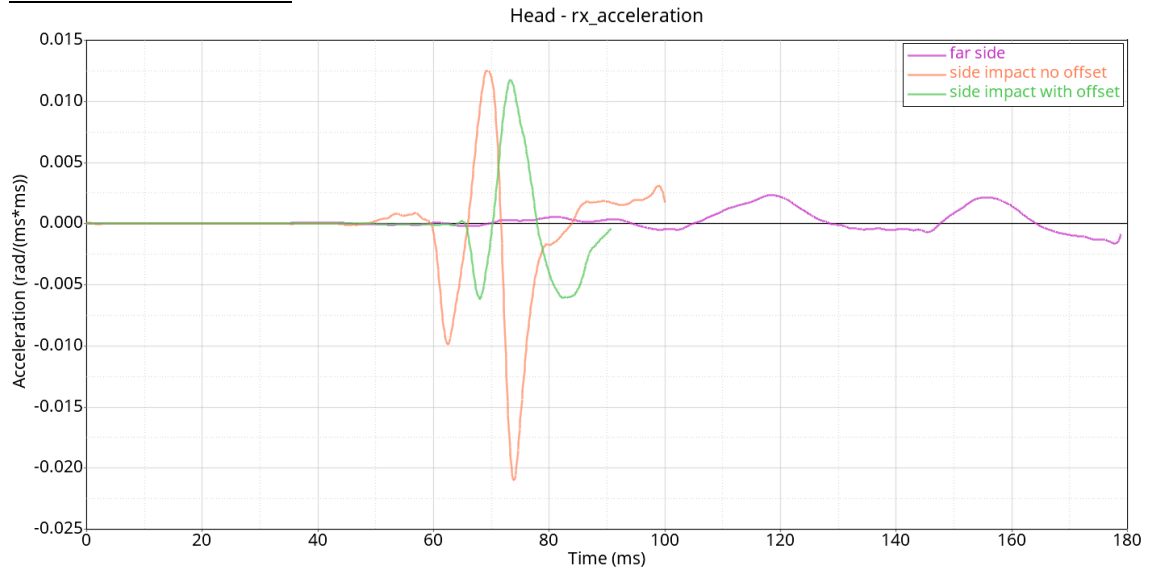


Figure 4-50 - Comparison rotational x accelerations

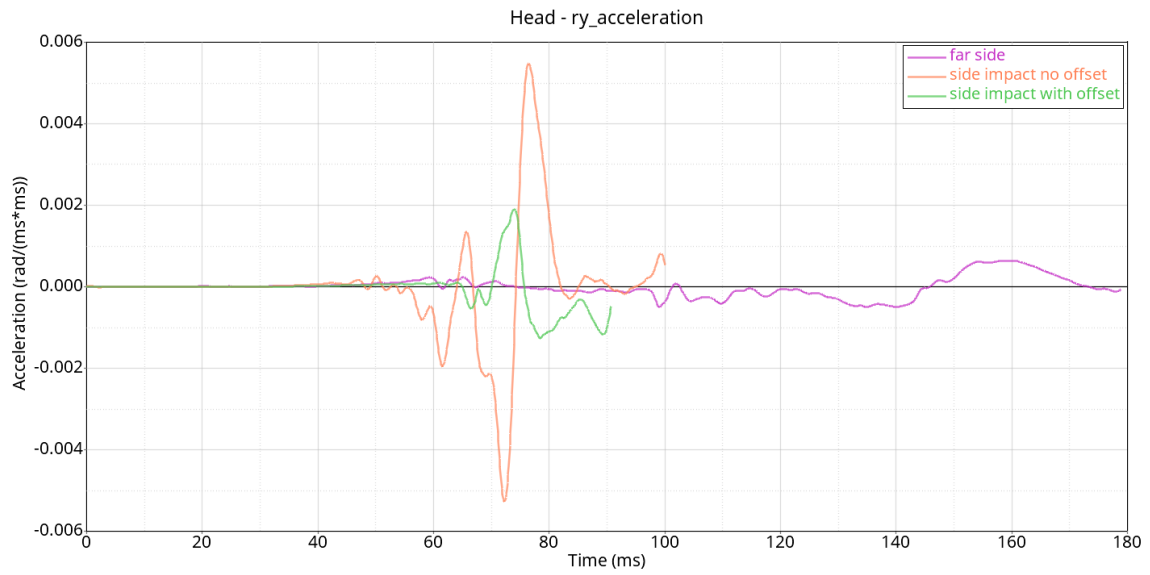


Figure 4-51 - Comparison rotational y accelerations

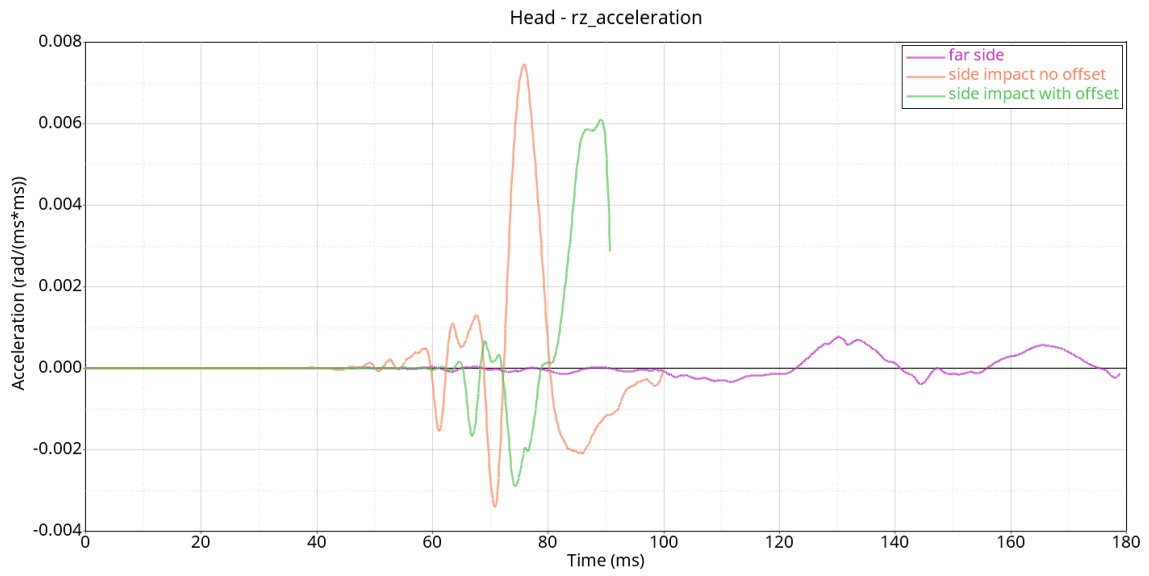


Figure 4-52 - Comparison rotational z accelerations

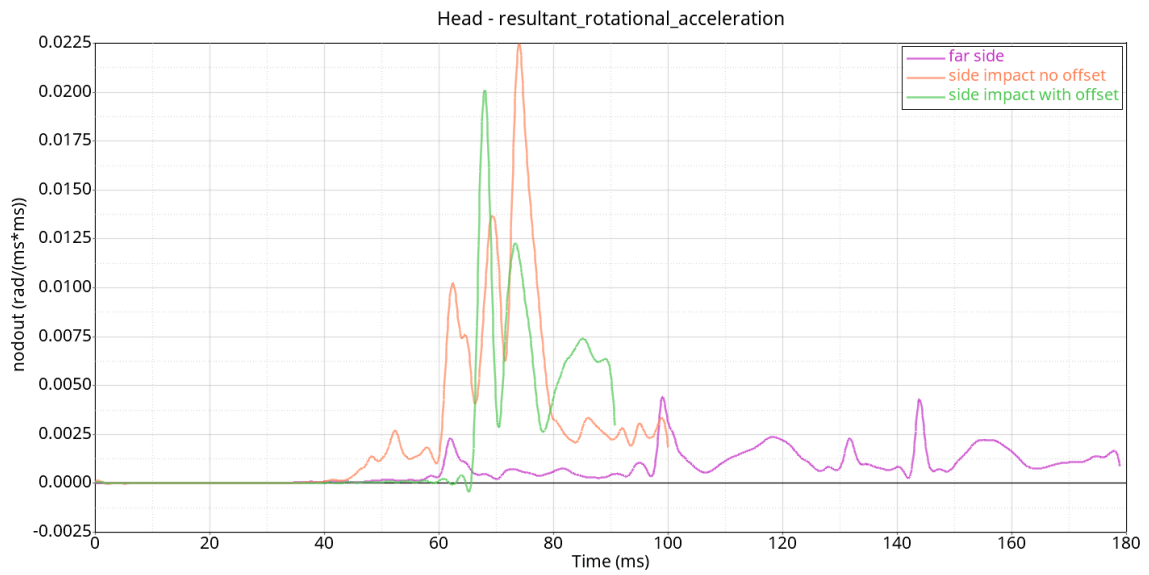


Figure 4-53 - Comparison resultant rotational accelerations

When analysing rotational accelerations of the head, in any direction the case without offset is more stressed than the case with offset. The far side impact is less dangerous than the others as it has a much lower angular acceleration in each direction.

Thorax T1

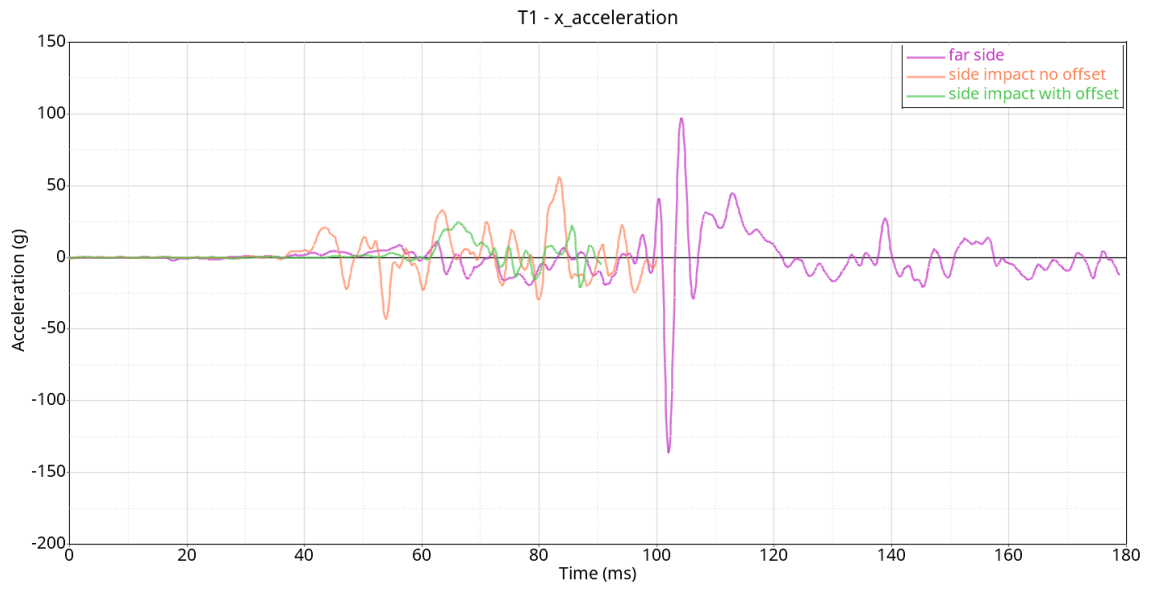


Figure 4-54 - Comparison T1 x accelerations

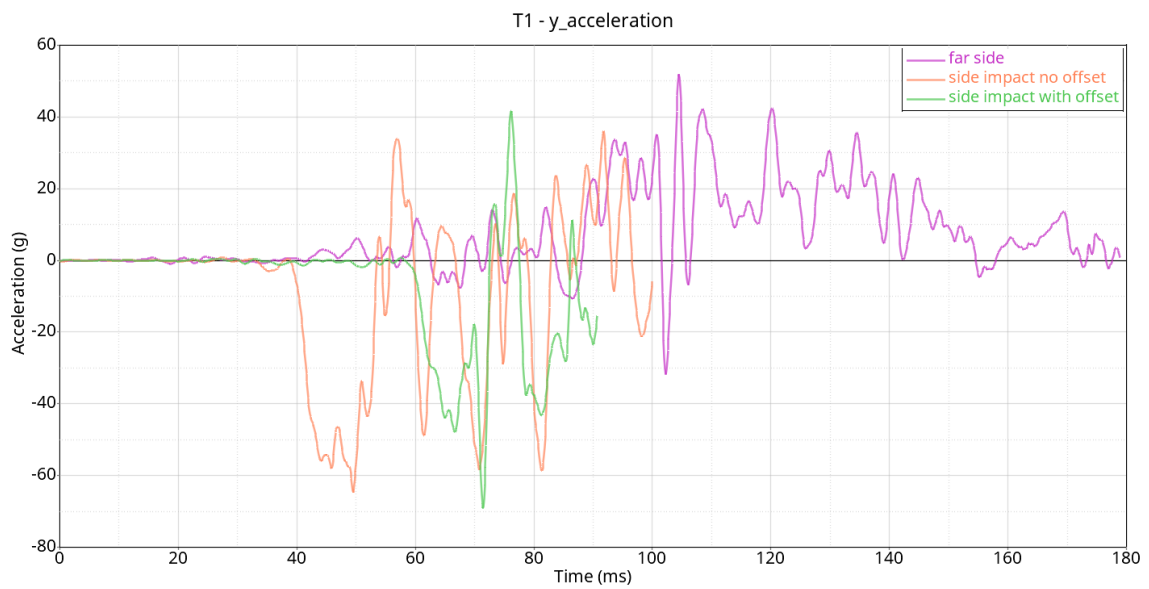


Figure 4-55 - Comparison T1 y accelerations

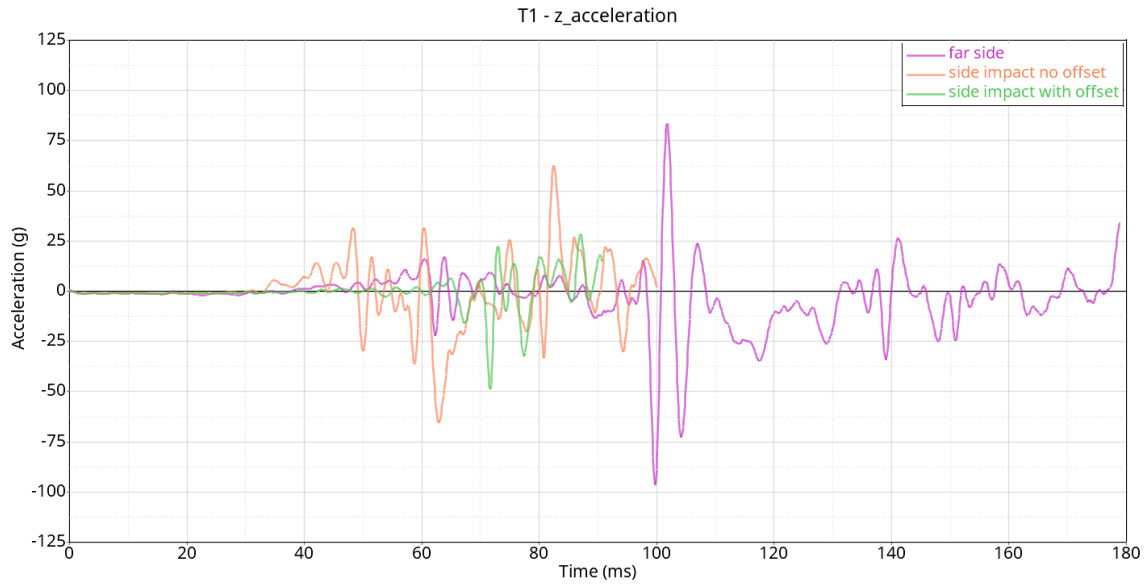


Figure 4-56 - Comparison T1 z accelerations

The opposite behaviour to the head occurs when analysing the acceleration to which the vertebra T1 is subjected. In all directions the far side case is the one with the highest values, maybe due to the type of impact and the movement of the driver which makes a wider excursion from the starting position than the other cases. The T1 vertebra is therefore more loaded in this type of impact.

Thorax T12

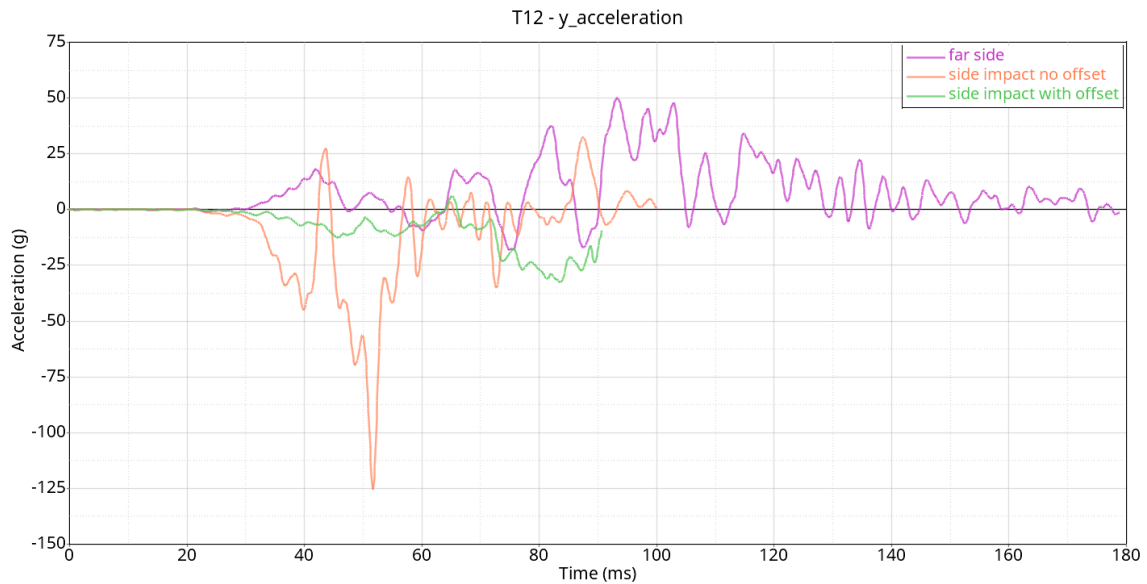


Figure 4-57 -- Comparison T12 y accelerations

Results

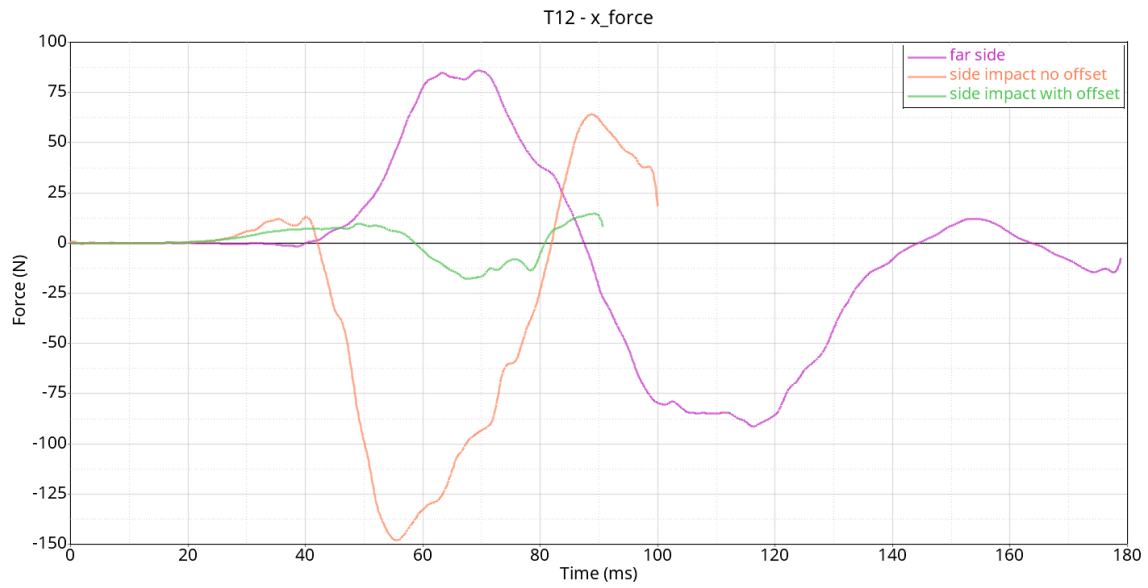


Figure 4-58 - Comparison T12 x forces



Figure 4-59 - Comparison T12 y forces

In the force along y direction, which is the direction of impact, a big difference can be observed, which makes the far side impact a more dangerous case for possible injury to the T12 vertebra. The behaviour of the vertebra T12 is therefore similar to that of the vertebra T1 as might be expected.

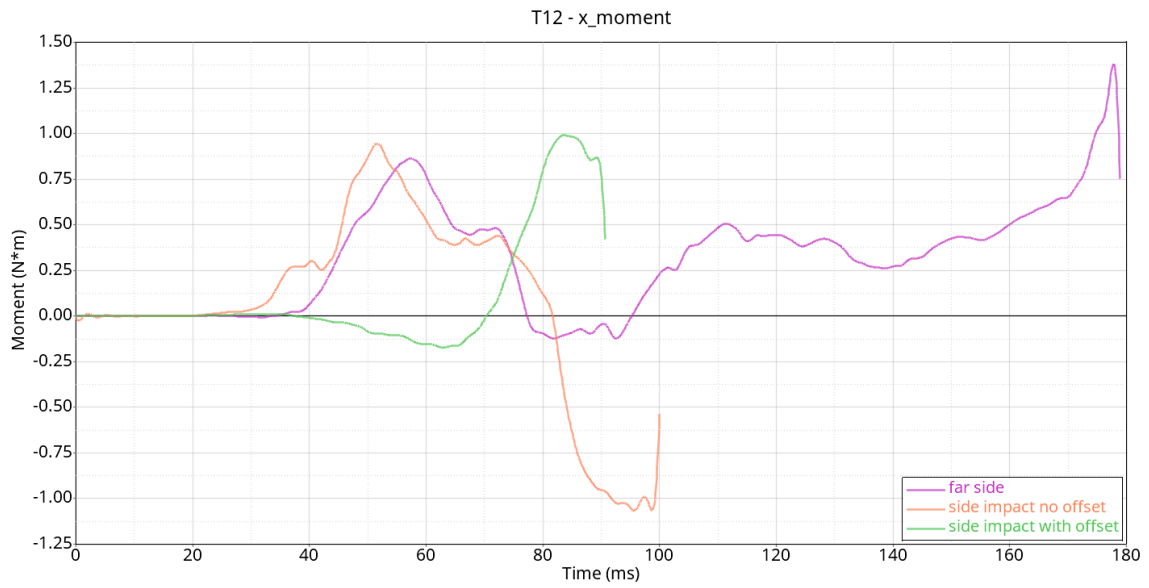


Figure 4-60 - Comparison T12 x moments

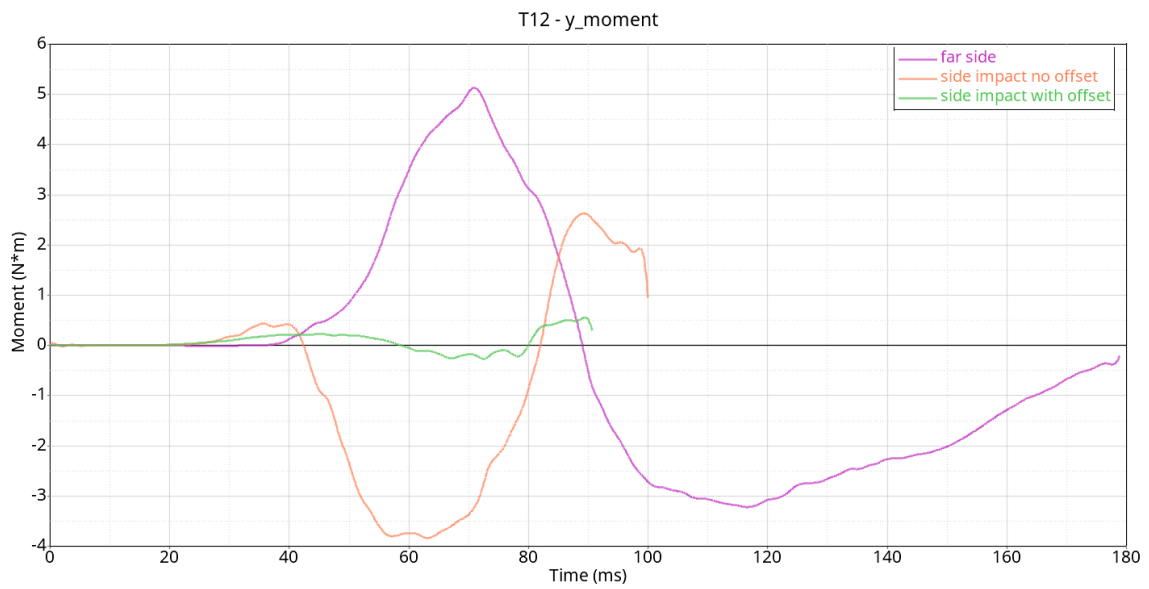


Figure 4-61 - Comparison T12 y moments

Ribs

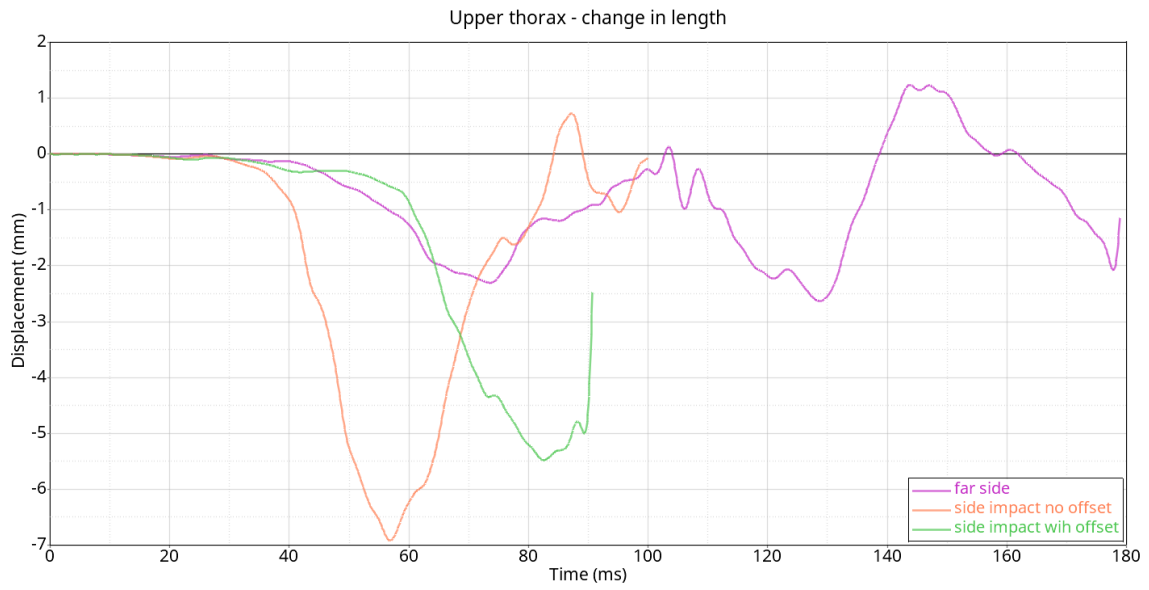


Figure 4-62 - Comparison upper thorax deflections

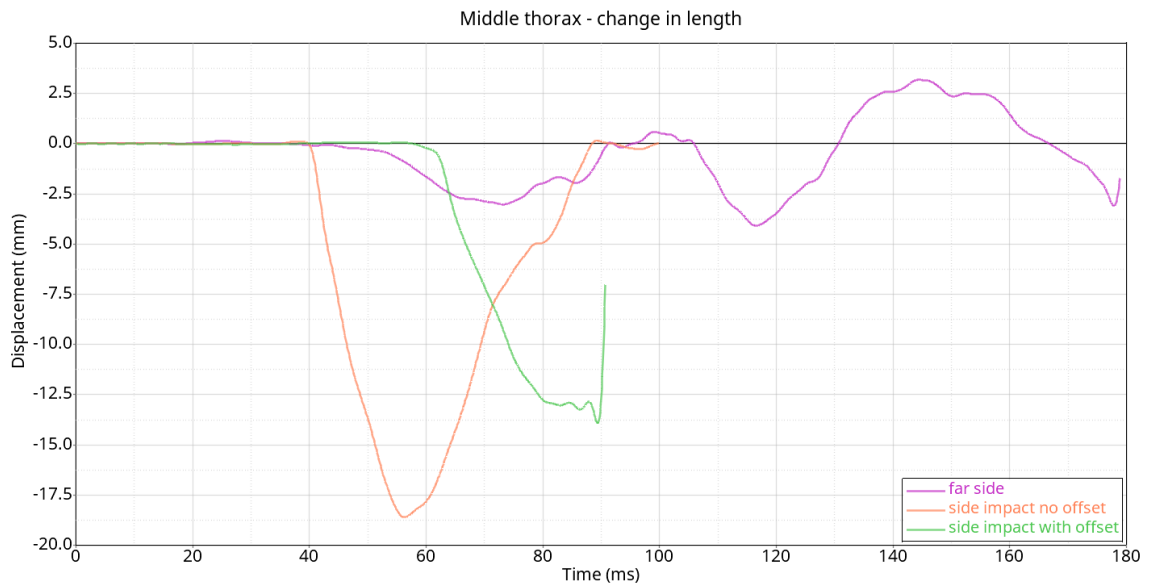


Figure 4-63 - Comparison middle thorax deflections

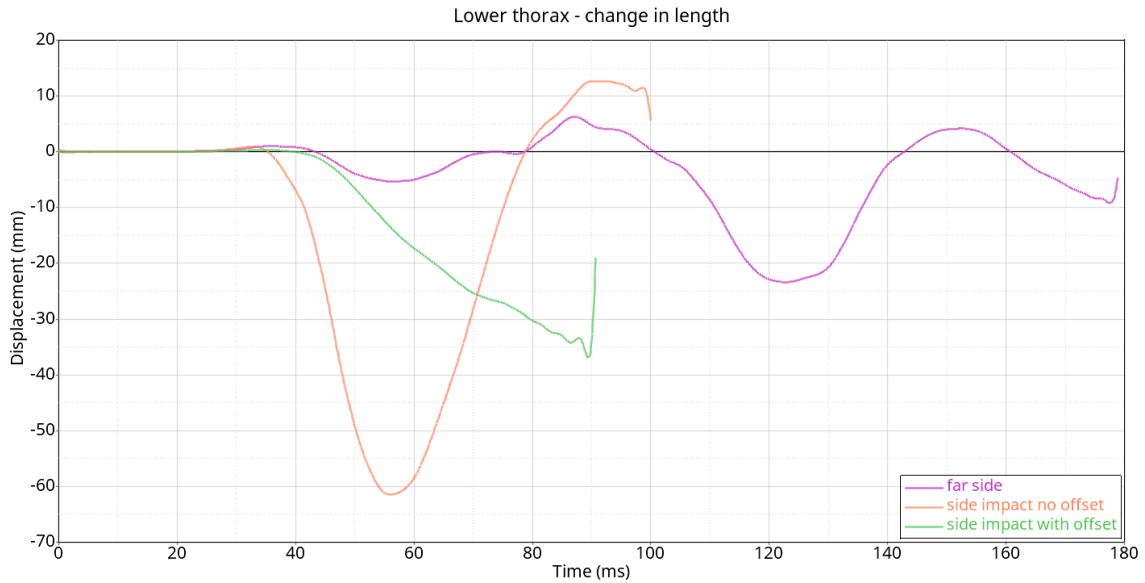


Figure 4-64 - Comparison lower thorax deflections

As can be seen in all cases the lower thorax is the one which suffers the greatest deflection, on this the viscous criterion can be calculated, although in the case of the far side the change in length is less than the others. In the case with offset the VC is equal to 0.64 m/s while in the case without offset is equal to 1.14 m/s. The far side case is the least stressed with a value of VC equal to 0.17 m/s.

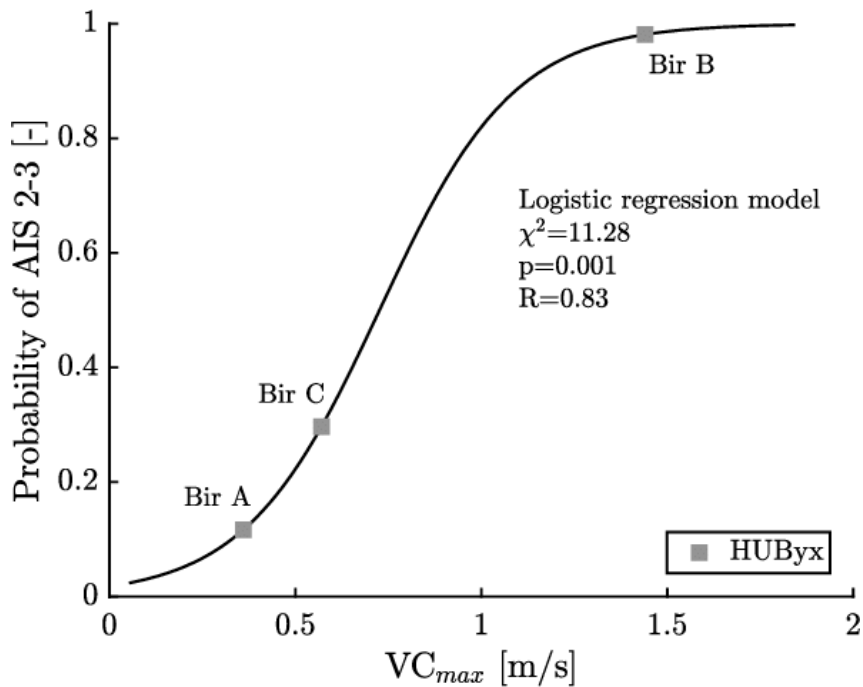


Figure 4-65 - Viscous criterion AIS 2-3

In the case with offset there is a 39% of probability of an injury of level AIS 2-3 while the case without offset is more dangerous with a 90% probability on an injury of level AIS 2-3, while in the case of the far side the risk of injury is less than 10%.

Backplate

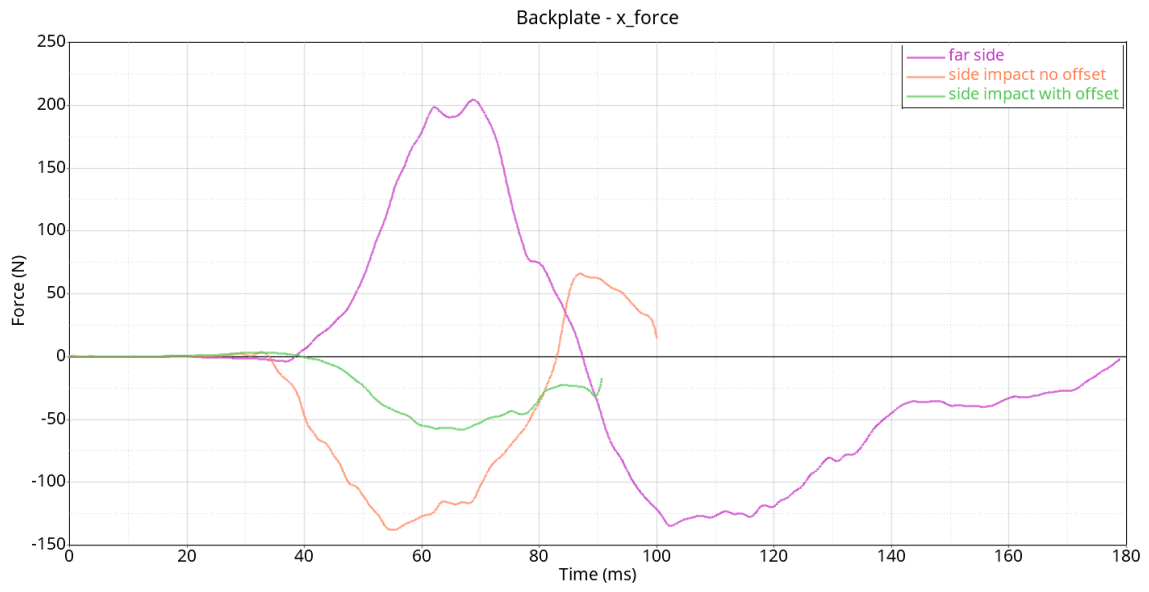


Figure 4-66 - Comparison backplate x forces

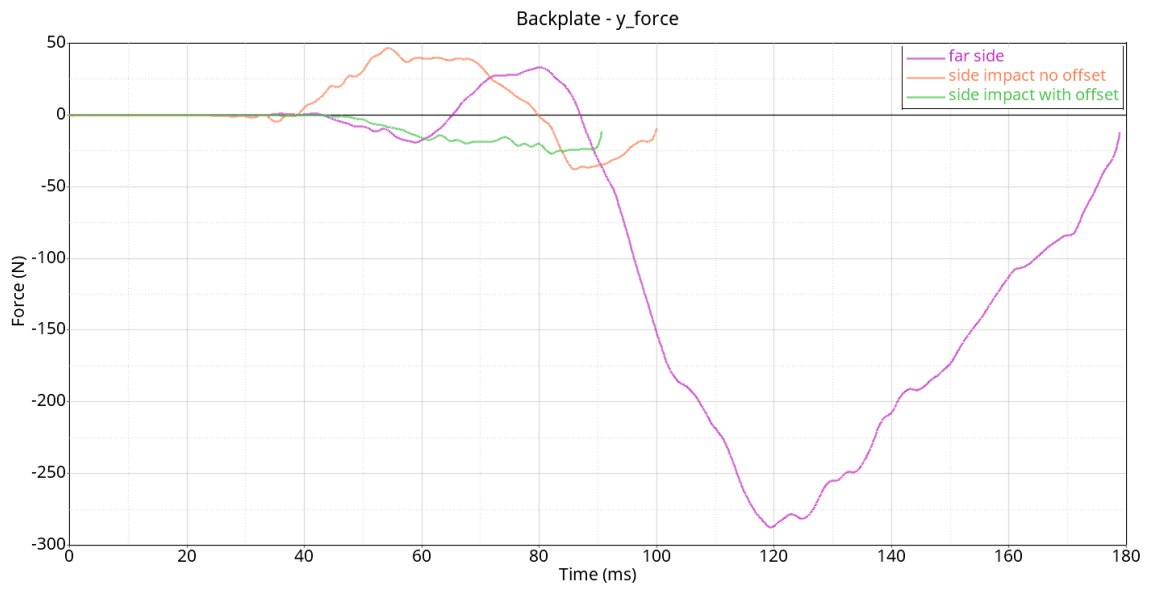


Figure 4-67 - Comparison backplate y forces

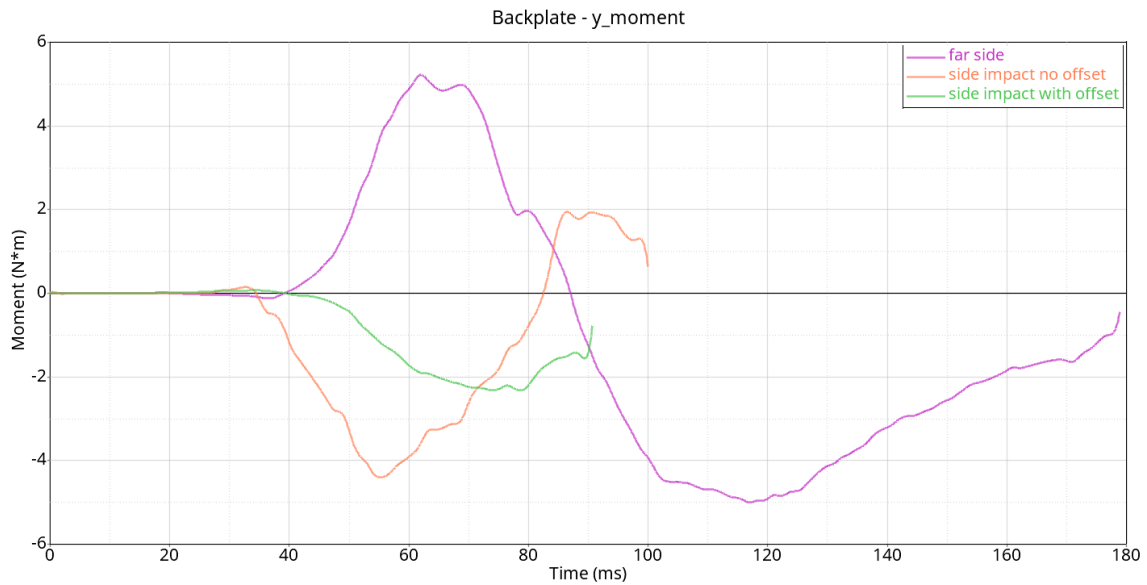


Figure 4-68 - Comparison backplate y moment

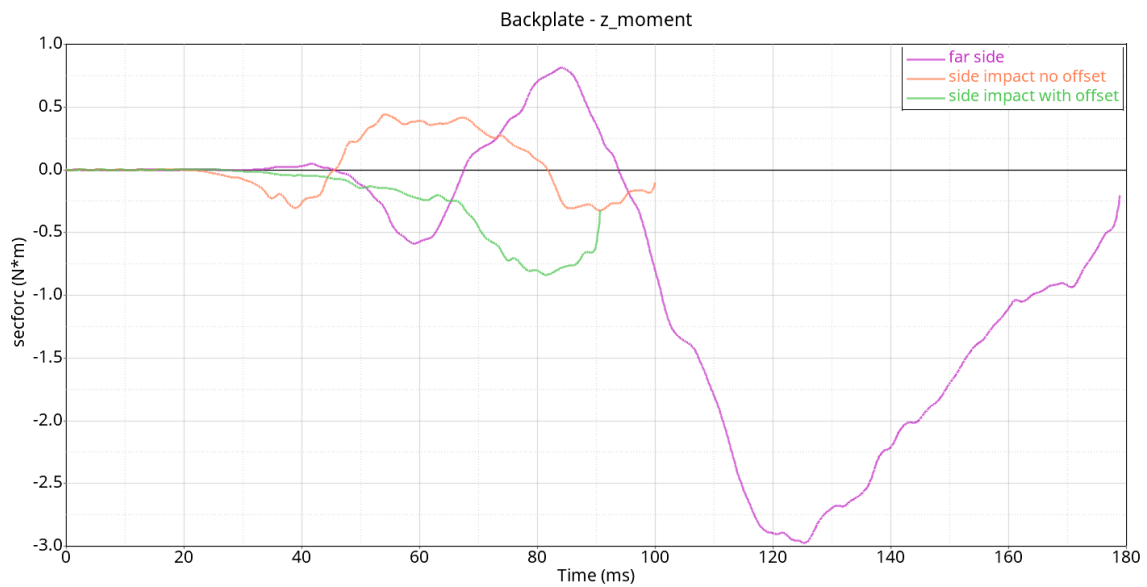


Figure 4-69 - Comparison backplate z moment

From the comparison it is immediately apparent that the backplate is subjected to a greater force along the direction of impact and along x in the case of the far side, while the loads in the case of side impacts are similar. This leads to the conclusion that in the case of the far side impact, the whole spine is more stressed, and from the simulation images this theory is confirmed by the large flexion of the spine.

Pelvis

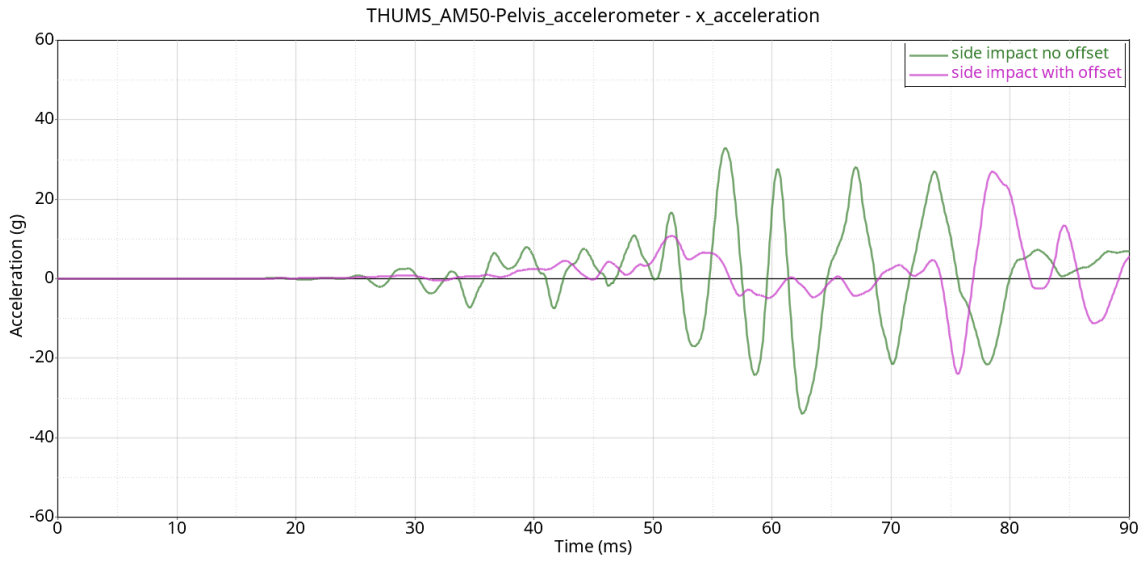


Figure 4-70 - Comparison pelvis x accelerations

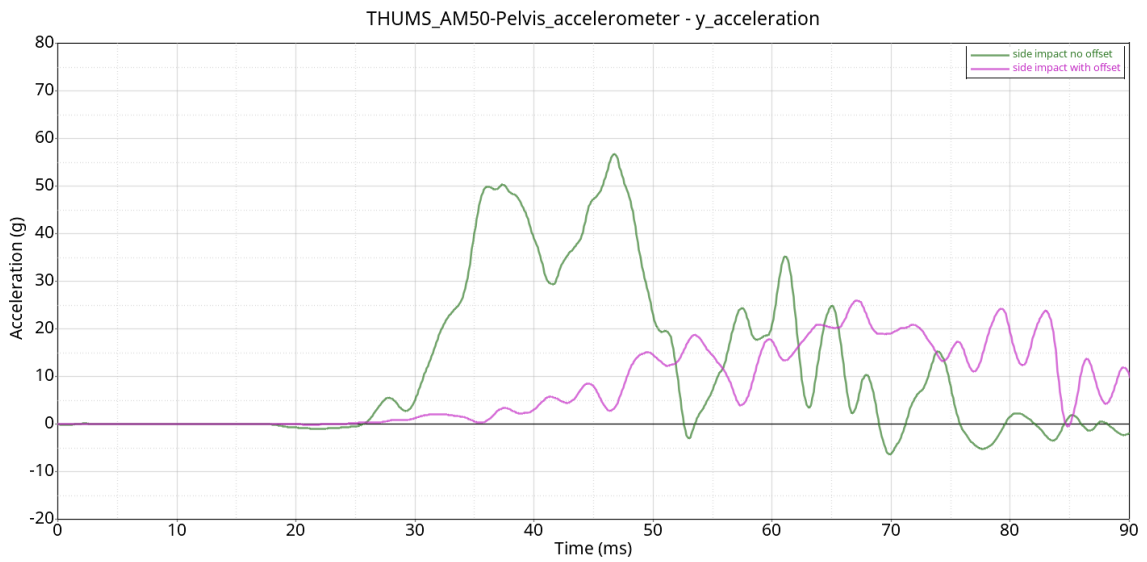


Figure 4-71 - Comparison pelvis y accelerations

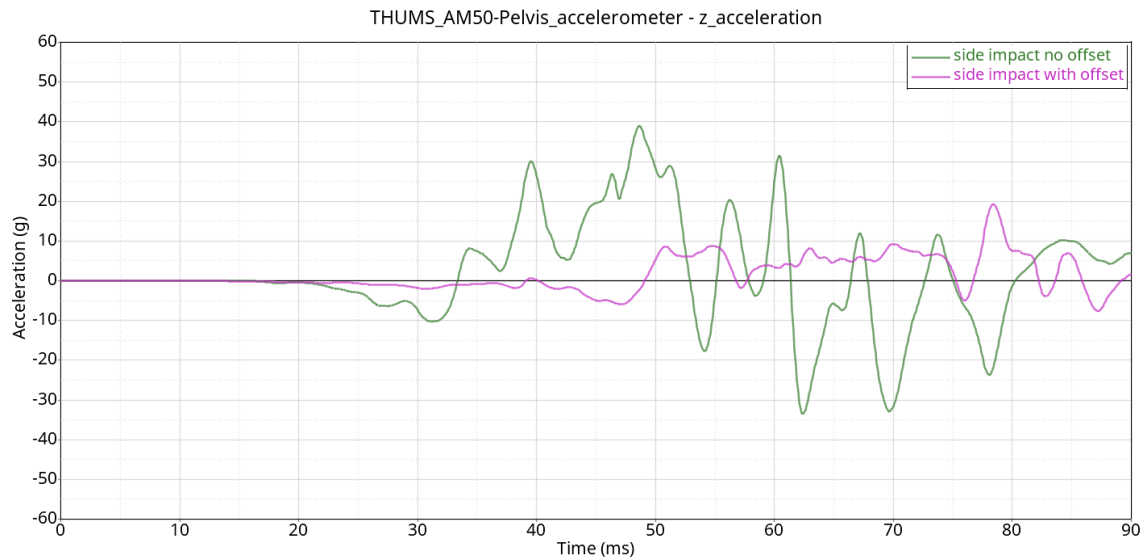


Figure 4-72 - Comparison pelvis z accelerations

From the graphs 4.70 to 4.72, it is evident that the pelvis in the side impact without offset is much more loaded as it is subjected to higher accelerations in all directions than in the case with offset. This result was to be expected as the pelvis is located closer to the point of impact in the case of the side impact standardised.

Pubic Symphysis

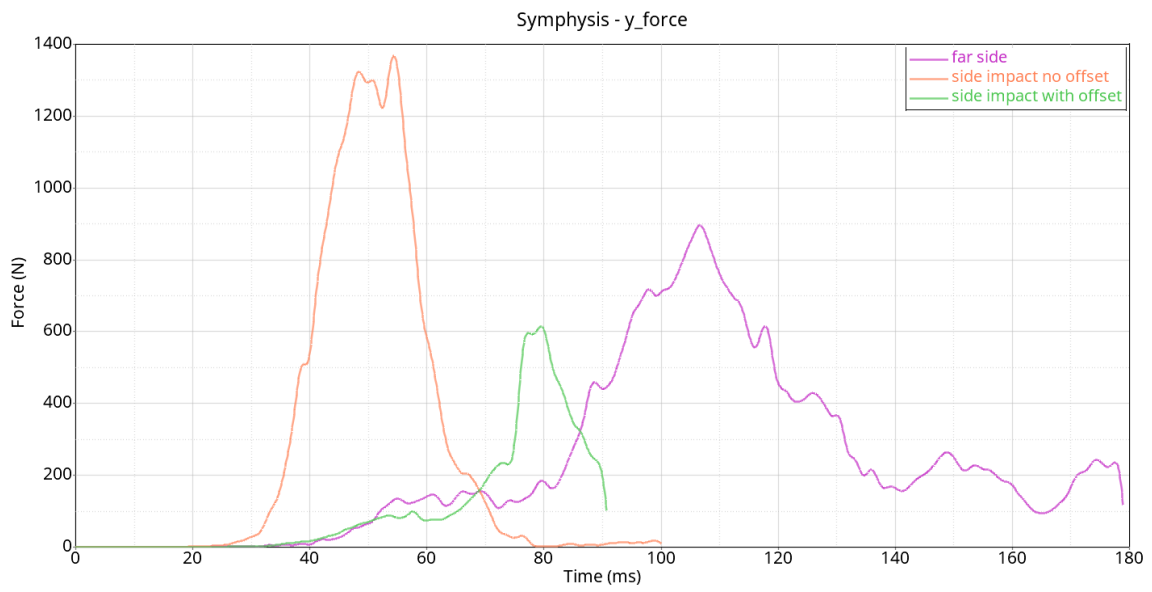


Figure 4-73 - Comparison pubic symphysis y forces

The same considerations made above for the pelvis are also valid for the pubic symphysis. In fact, the case without offset has more than twice the force applied in the direction of the impact.

Right Femur

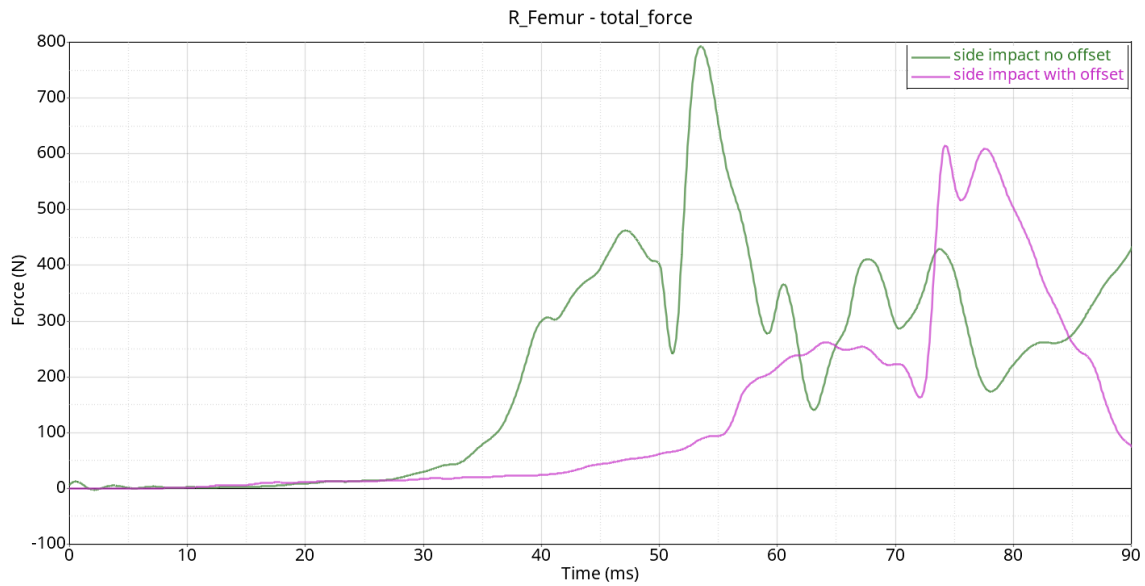


Figure 4-74 - Comparison right femur total forces

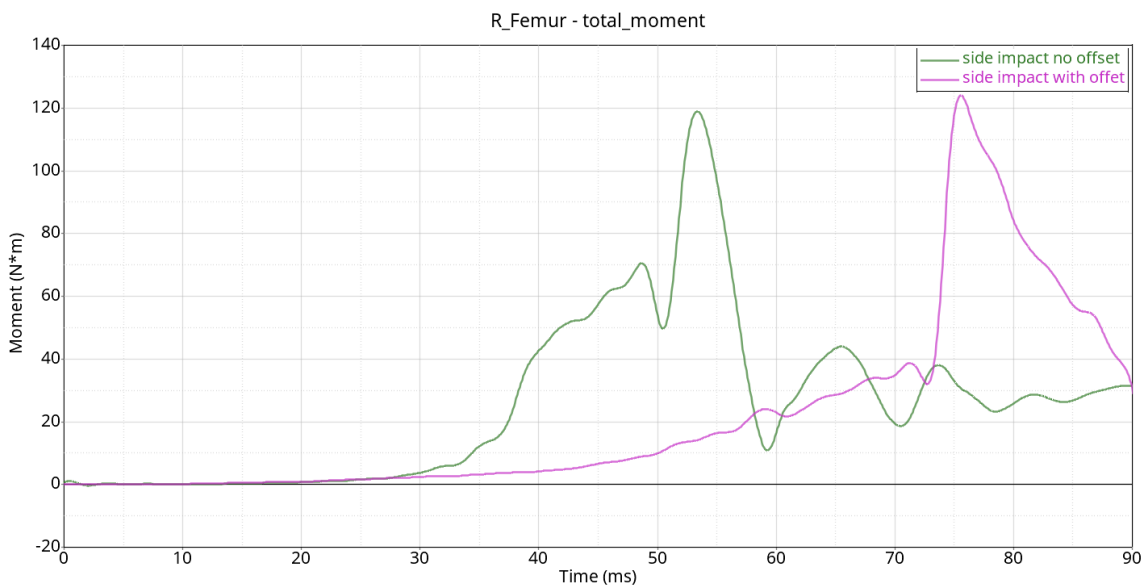


Figure 4-75 - Comparison right femur total moments

With regard to the comparison of the forces on the right femurs, it can be seen in figure 4.74 that the case without offset is subjected to a higher force, whereas if the moments to which they are exposed are analysed, it can be observed in figure 4.75 that in the case with offset the resulting moment is slightly higher.

Left Femur

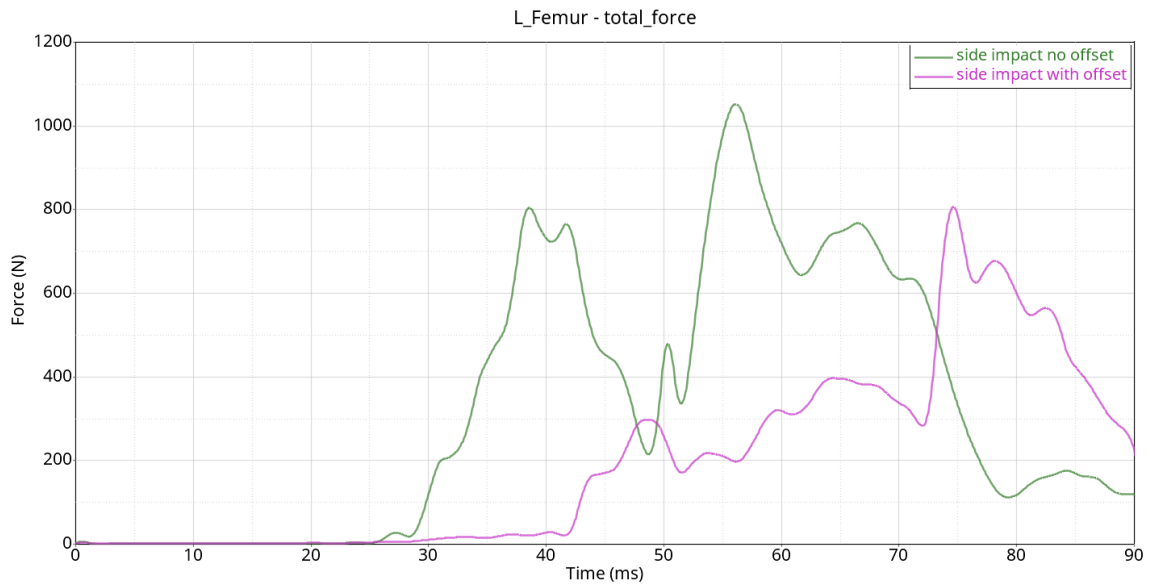


Figure 4-76 - Comparison left femur total forces

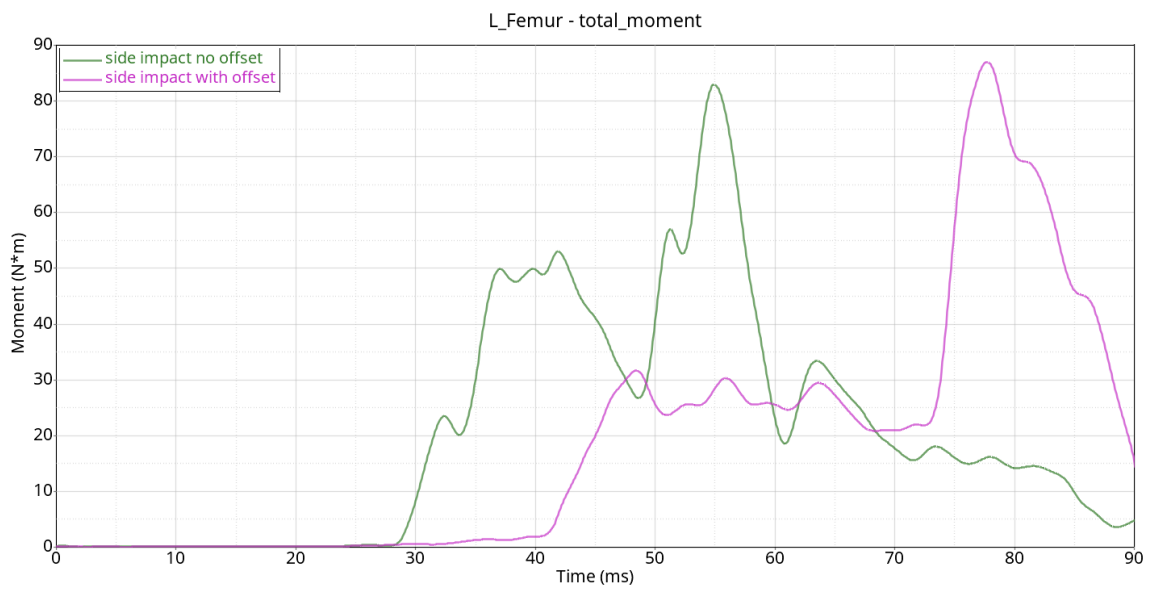


Figure 4-77 - Comparison left femur total moments

In the case of left femurs, the same considerations can be made as for right femurs.

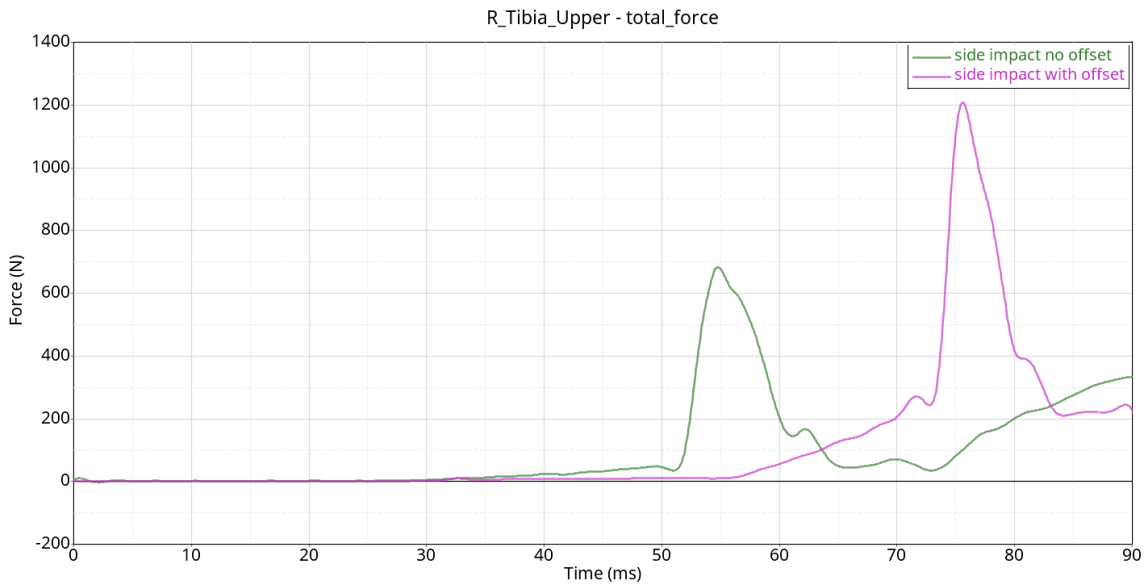
Right upper Tibia

Figure 4-78 - Comparison right upper tibia total forces

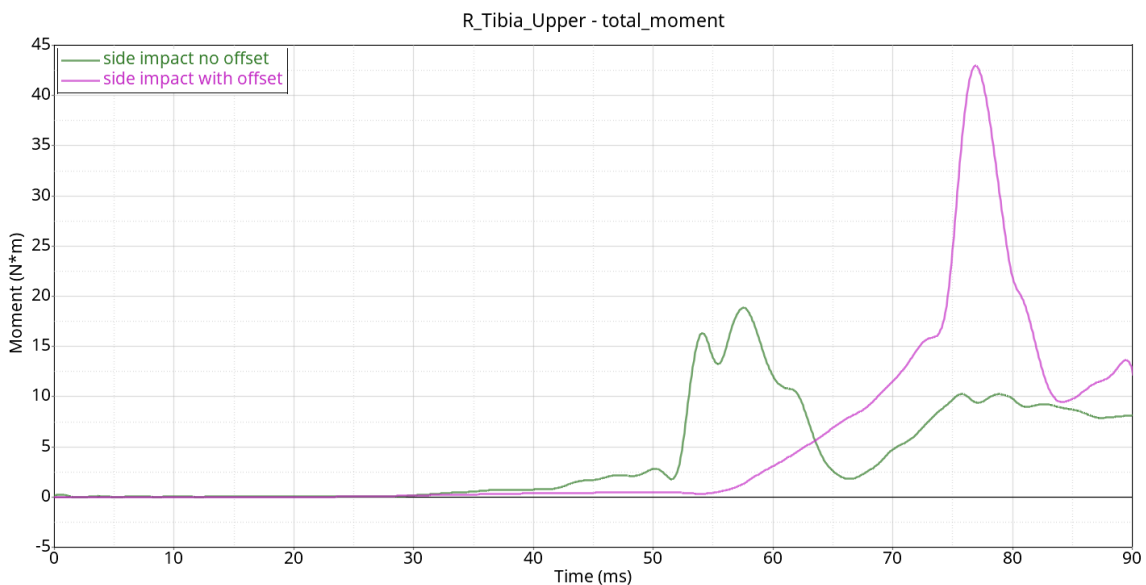


Figure 4-79 - Comparison right upper tibia total moments

When analysing the data on the comparison of the two impact cases on the upper section of the right tibia, a difference to the other parts of the body is immediately apparent. The case with offset is highly loaded, in particular, it can be observed in the figure 4.78 that it has a much more higher resultant force. The right tibia is more loaded because in the case with offset the point of impact is closer to the tibiae being closer to the front axle. In figure 4.79, a total moment more than two times than the case without the offset. This result is justified by the fact that the right tibia is hit by the left and has a rotation.

Right lower Tibia

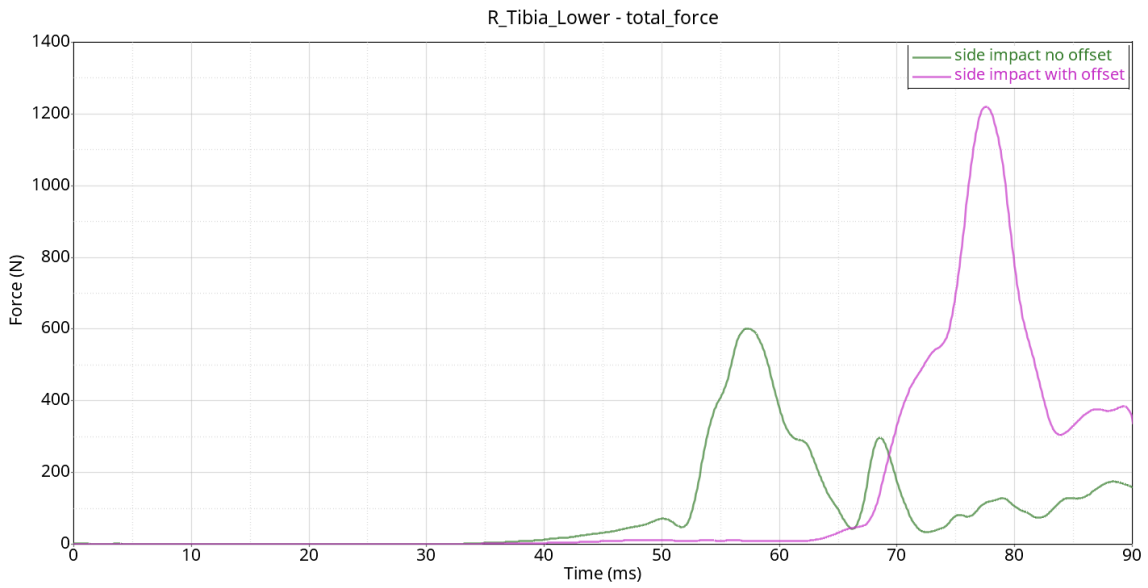


Figure 4-80 - Comparison right lower tibia total forces

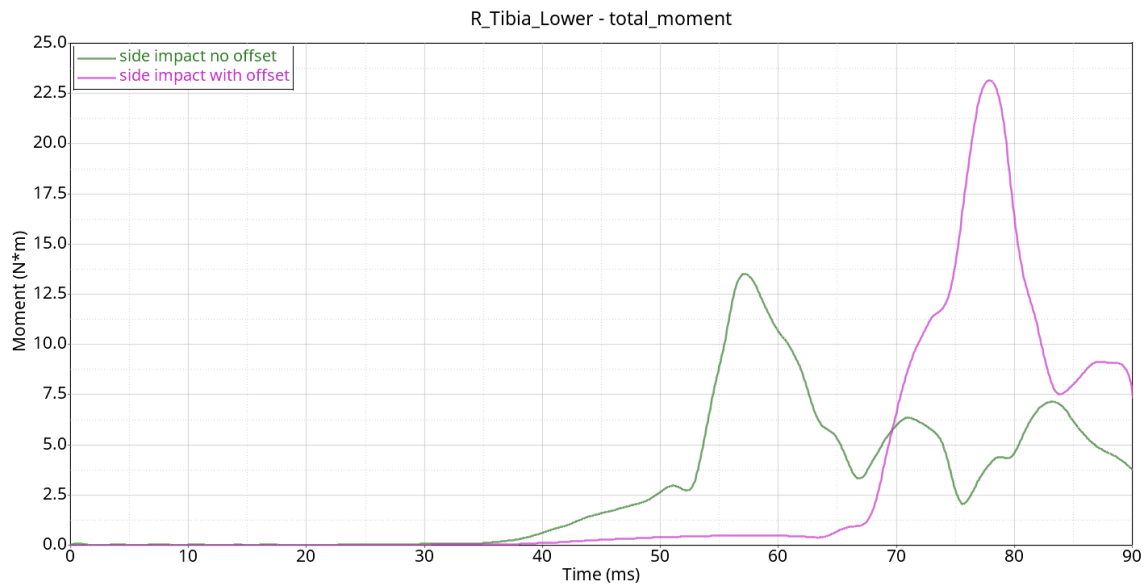


Figure 4-81 - Comparison right lower tibia total moments

The same trend as above can be seen when analysing the lower section of the right tibia. Considering both sections, it can therefore be stated that in the case with offset the right tibia, i.e. the one furthest from the point of impact is more stressed.

Left upper Tibia

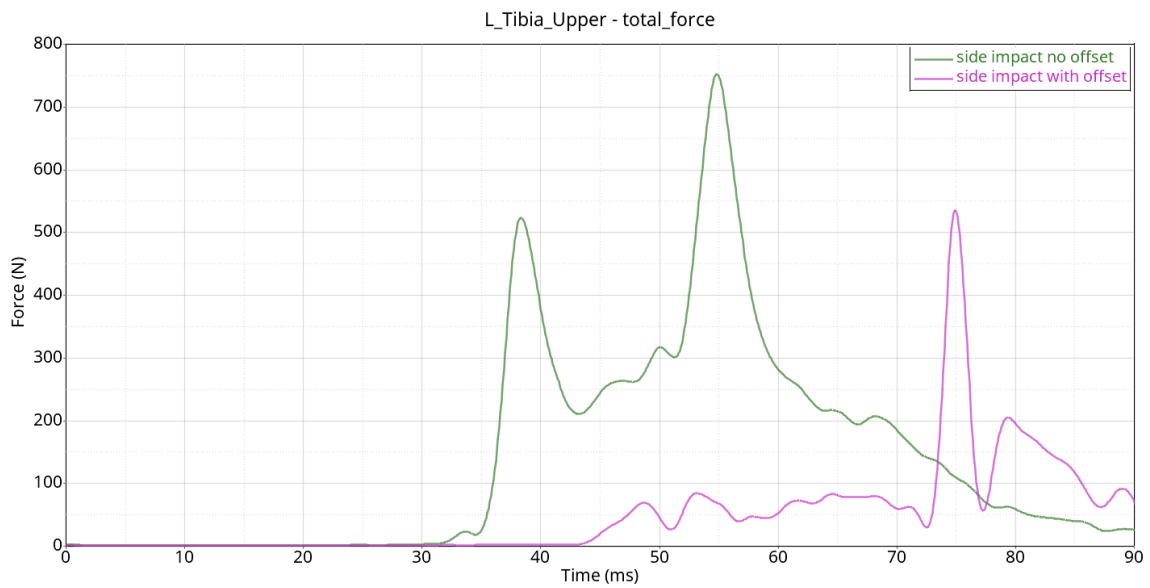


Figure 4-82 - Comparison left upper tibia total forces

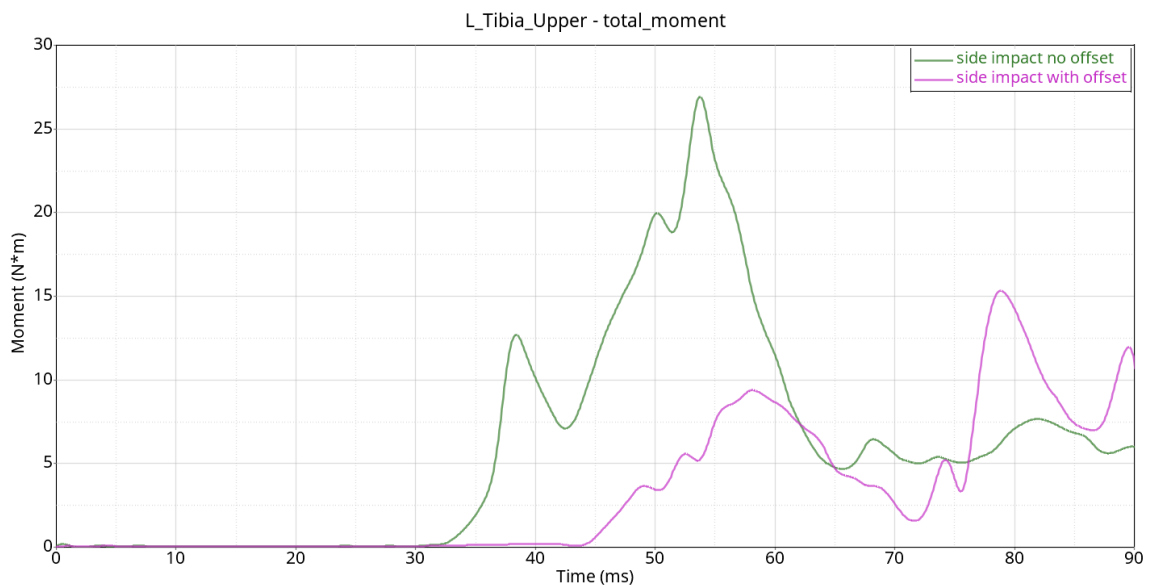


Figure 4-83 - Comparison left upper tibia total moments

Inversely to the considerations made above for the right side, the upper section of the left tibia undergoes greater forces and moments in the case without offset, as you can notice in figure 4.82, 4.83.

Left lower Tibia

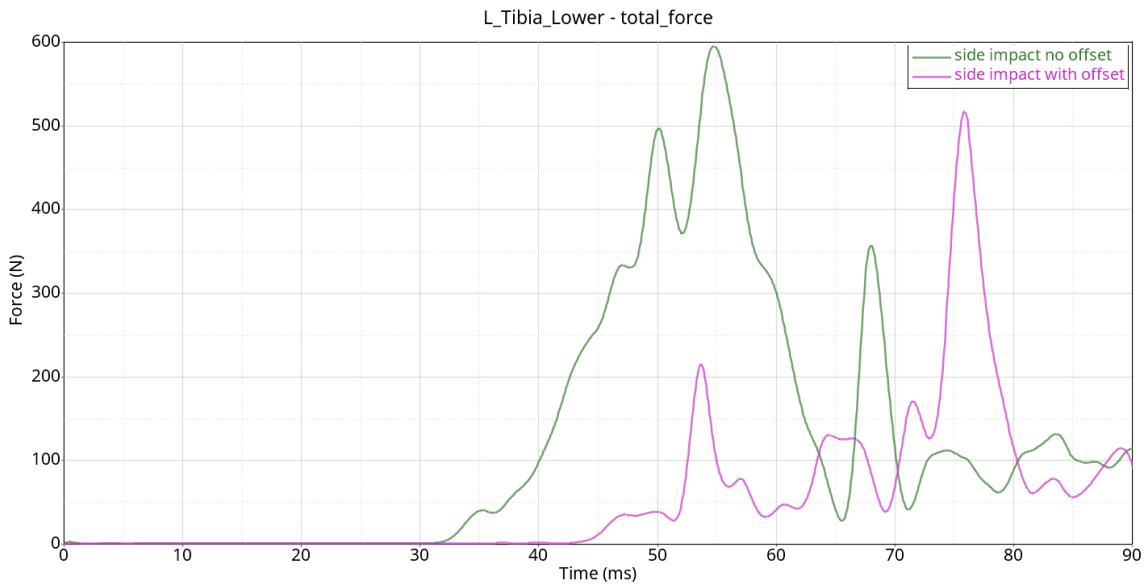


Figure 4-84 - Comparison left lower tibia total forces

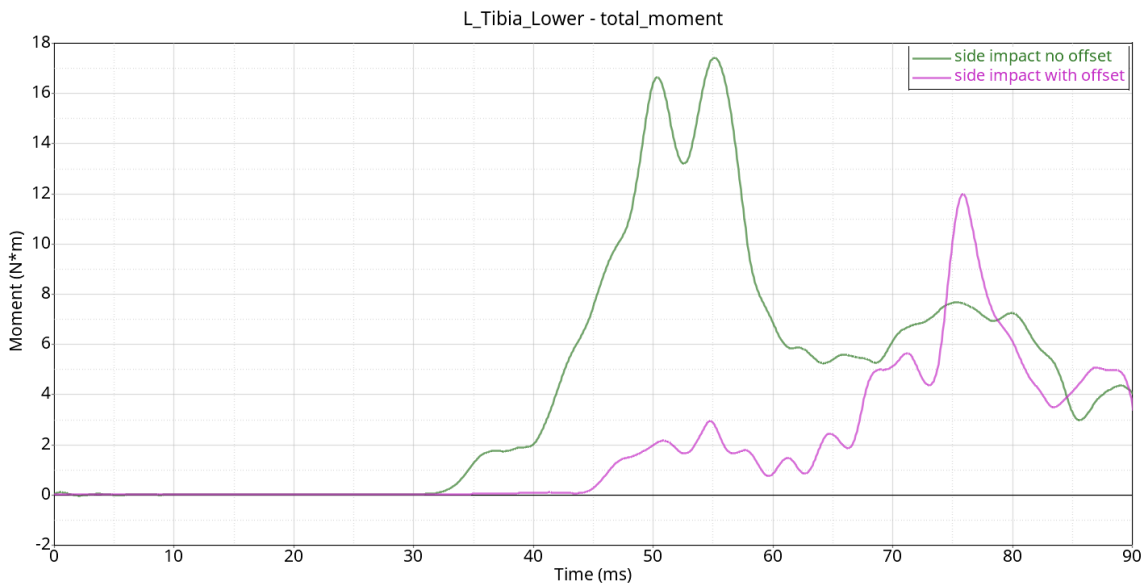


Figure 4-85 - Comparison left lower tibia total moments

The same trend for the upper left tibia is repeated in the left lower section of the tibia but with smaller differences in term of forces and moments. If both sections are analysed, it can be deduced that the left tibia is more stressed in the case without offset. The Tibia Index can now be calculated as proposed in the chapter 1.2.4 taking into account the worst case. In the case without offset the TI is equal to 0.107 while in the case with offset it is 0.152.

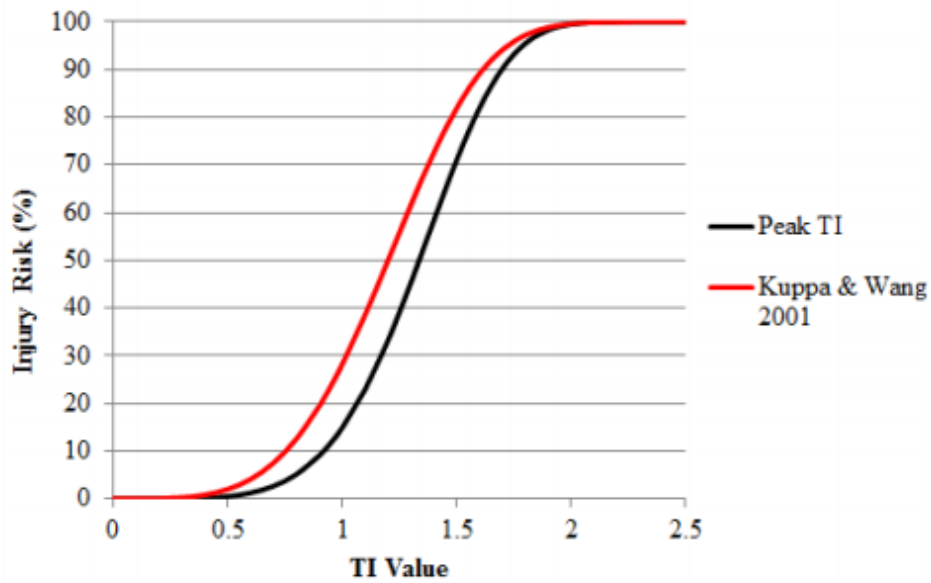


Figure 4-86 - Tibia index risk curve

The probability of injury can be calculated using the experimental curve of Kuppala & Wang [28], which shows that in both cases the risk of injury is practically zero. This is due to the fact that the forces are not too high and are damped during the impact by the non-rigid but deformable parts of the vehicle.

Chapter 5: Conclusions

In this thesis a side impact with an offset respect to the R point was studied with a FE simulation and Human Body Model. This type of crash test is not regulated by Euro NCAP but to recreate this type of impact it refers to the standard of Euro NCAP for lateral impacts in order to compare the results. The Euro NCAP side impact test consist in the side impact of a movable deformable barrier thrown against the car tested, at 50km/h. The direction of impact of the barrier is perpendicular to the car, the MDB strikes the vehicle with an offset respect to the standard case, in particular the point of impact at the front axle has been chosen. All the simulations were run using LS-DYNA version R9 and LS-PP software was used for the pre-processing.

The FE simulation was composed by the following FE models:

- Advance European Movable Deformable Barrier (AE-MDB)
- 2012 Toyota Camry mid sedan
- Total Human Model for Safety (THUMS)

First the AE-MDB was validated according to the documentation provided by LSTC, then a fully simulation without the HBM was set and run. The results were completed and showed a correct and satisfying behaviour.

After this step the Human Body Model was positioned, through the PIPER software and a seatbelt model was created and fit on the THUMS to ensure the driver to the seat, previously deformed with a sitting simulation. A set of accelerometers and load sensors was implemented in the human model to track the behaviour of critical parts of the human body during the impact. Head, neck, thorax, pelvis, and lower limbs were tracked, according to the Euro NCAP standard and not. Some sensors were added to track the volume and surface area of defined internal organs and the ribcage, lastly some markers were positioned along the spine of the HBM, in order to track the deformation of it during the impact. This allows to have a complete idea of the severity of the impact and fully use the potential of the THUMS. The FE simulation was then run for a considered time interval of 90ms, where, according to the literature, there is the peak value of acceleration. The simulation was completed after around 32 hours with 64 cores with 27.7 Gb of memory utilized.

The biomechanical results were then analysed and injury criteria , described in chapter 2.2 were calculated. The data obtained from the simulation are then compared with those from the side impact case and the far side in order to analyse the differences in the three types of impact.

The results show a satisfying behaviour of the vehicle and the MDB, this is also confirmed by the energy analysis and by the energy ratio, tending towards unity.

Analysing the sensor's output, an important acceleration of the head was detected, with a peak value of 88g. The severity of the head injury was analysed also with the Head Injury Criteria, the value obtained is 220. Using the Prasad-Mertz set of curves to have a better idea of the injury level, it was obtained a very low probability of severe injury of 2.4% and a probability of minor injury of 28%.

Continuing the analysis, an important deflection of the neck was noticed by the images of the simulation and indagated, analysing the moments and the forces of the upper and lower neck, i.e., C1 and C7 vertebrae, and through the Neck Injury Criteria (Nij). Both the results were found not to be significant enough to generate an injury, which was confirmed by the very low Nij calculation.

As expected, the chest is the area most at risk for injury and cause of death. This aspect is confirmed in the case of offset, in fact, this evidence was found through the thorax deflection and the Viscous Criterion (VC). In particular, the lower thorax, corresponding to the 9th ribs is subjected to a large deformation of 35mm and the VC calculated was 0.64 m/s which is correlated to a 39% of a medium or severe injury. The accelerations of the upper set of thorax vertebrae (T1, T4) are all relatively high.

Analysing the biomechanical data obtained from the sensors placed on the lower part of the body, there are no peaks that could lead to possible injuries, in particular, analysing the tibiae, it is possible to calculate the TI, which is very low. Despite the proximity of the tibiae to the point of impact, they are not subjected to high loads, since the largest amount of the impact energy is lost in the deformation of the vehicle.

These results shows that the severity of the injury is higher in the upper part of the body and then it slightly decreases as soon as the lower part of the body is considered. This confirms that the statistics found on the literature for side impact are also valid for the side impact with offset. These in fact state that the upper part of the body (head and thorax) is the most injured during side impact crashes. It is important to remember that the car model used in this thesis was not provided with any passive safety system, like the side airbag.

The comparison with the other two impact cases allows us to note some interesting things. The data considered in the comparison are mainly those required by the Euro NCAP regulations, so there is no lower body data for the far side. It can be seen immediately that, although the peak acceleration to which the head is subjected in the case with offset is slightly higher than the others, the case without offset turns out to be the one with the highest HIC and therefore the most dangerous for the head. this is because it has a high acceleration but for a longer time interval. The head however results to be less stressed in the case of the far side.

Analysing the back, the comparison with the greatest differences is in the study of the T12 vertebra. The force along the direction of impact is much higher in the far side case.

The same is valid for the backplate that is more stressed in the case of far side compared to the others. If we analyse the thorax instead the side impact without offset is the worst case with more probability of injury followed by the case with offset.

Taking into consideration the inferior limbs it is noticed as the tibias in the case with offset are more solicited but however under every limit of risk of injury.

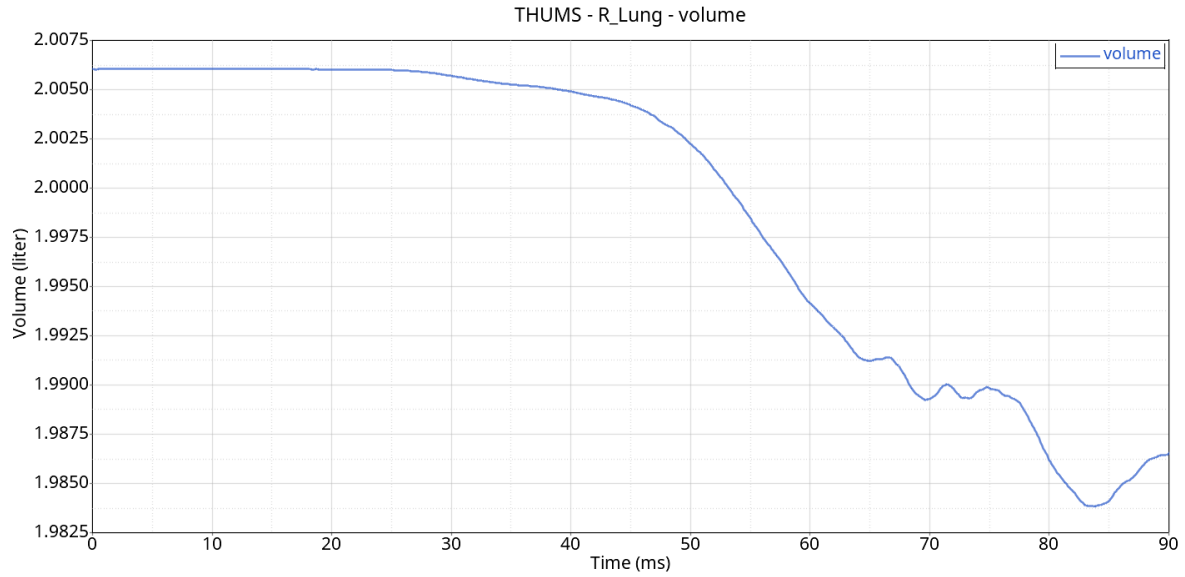
The side impact without offset is more dangerous for the upper body, in particular for the head, the back instead is more loaded in the case in the far side because of the great excursion of the spine during the impact. In the offset case the legs are more loaded than in the other cases because they are closer to the point of impact but are not at risk of injury. The case with offset is therefore less severe than the corresponding case without offset.

The use of an HBM in this thesis allow to have a complete idea of the body behaviour during the impact and give to the user the possibility of analysed more data, compared to the real dummy used in the NCAP test, like the internal organs volume, the surface area of them and the spine deformation. The advantages of the HBM results clear, with a low budget analysis and a potential complete understanding of the body behaviour. The implementation of this type of analysis in the automotive industry can give a preliminary view of a crash scenario and will be a fundamental tool for the passive safety systems design and beyond.

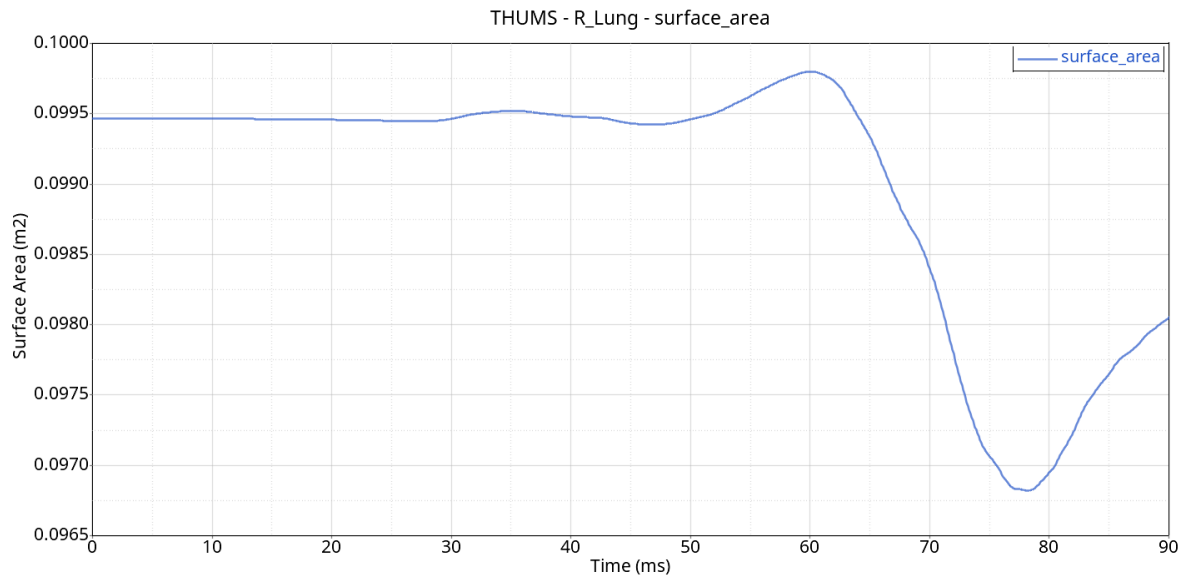
Appendix A

In this appendix results of the variation of volume and surface area of the internal organs are shown below:

Right Lung

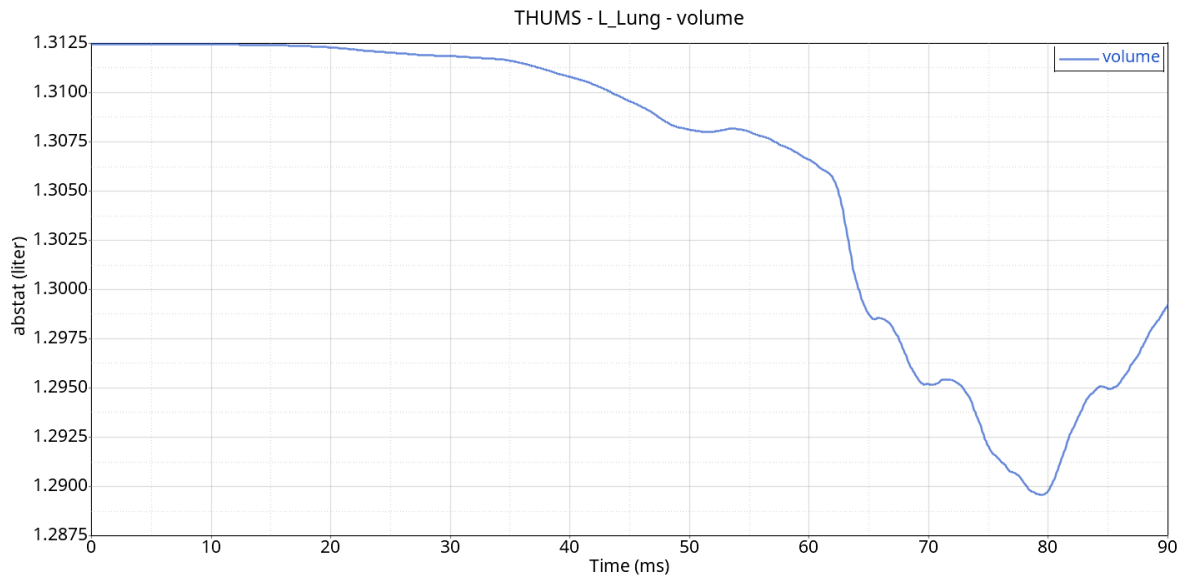


Appendix A 1 - Right lung volume

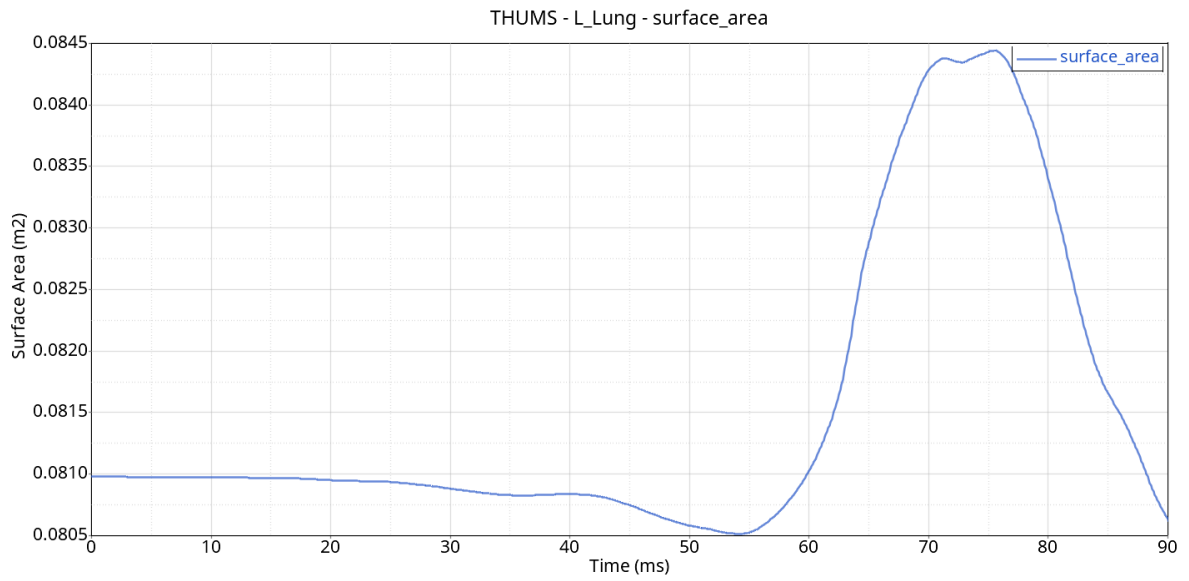


Appendix A 2 - Right lung surface area

Left Lung

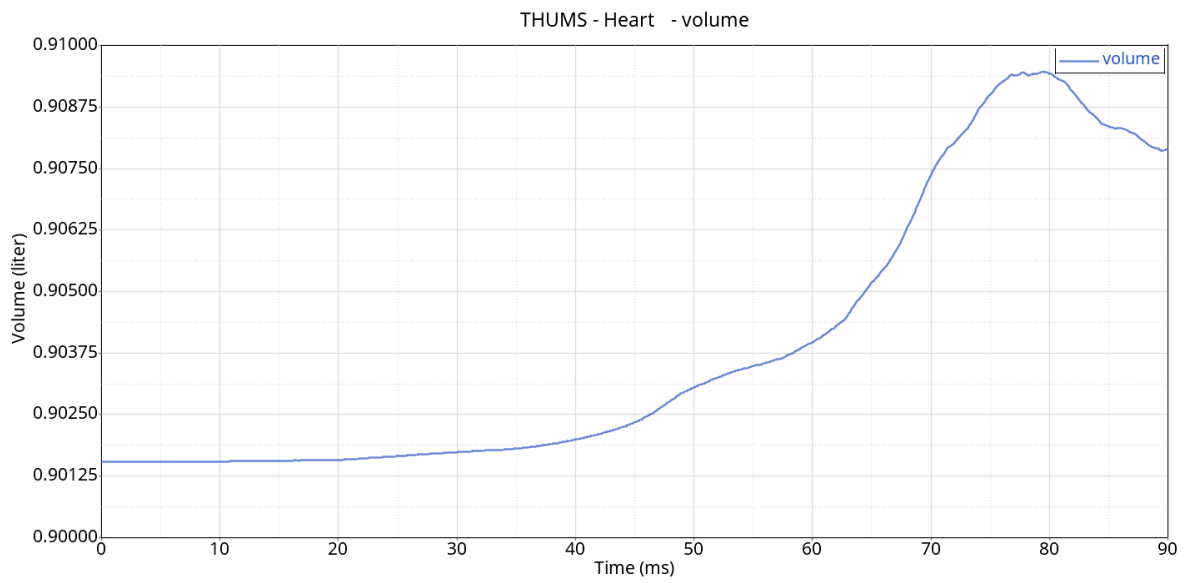


Appendix A 3 - Left lung volume

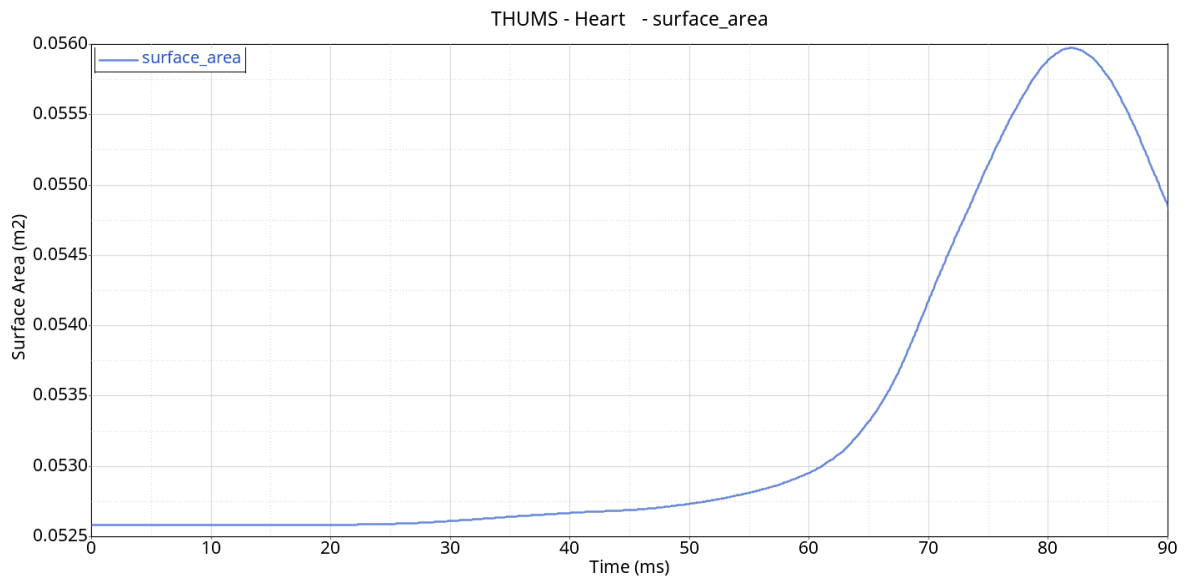


Appendix A 4 - Left lung surface area

Heart

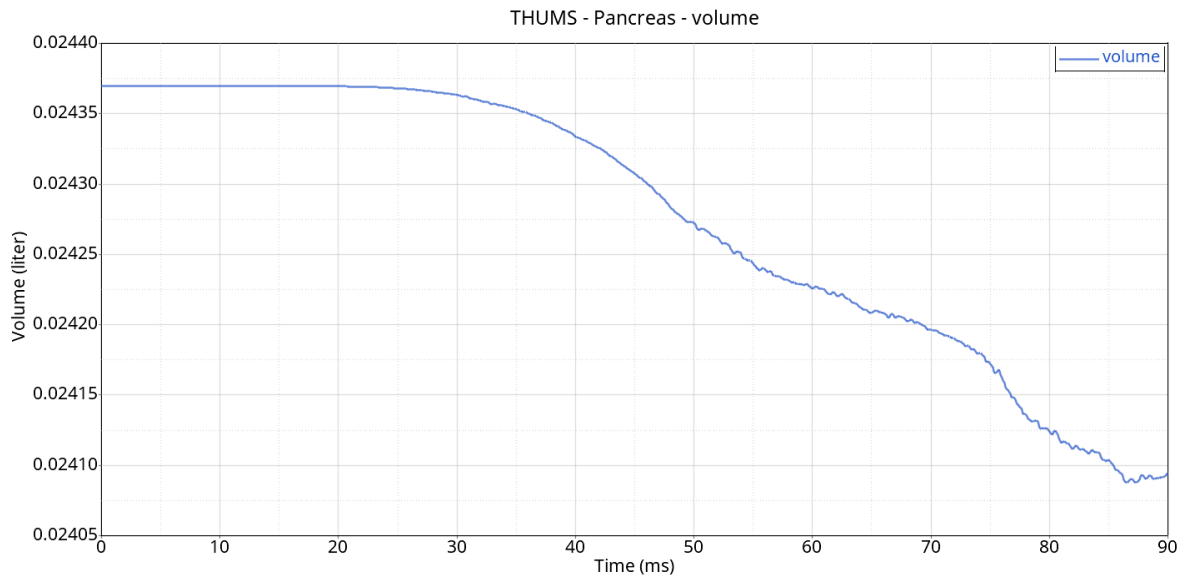


Appendix A 5 - Heart volume

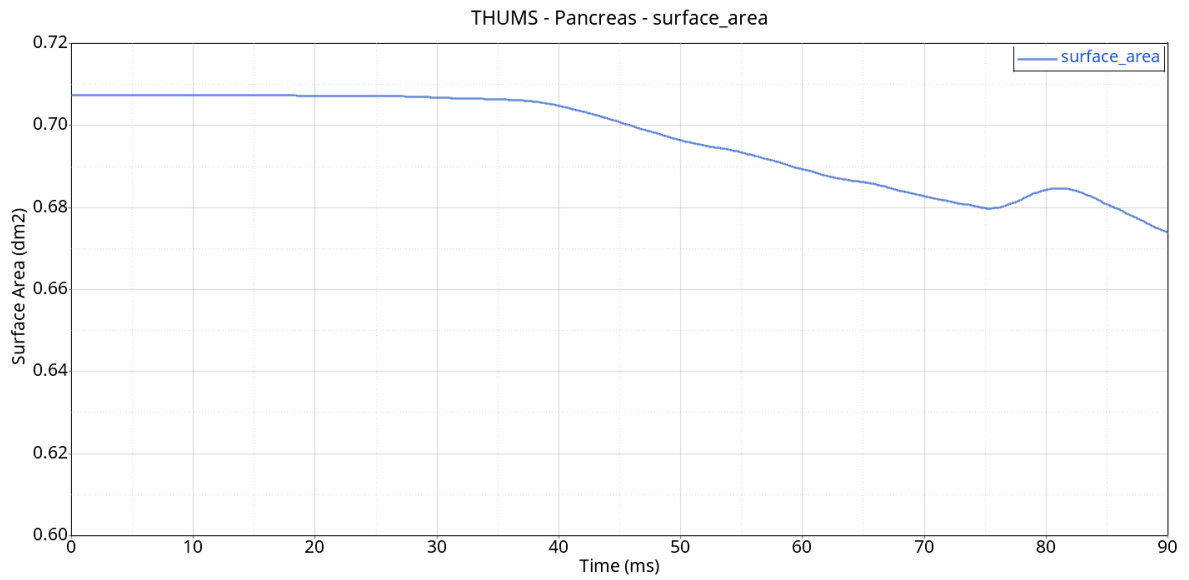


Appendix A 6 - Heart surface area

Pancreas

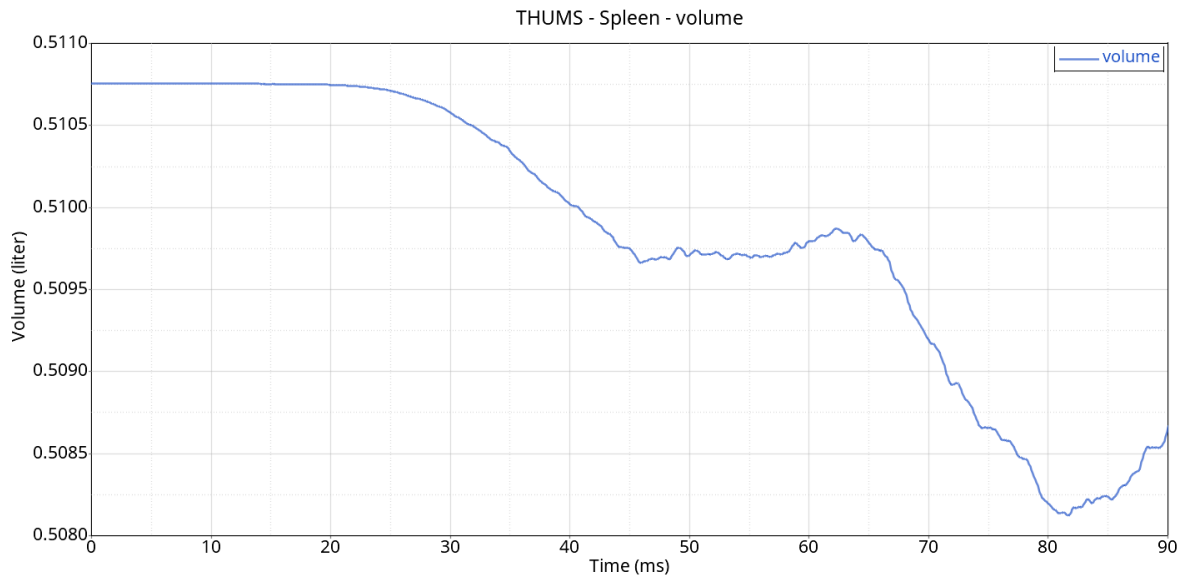


Appendix A 7 - Pancreas volume

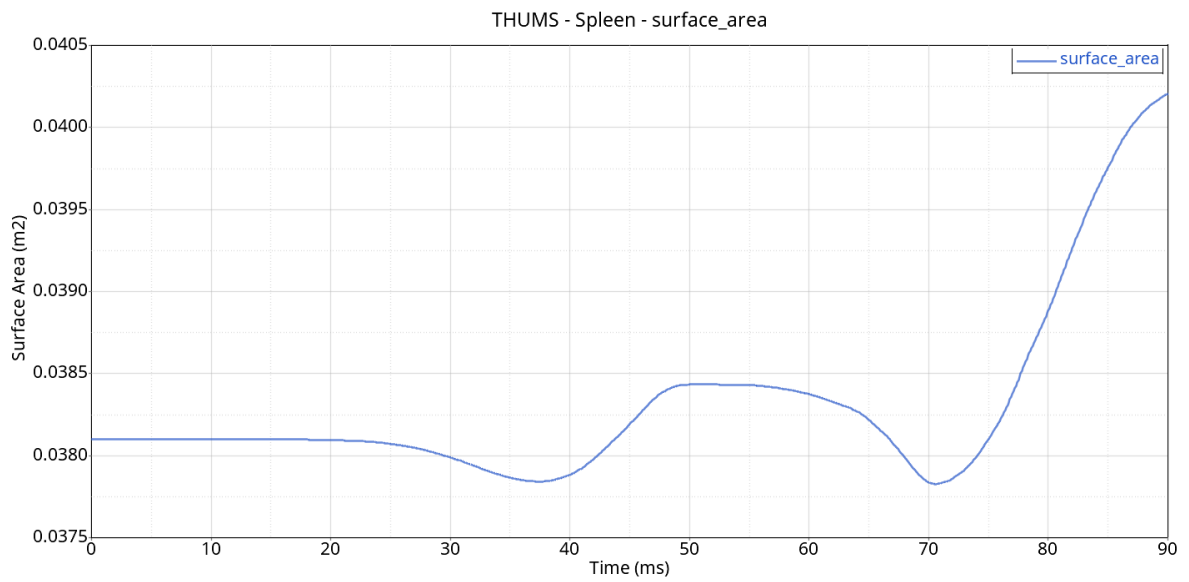


Appendix A 8 - Pancreas surface area

Spleen

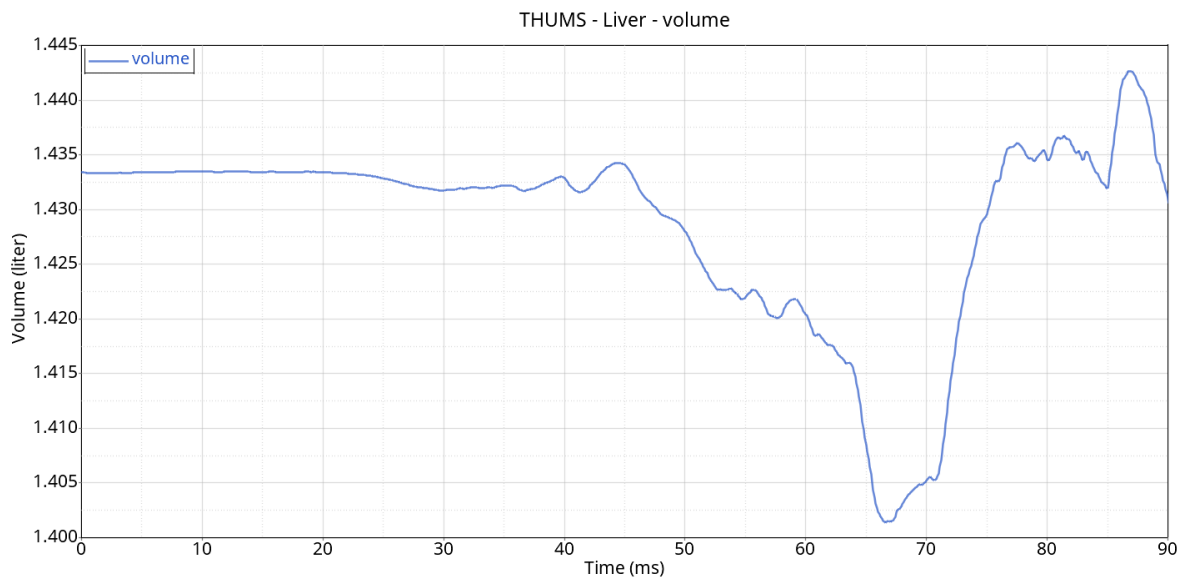


Appendix A 9 - Spleen volume

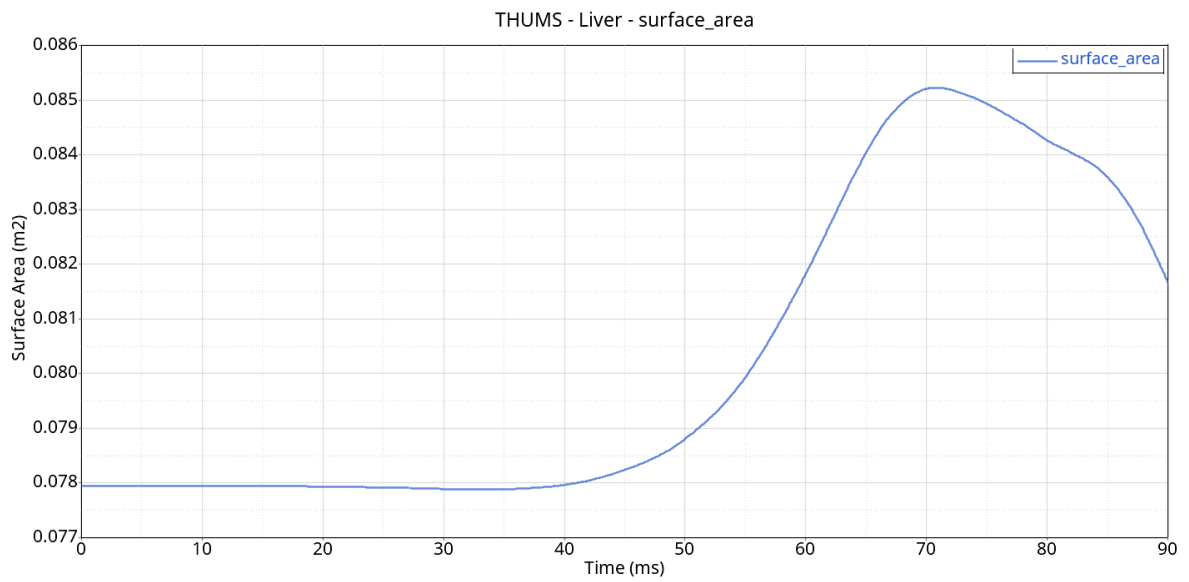


Appendix A 10 - Spleen surface area

Liver

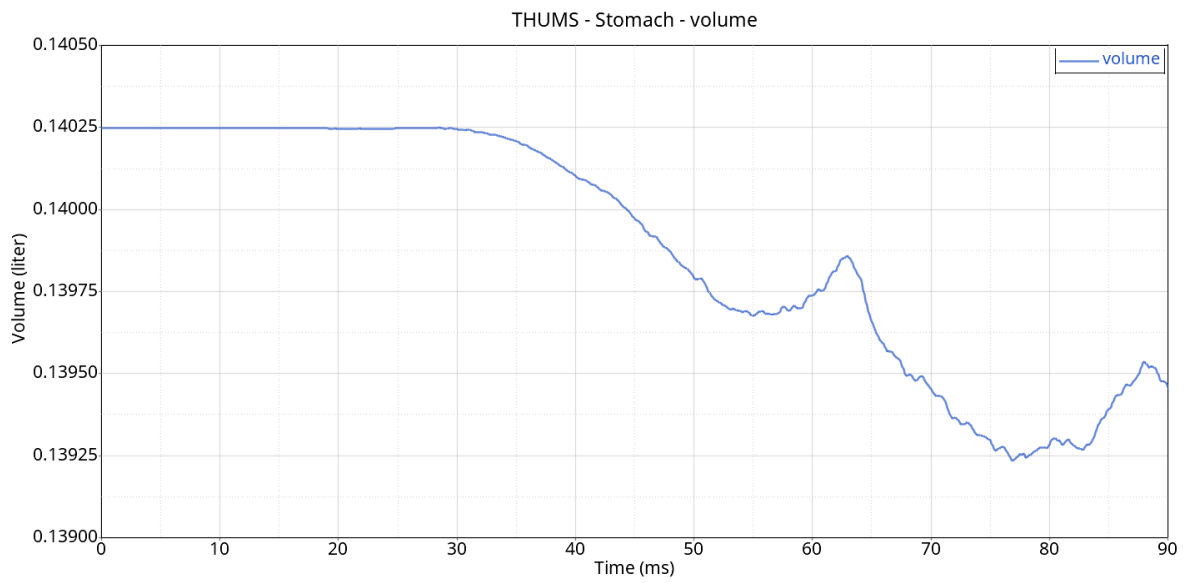


Appendix A 11 - Liver volume

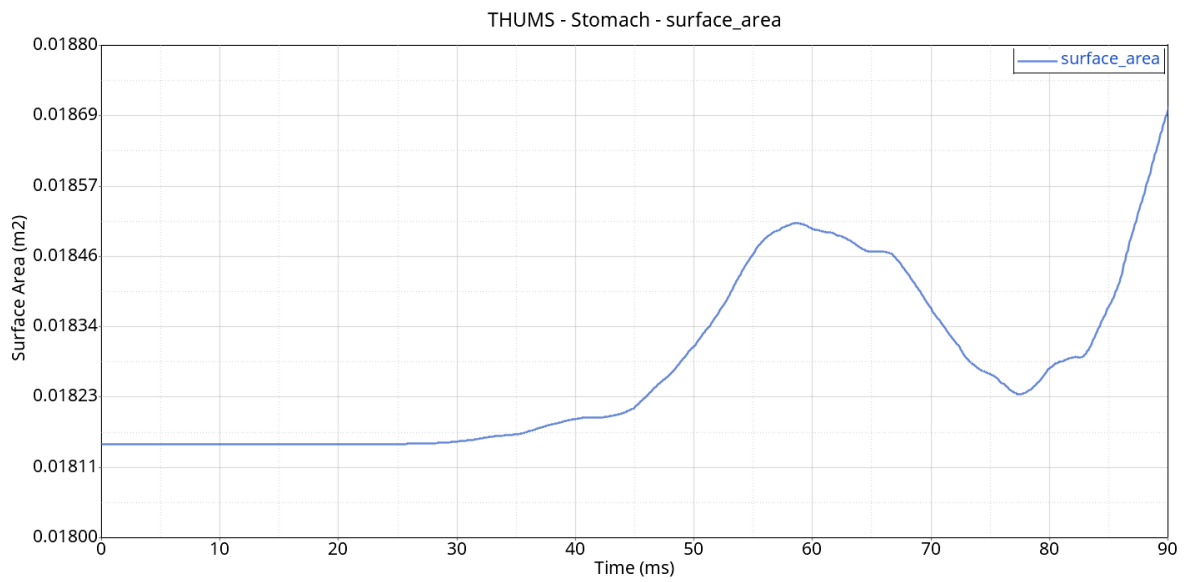


Appendix A 12 - Liver surface area

Stomach

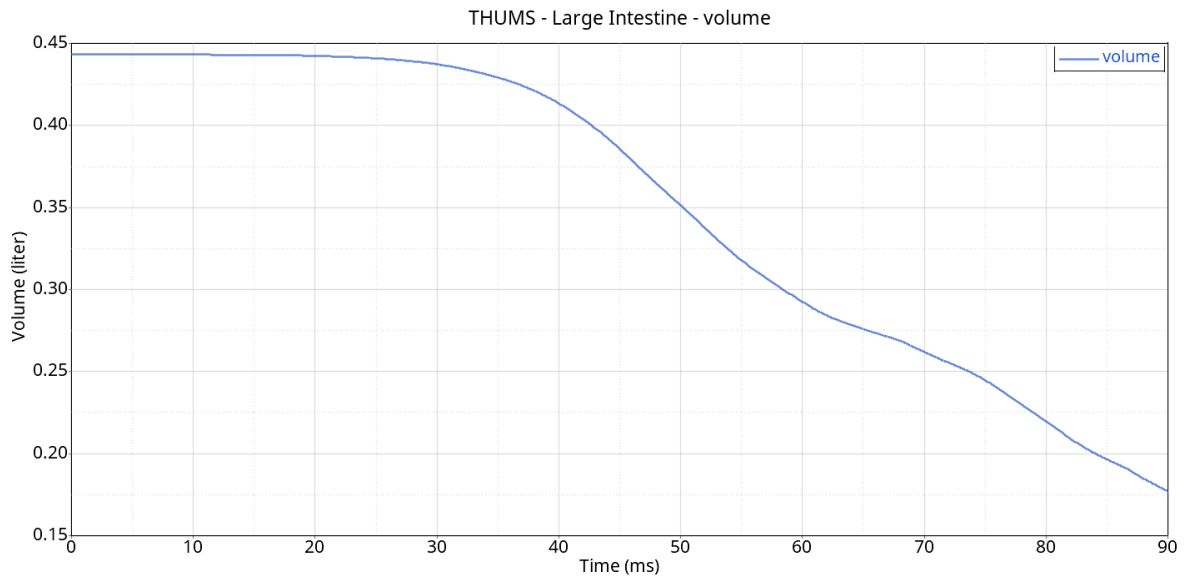


Appendix A 13 - Stomach volume

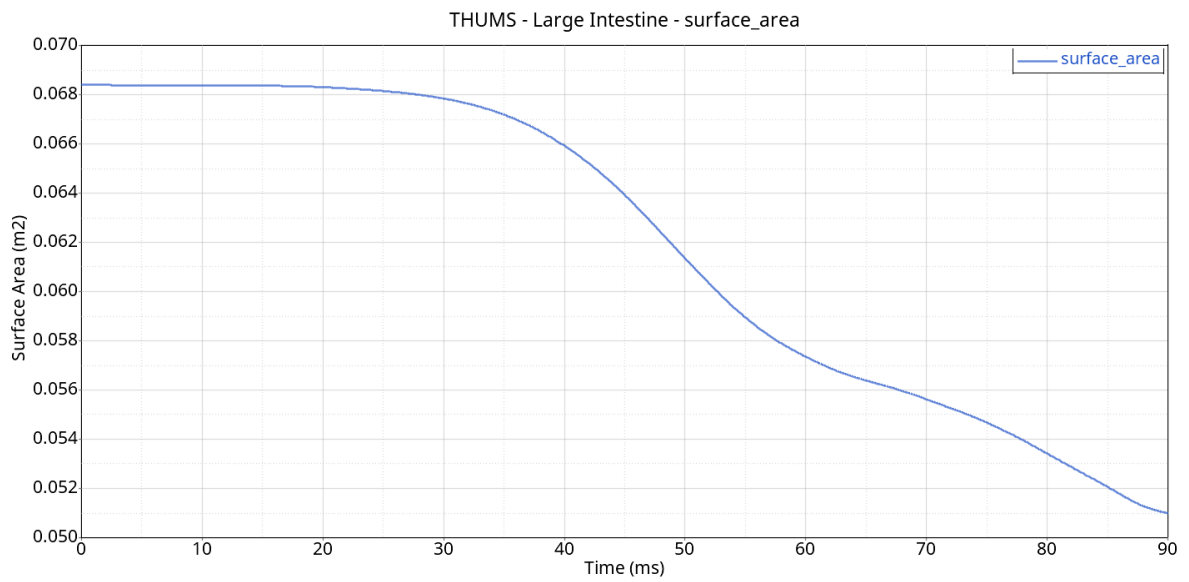


Appendix A 14 - Stomach surface area

Large Intestine

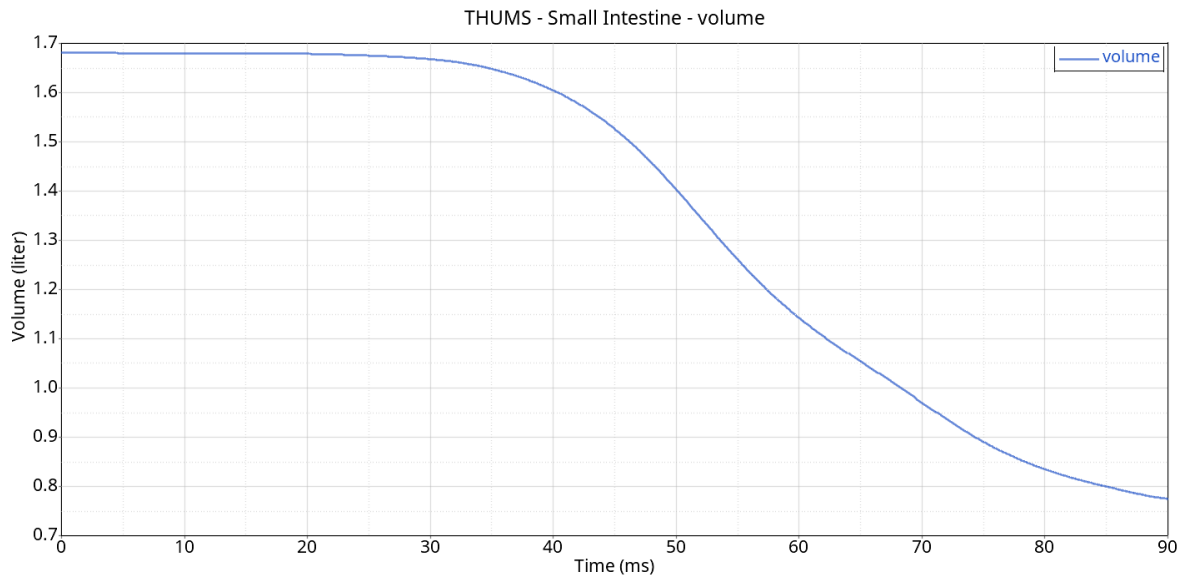


Appendix A 15 - Large intestine volume

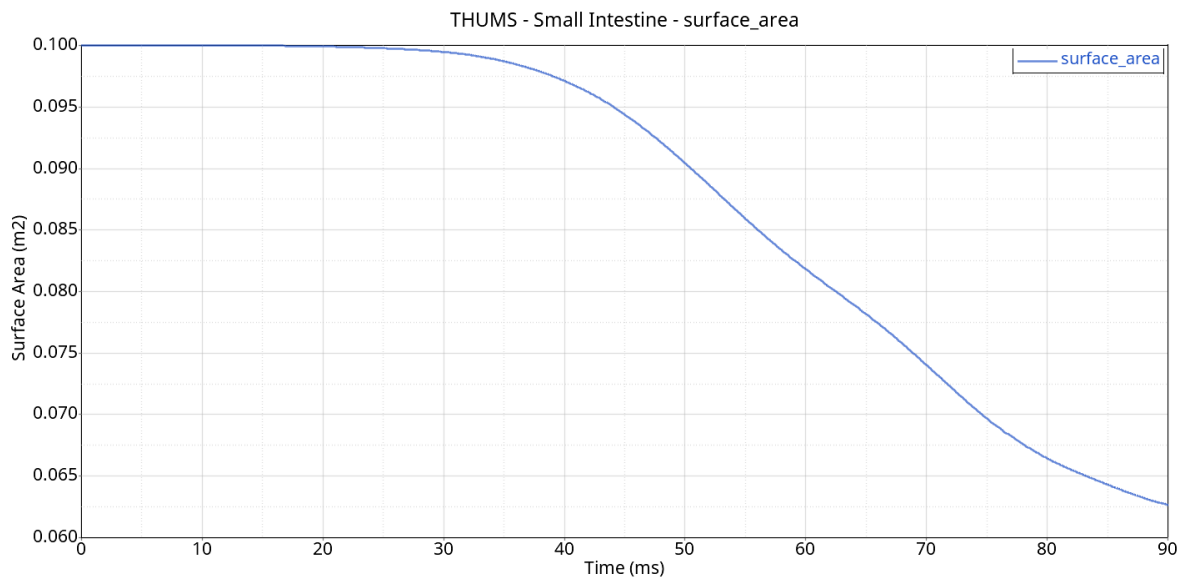


Appendix A 16 - Large intestine surface area

Small Intestine

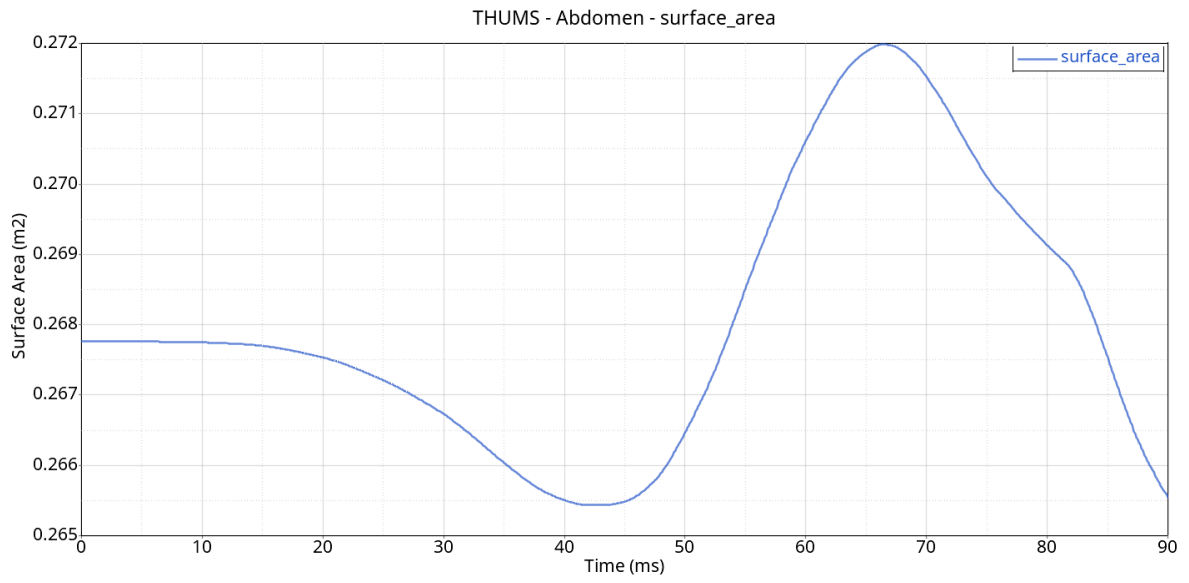


Appendix A 17 - Small intestine volume

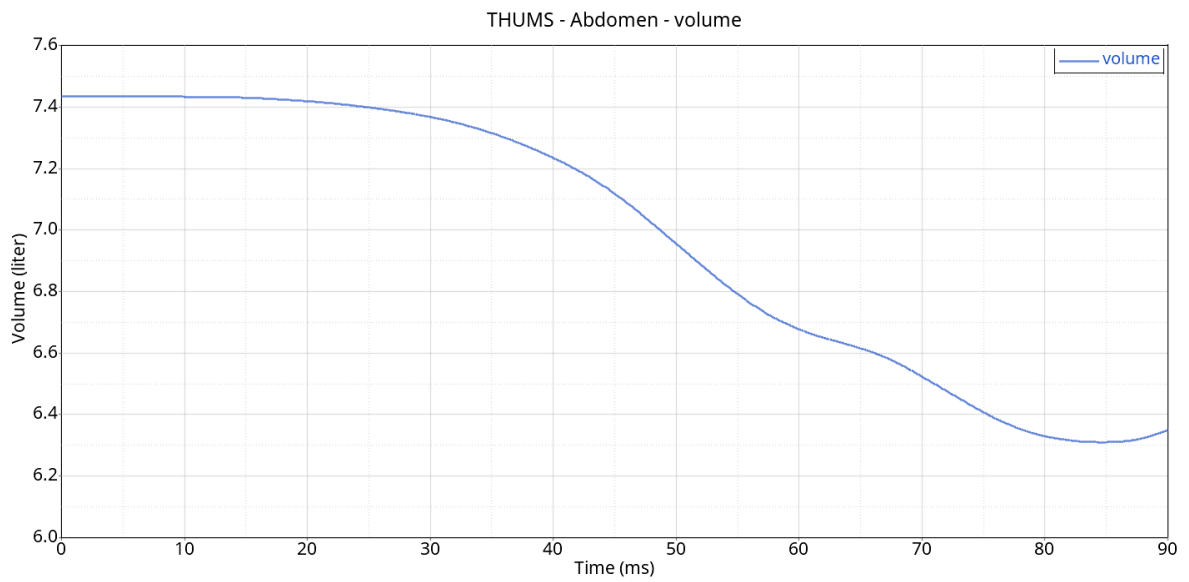


Appendix A 18 - Small intestine surface area

Abdomen



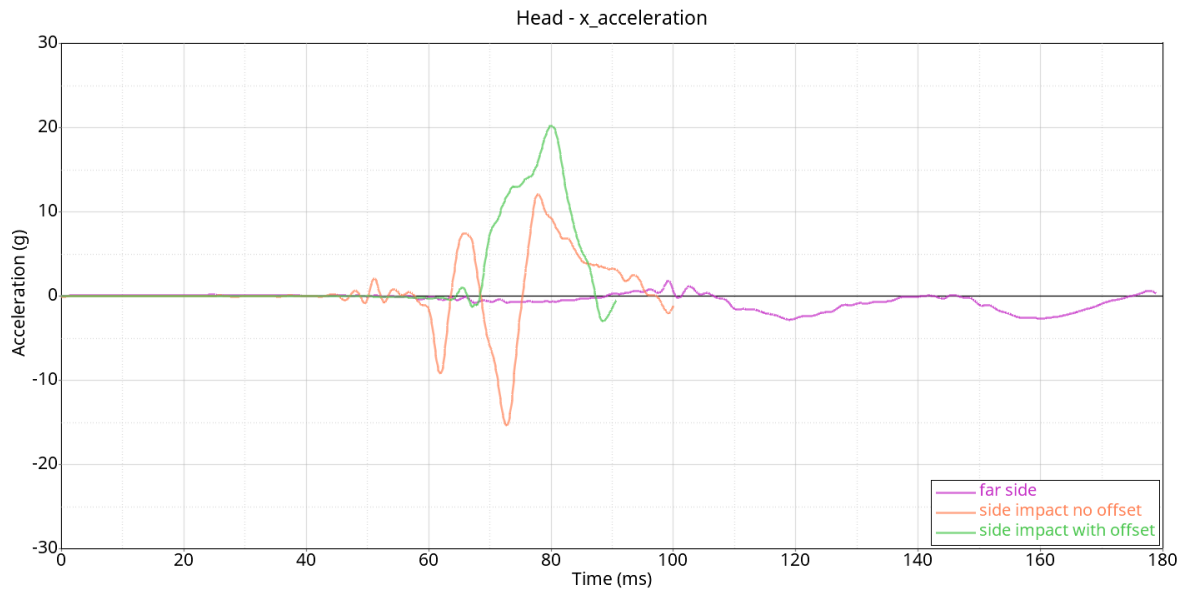
Appendix A 19 - Abdomen volume



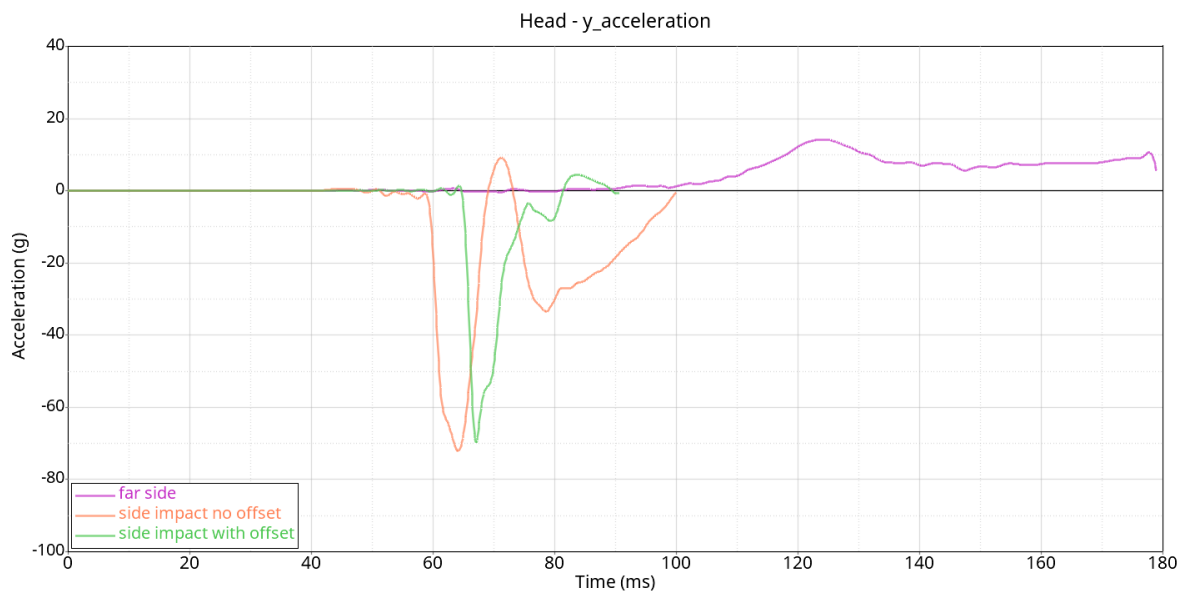
Appendix A 20 - Abdomen surface area

Appendix B

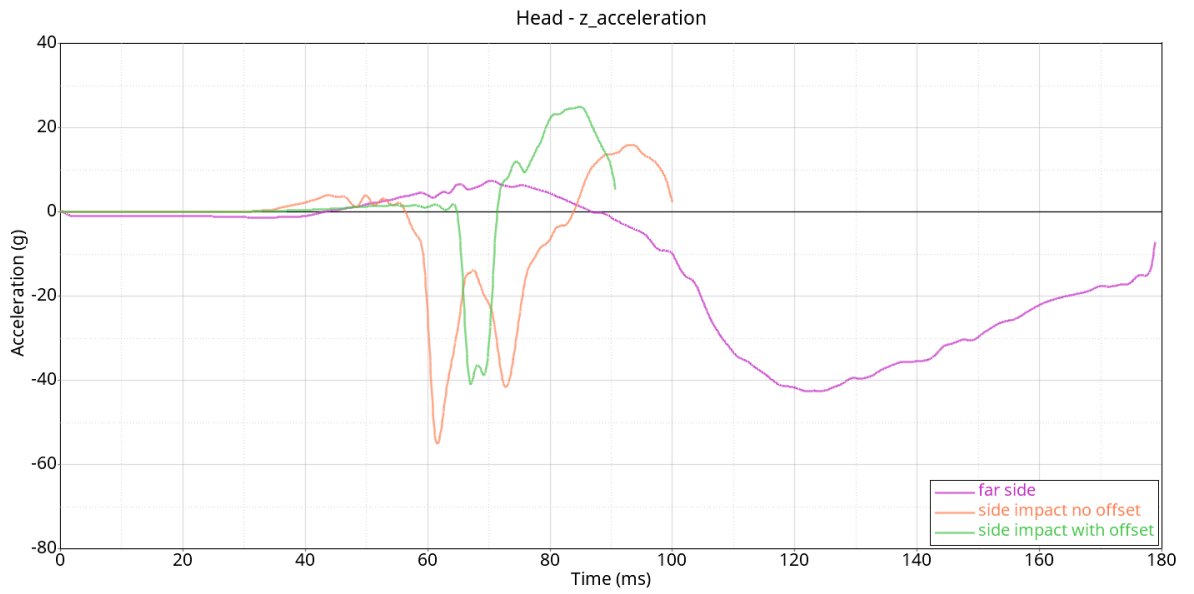
This appendix provides graphs of complementary data, some of which are not required by normative but, as in the case of the neck, are useful in highlighting differences between the various cases of impact.



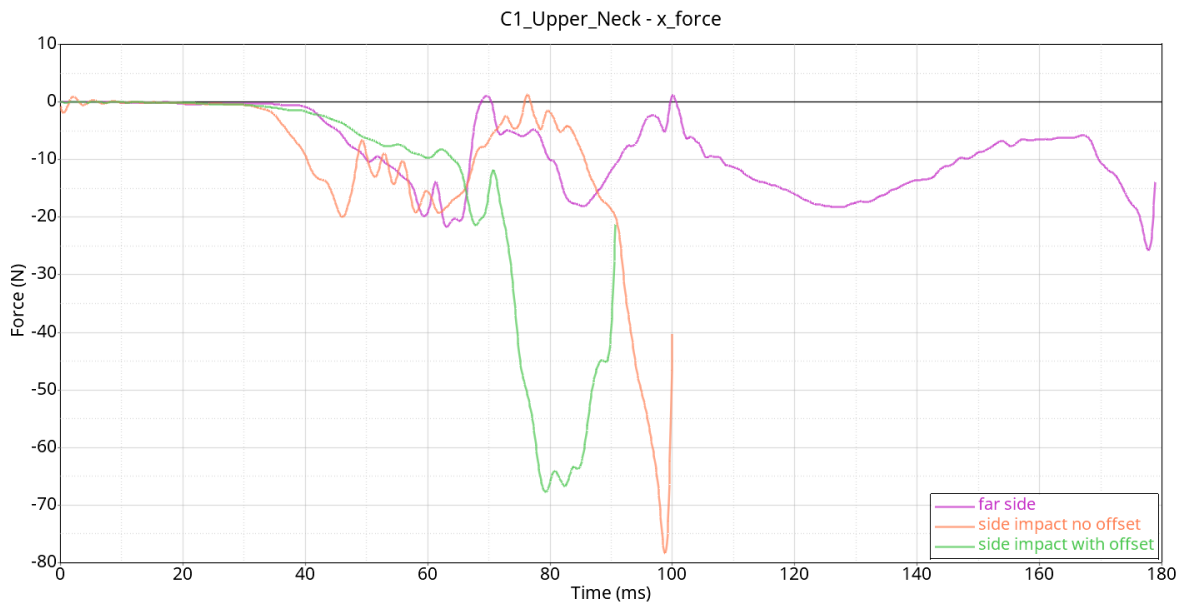
Appendix B 2 - Head x_acceleration



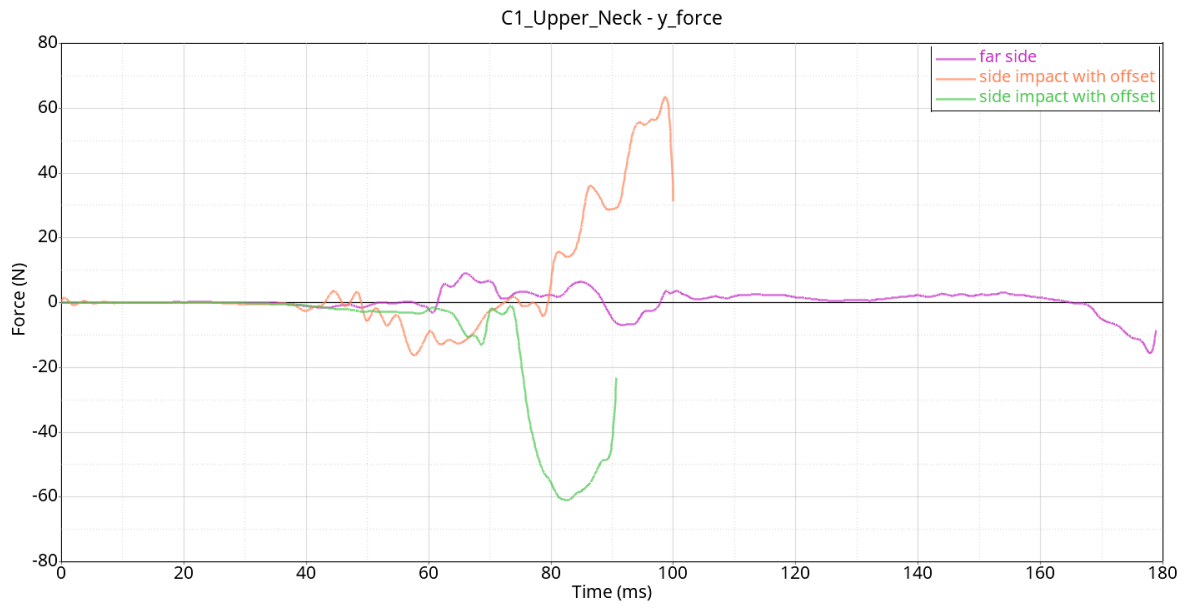
Appendix B 1 - Head y_acceleration



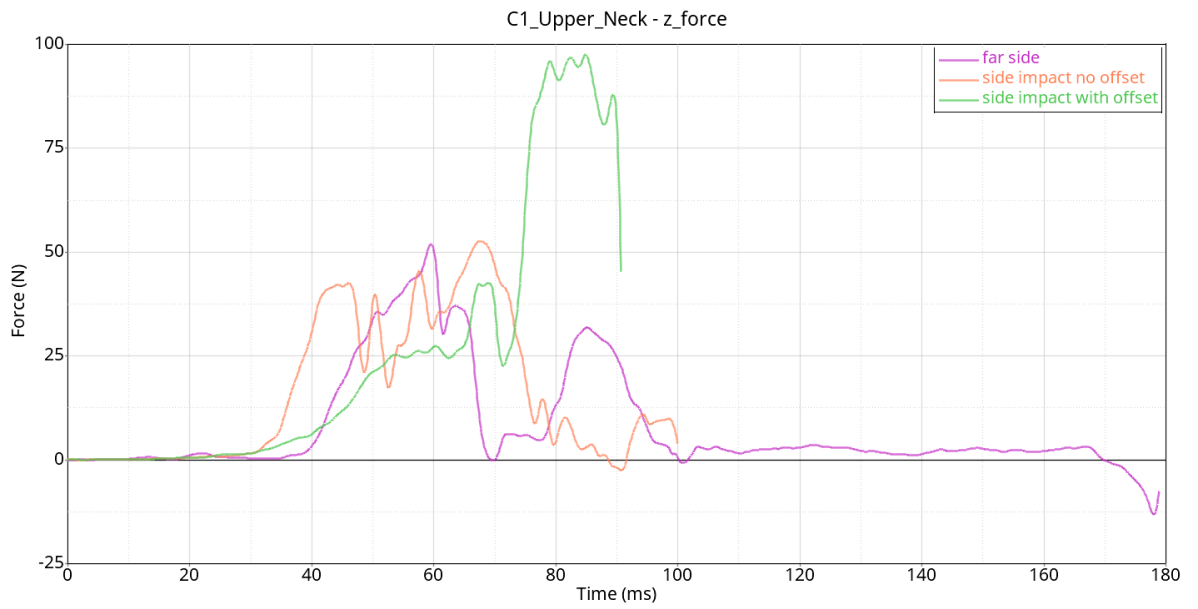
Appendix B 3 - head z_acceleration



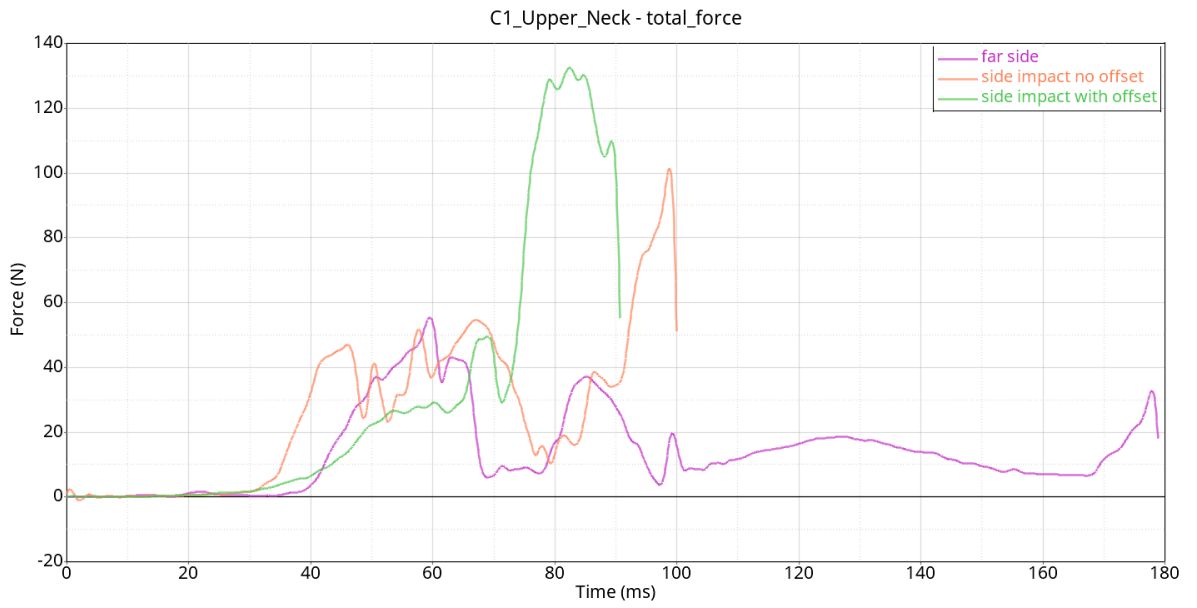
Appendix B 4 - Upper neck x_force



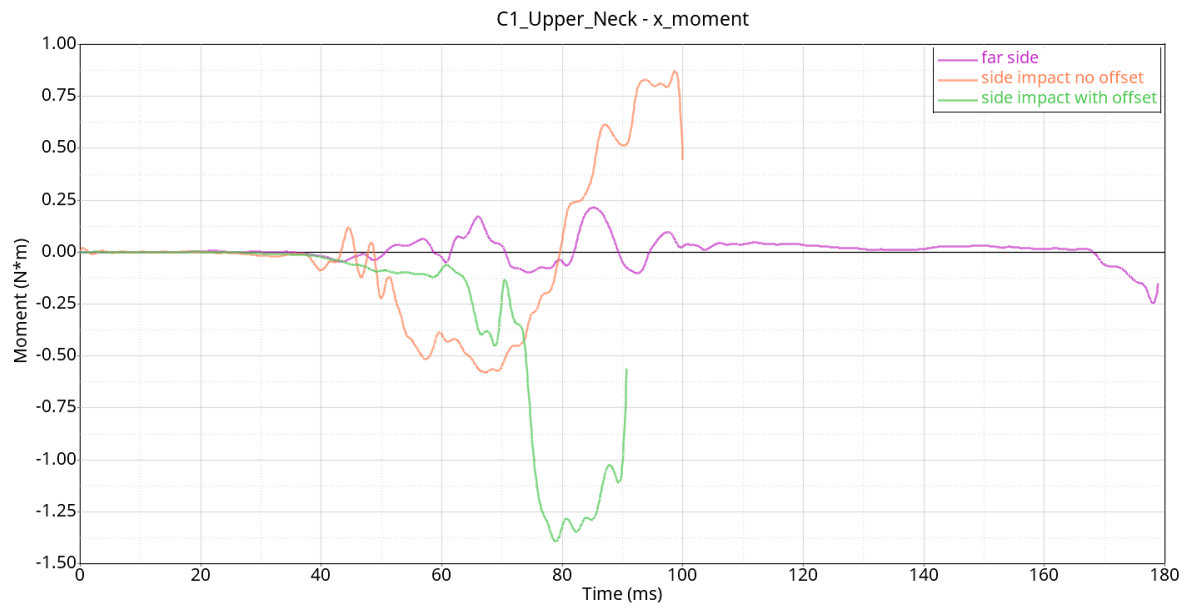
Appendix B 5 - Upper neck y_force



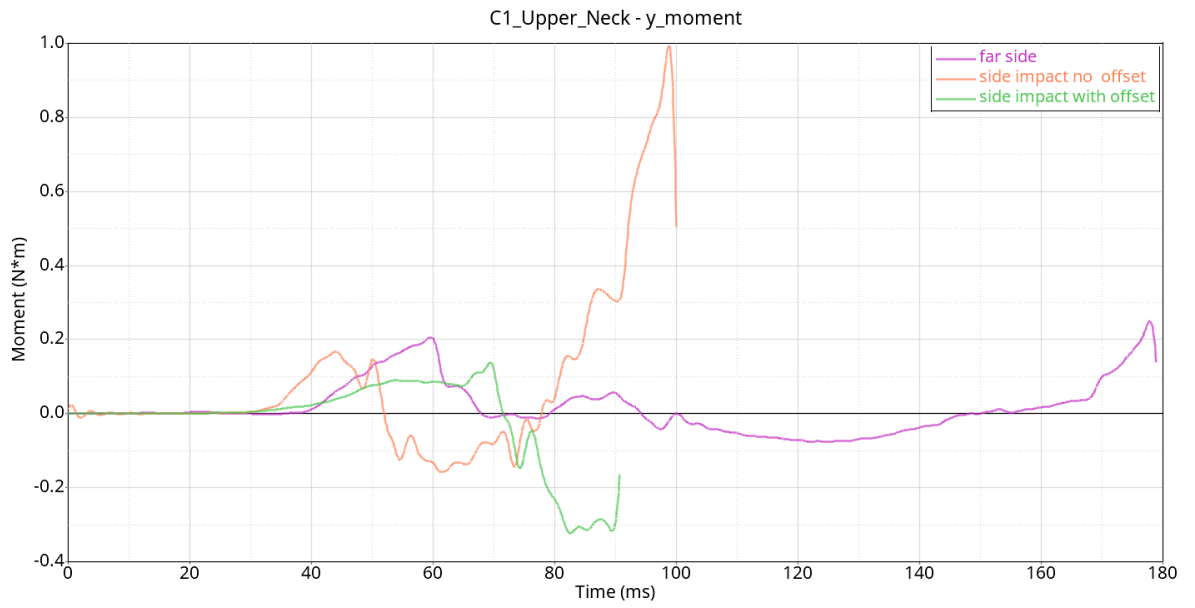
Appendix B 6 - Upper neck z_force



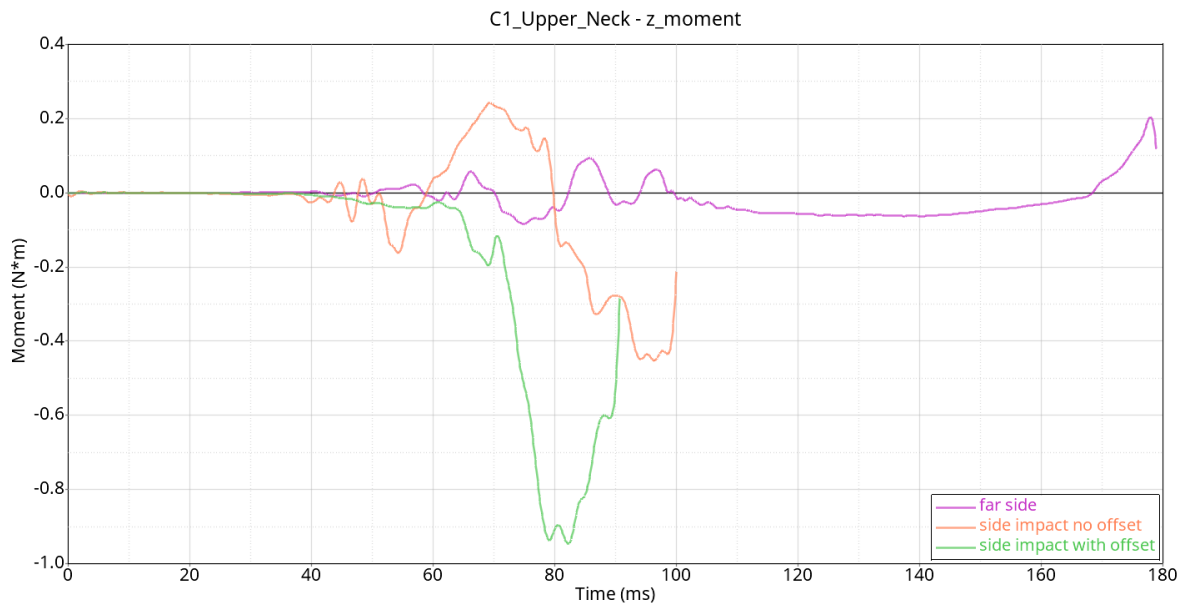
Appendix B 7 - Upper neck total_force



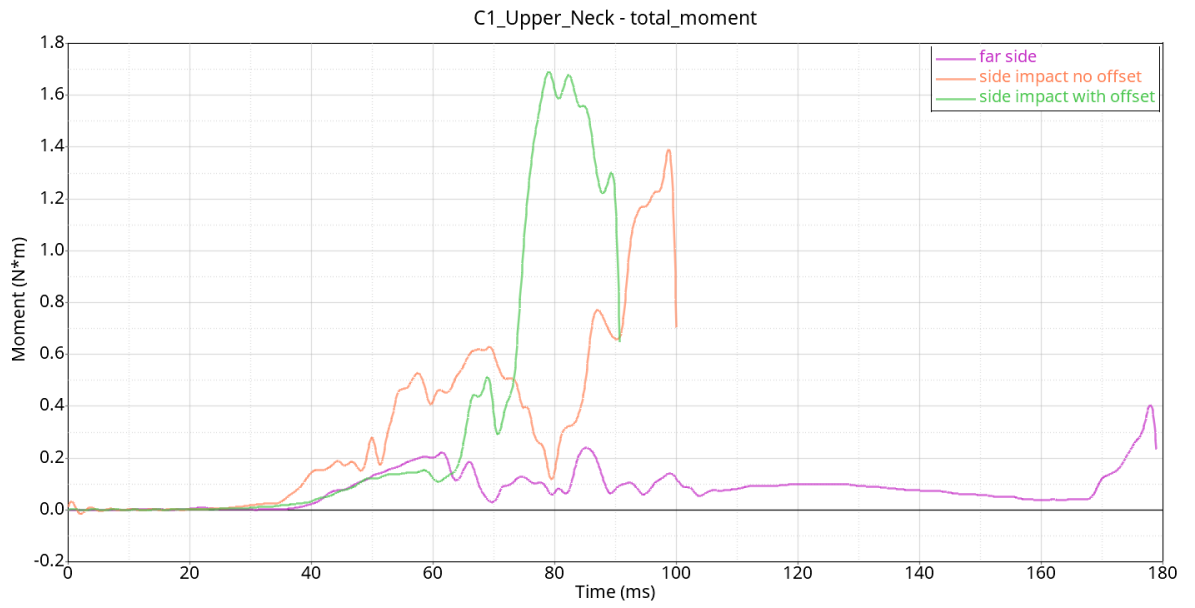
Appendix B 8 - Upper neck x_moment



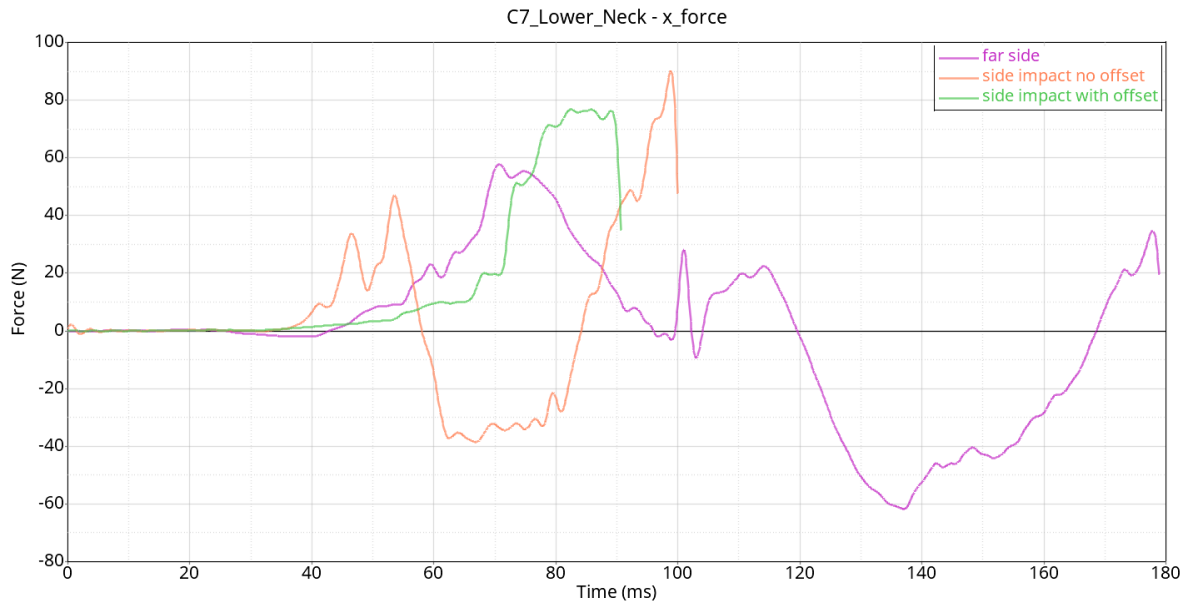
Appendix B 9 - Upper neck y_moment



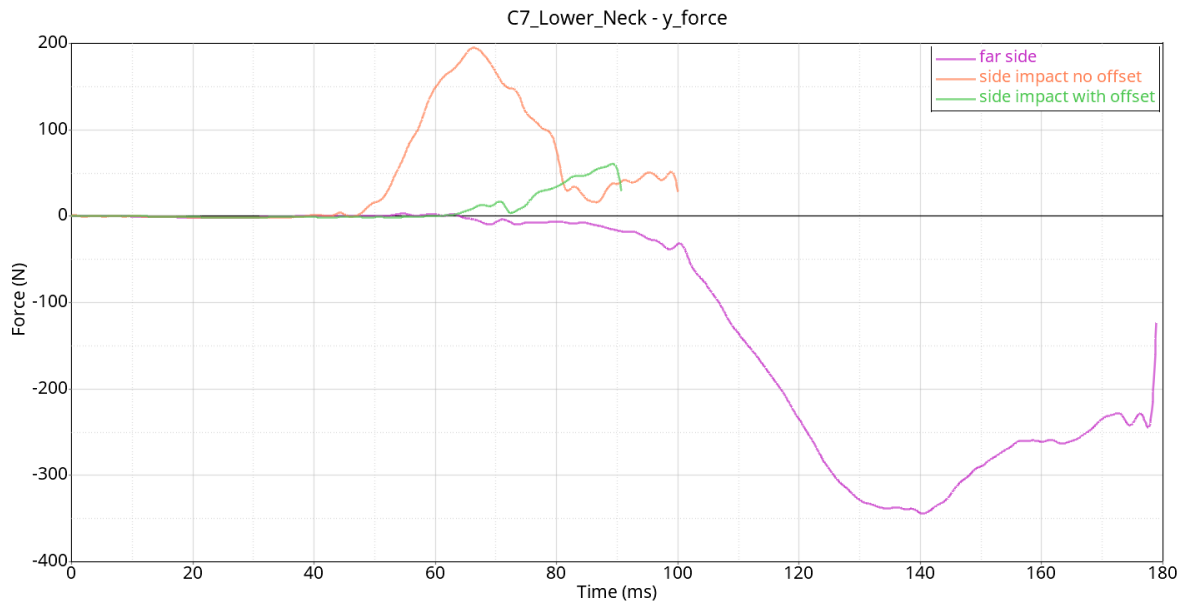
Appendix B 10 - Upper neck z_moment



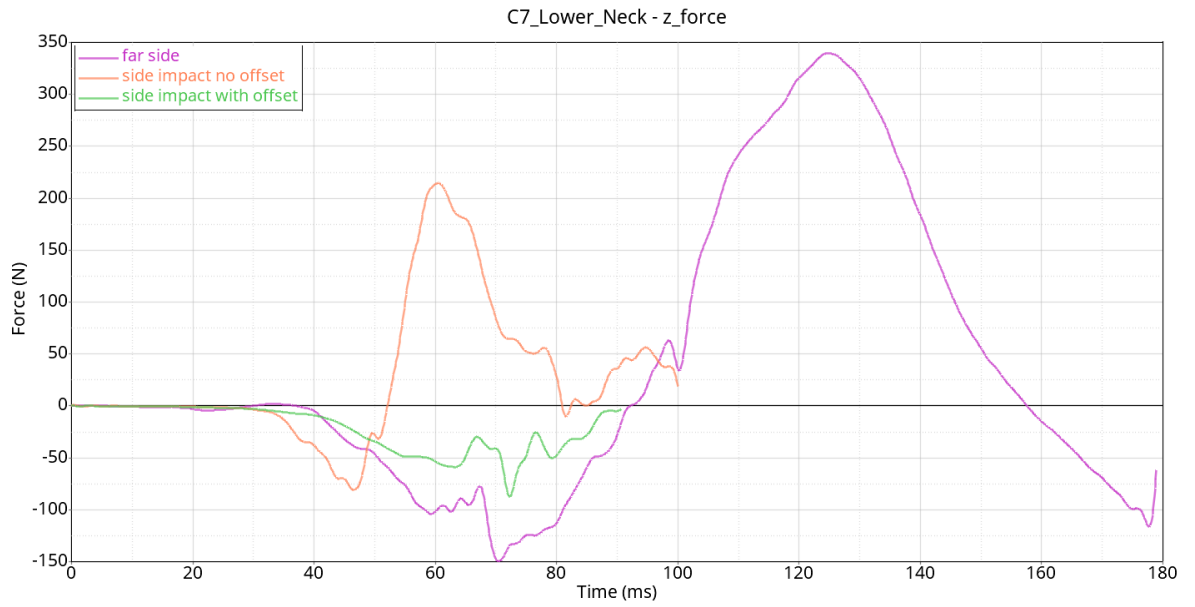
Appendix B 11 - Upper neck total_moment



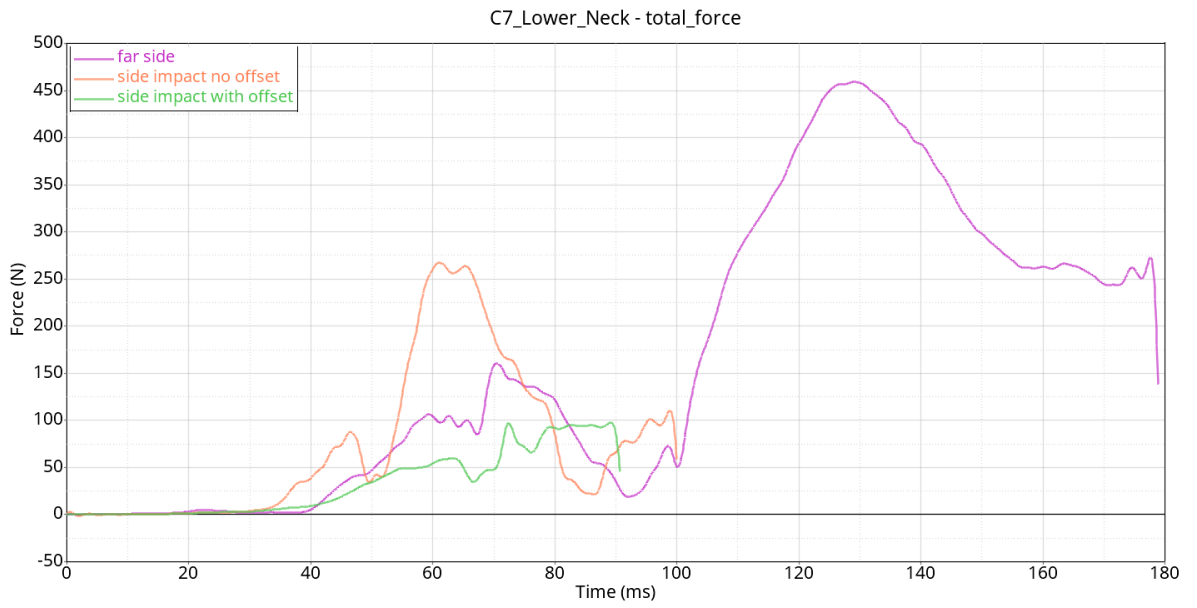
Appendix B 12 - Lower neck x_force



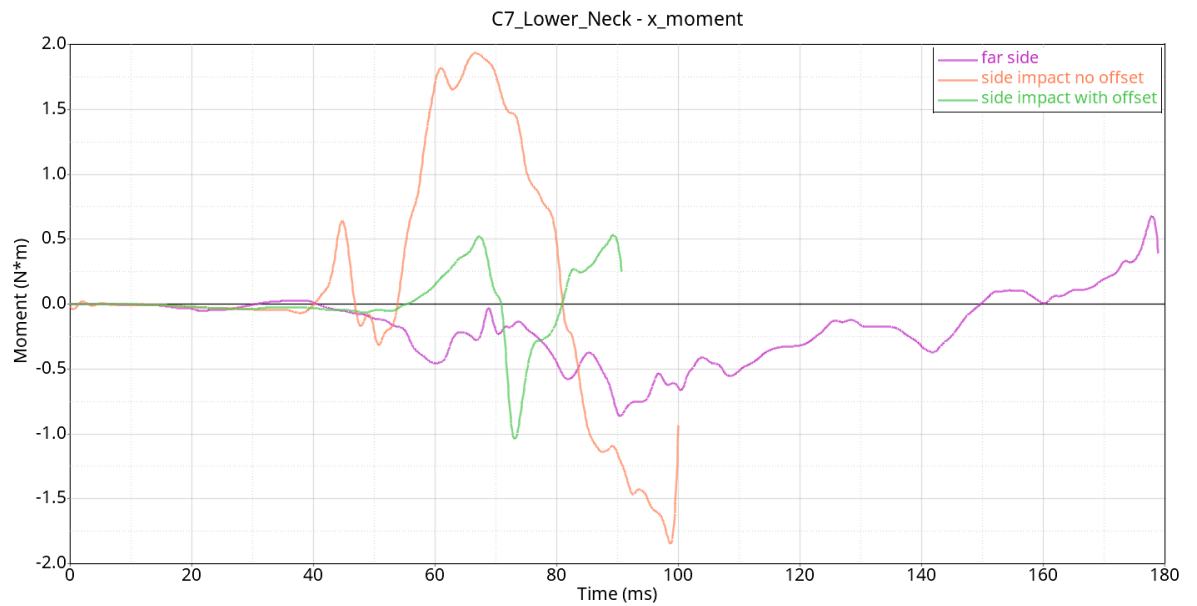
Appendix B 13 - Lower neck y_force



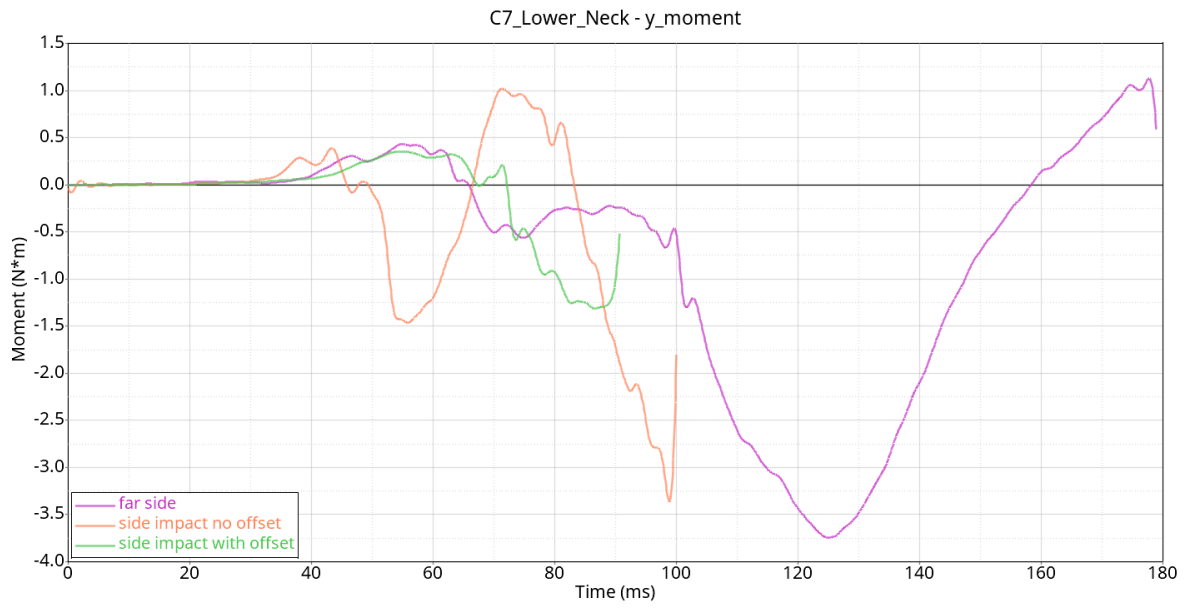
Appendix B 14 - Lower neck z_force



Appendix B 15 - Lower neck total_force



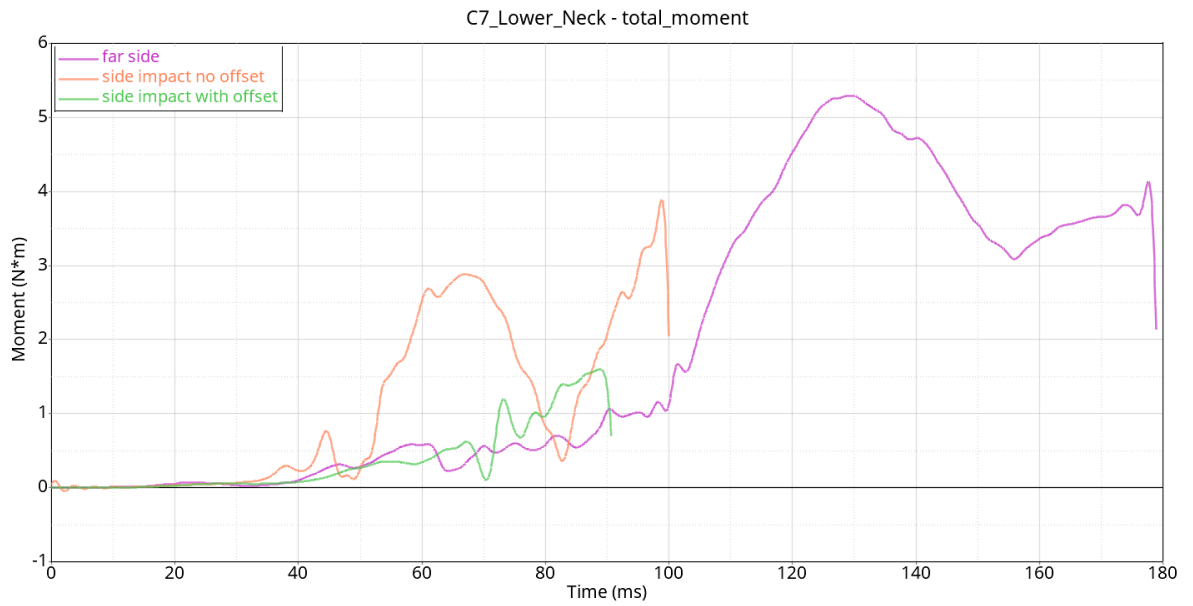
Appendix B 16 - Lower neck x_moment



Appendix B 17 - Lower neck y_moment



Appendix B 18 - Lower neck z_moment



Appendix B 19 - Lower neck total_moment

It's evident that in the case of the far side impact the neck has a different behaviour depending on the section analysed, while in the cases of the side impacts the behaviour is similar for both sections. The upper section is in fact subjected to low moments and forces, while the lower section is subjected to very high forces, especially in the direction of the impact, perhaps due to the fact that the driver does not encounter any obstacles during the impact and therefore has a greater excursion.

References

- [1] Insurance Institute for Highway Safety (IIHS), “2016, Fatality facts,” 2017.
- [2] Donata Gierczycka, Brock Watson and Duane Cronin, “Investigation of occupant arm position and door properties on thorax kinematics in side impact,” 2015.
- [3] Donata Gierczycka, Brock Watson and Duane Cronin, “Investigation of occupant arm position and door properties on thorax kinematics in side impact,” Department of Mechanical and Mechatronics Engineering, University of Waterloo, Waterloo, ON, Canada, 2014.
- [4] Euro NCAP, “<https://www.euroncap.com/>”.
- [5] “Wikipedia,” [Online]. Available: https://it.wikipedia.org/wiki/Euro_NCAP.
- [6] Adam J. Golmana, Kerry A. Danelsona, Logan E. Millera, Joel D. Stitzel, “Injury prediction in a side impact crash using human body,” 2013.
- [7] LSTC, “<https://www.lstc.com/products/models/barriers>”.
- [8] Euro NCAP, “L7e SIDE IMPACT TESTING PROTOCOL,” 2014.
- [9] Michael Kleinberger, Emily Sun, Rolf Eppinger, “Development of Improved Injury Criteria for the Assessment of Advanced Automotive Restrain System,” 1998.
- [10] Algorithm workgroup: D. Cichos (bast), D. de Vogel (Ford), M. Otto (TUV), “Crash Analysis Criteria Description (version 2.3),” 2011.
- [11] Dilip Bhalsod, Raghavendra Chivukula, “Advance European Movable Deformable Barrier documentation, Version: LSTC.AE-MDB_VERSION_R1.0.070613 V1.0”.
- [12] Euro NCAP, “AE-MDB specification version 1.0,” 2013.
- [13] Center for Collision Safety and Analysis (CCSA), “<https://www.ccsa.gmu.edu/models/2012-toyota-camry/>”.
- [14] CCSA, “2012 Toyota Camry Detailed Model V5 - Validation”.

- [15] CCSA, “Development & Validation of a Finite Element Model for the 2012 Toyota Camry Passenger Sedan”.
- [16] Toyota Central R&D Labs. Inc., “THUMS AM50 Occupant Model Version 4.1,” 2020.
- [17] G. Biasi, “Human Body Model and passive safety of vehicles: study of injuries on abdominal organs using the Peak Virtual Power method (PVP),” a.a. 2020/2021.
- [18] I. Yeh, “LS-DYNA Seat Belt Modelling Guideline,” ftp.lstc.com, 2017.
- [19] S. Guha, Occupant Modelling Workshop & Other Learning Aids, LSTC, 2011.
- [20] LSTC ftp site, “seatbelt modeling”.
- [21] TOYOTA MOTOR CORPORATION Toyota Central R&D Labs. Inc., “Documentation - Total Human Model for Safety (THUMS) - AM50 Pedestrian/Occupant Model Academic Version 4.02,” 2015.
- [22] F. Germanetti, “Finite Element Simulation of Impact of Autonomous Vehicle with Human Body Model in Out-of-Position Configuration,” Politecnico di Torino, a.a. 2019/2020.
- [23] D. Soliman, “Finite element modelling of vehicles in human body models for passive safety,” Politecnico di Torino, a.a. 2019/2020.
- [24] J. C. Parr, M. E. Miller, J. A. Pelletiere and R. A. Erich, “Neck injury criteria formulation and injury risk curves for the ejection environment: a pilot study,” 2013.
- [25] Mertz, H.J., “Anthropometric Test Device in Accidental Injury: Biomechanics and Prevention,” 1993.
- [26] F. Garelli, “Side impact crash studied with FE simulation and human body model,” 2021.
- [27] P. Assandri, “Human Body Model and Passive Safety in Autonomous Vehicles: Far Side Impact,” 2021.
- [28] Avery B. Chakravarty, “The effects of off-axis loading on fracture risk in the human tibia,” 2016.

Acknowledgements

Ci tengo a ringraziare in primis il mio relatore, il professor Alessandro Scattina, per avermi seguito in questo lavoro di tesi e il team di lavoro che si è creato con i colleghi Paolo Ascia, Pietro Assandri, Kungwani Bharat, Gianluca Di Blasi e Federico Garelli.

Con la stesura di questa tesi si conclude il mio percorso universitario ricco di gioie e soddisfazioni, ma anche con alcuni momenti difficili. Vorrei ringraziare soprattutto la mia famiglia per essermi sempre stata vicina e avermi supportato in ogni momento non facendomi mai mancare il loro appoggio. Un grazie alla mia ragazza per avermi sostenuto e spronato. Grazie ai miei coinquilini, Paolo, Gabriele e Matteo con i quali ho condiviso questi anni universitari a Torino. Un grande grazie va, poi, a tutti i miei amici per essere stati presenti e per avermi accompagnato in questi anni.

